University of South-Eastern Norway
Faculty of Technology, Natural Sciences and Maritime Studies
—
Doctoral dissertation no. 120
2022

Nora Cecilie Ivarsdatter Skau Furuvik

Modelling of ash melts in gasification of biomass

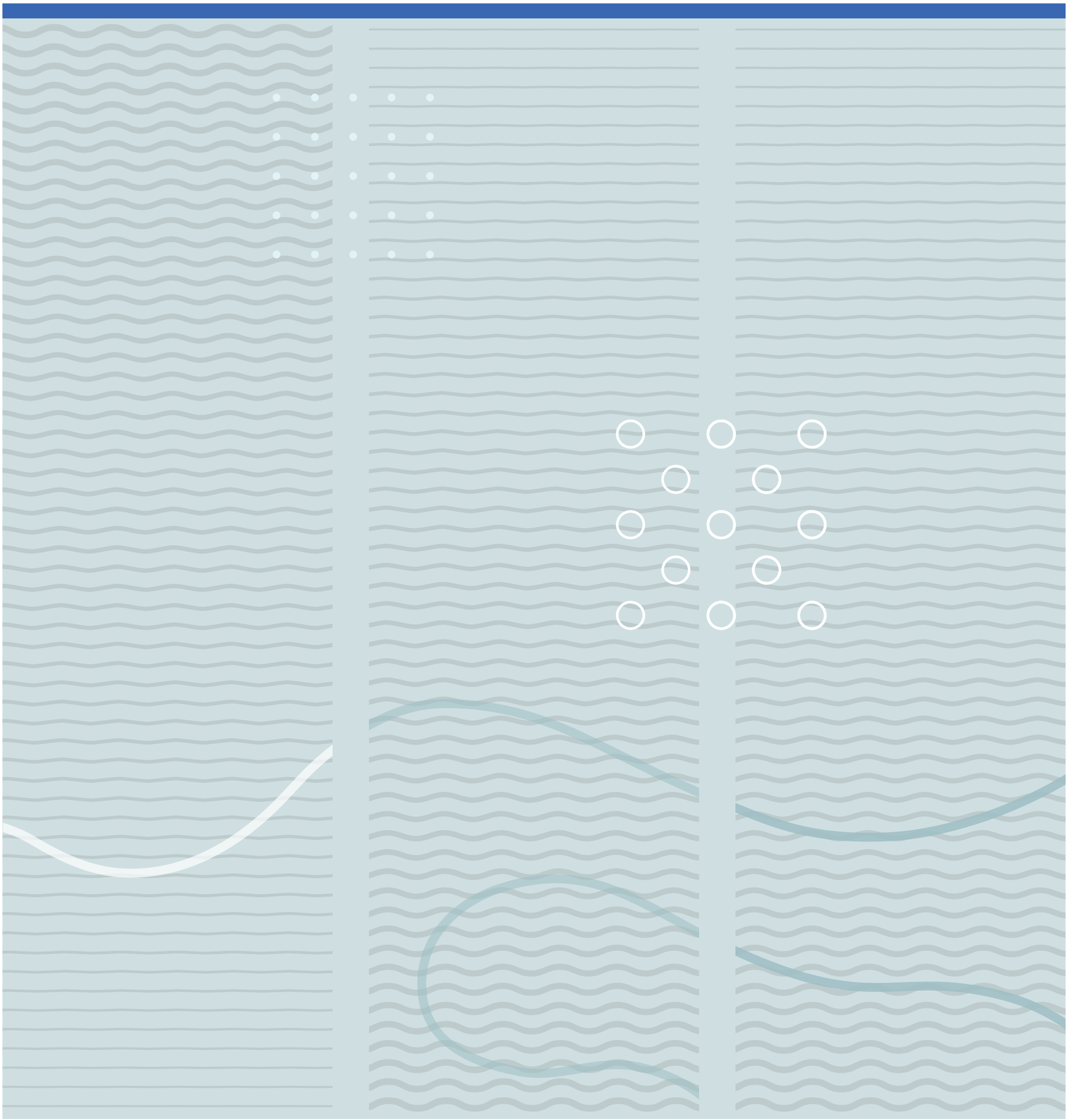

Nora Cecilie Ivarsdatter Skau Furuvik

Modelling of ash melts in gasification of biomass

A PhD dissertation in

Process, Energy and Automation Engineering

© 2022 Nora Cecilie Ivarsdatter Skau Furuvik
Faculty of Technology, Natural Sciences and Maritime Studies
University of South-Eastern Norway
Porsgrunn, 2022

Doctoral dissertations at the University of South-Eastern Norway no. 120

ISSN: 2535-5244 (print)
ISSN: 2535-5252 (online)

ISBN: 978-82-7206-649-8 (print)
ISBN: 978-82-7206-650-4 (online)

This publication is, except otherwise stated, licenced under Creative Commons. You may copy and redistribute the material in any medium or format. You must give appropriate credit provide a link to the license, and indicate if changes were made.
http://creativecommons.org/licenses/by-nc-sa/4.0/deed.en

Print: University of South-Eastern Norway

Preface

This thesis is submitted in partial fulfilment of the requirements for the degree of Doctor of Philosophy (PhD) within the program for Process, Energy and Automation Engineering at the University of South-Eastern Norway (USN). The PhD work has been carried out at USN, campus Porsgrunn, in the period from September 2018 to December 2021. The thesis is divided into two parts, Part 1 consists of an overview of the research project, and Part 2 consists of the eight scientific papers that the dissertation is based on.

First and foremost, I would like to thank my main supervisor Professor Britt Margrethe Emilie Moldestad. Thank you for expert guidance, for being both supportive, motivating and patient, for pushing me when needed and keeping me on track when interest in other topics challenged my focus.

I would also like to thank my co-supervisors, Professor Marianne Sørflaten Eikeland and associate Professor Rajan Kumar Thapa for their contribution and supportive supervision. Thanks to the rest of the Alternative Fuels research group, Rajan Jaiswal, Ramesh Timsina, Hildegunn Hegna Haugen, Janitha Bandara, and Cornelius Agu for great cooperation and for always being helpful in solving my technical questions.

A further thanks to all my friends and colleagues that were there to help and give me kind support. Special thanks to Rajan Jaiswal for being my partner in crime in both experimental and simulation work, for valuable assistance, input and suggestions, and to Øyvind Johansen for technical and practical help in development and rigging of experimental setups. I would also like to extend a special thanks to Henrik Kofoed Nielsen at the University of Agder (UiA) for always being positive to let me borrow necessary facilities at UiA, and to Christoph Pfeifer at University of Natural Resources and Life Sciences (BOKU) for the hospitality during my visit to Vienna. Thanks to Liang Wang from SINTEF Energy Research for performing SEM-EDS analysis, and Krister Jakobsen and Harald Pleym for spending valuable time with contributions on the work for present papers.

Thanks to my parents, Ingrid and Ivar, my sister, Inger Marie, and my brother, Fredrik, for moral support and for always believing in me.

Finally, a huge, warm thank you to my husband Frank Robert and our two daughters Sarah Adele and Line. Thank you for your unlimited support, patience and understanding throughout this period.

Porsgrunn 03.12.2021

Nora Cecilie Ivarsdatter Skau Furuvik

Acknowledgements

This study was funded by the Research Council of Norway, program for Energy Research (ENERGIX), through project no. 280892 “Prediction of FLow behaviour of ASH mixtures for transport biofuels in the circular economy (FLASH)”.

Abstract

The need for advanced biofuels produced from sustainable sources is stressed, both on national and international level due to a global agreement to limit the Earth's global warming. The major goals in the Norwegian agreement on climate policy are to become climate neutral by 2030 and to become a net-zero emission society by 2050. One of the priority areas for action is to reduce the sources of greenhouse gases by speeding up the introduction of low-emission alternative transport fuels, such as liquid transport biofuels.

A well-known process for converting biomass resources into liquid transport biofuels involves gasification, a thermochemical process that converts the biomass into a gaseous mixture of syngas in the presence of heat and a gasifying agent. The syngas consists of mainly hydrogen (H_2) and carbon monoxide (CO), and can be further processed into biofuels. Among the different technologies applied for biomass gasification, fluidized beds have industrial advantages due to the ability to process a wide range of biomass under controlled operating conditions. The fluidized bed gasifiers also offer several other advantages, including good mixing, high heat and mass transfer and high productivity at a relatively low process temperature. However, processing biomass-derived fuels in fluidized beds suffers from ash related problems. The major challenge is associated with molten biomass ash and the formation of agglomerates that cause fluid dynamic disturbances in the bed. If not counteracted, the bed disturbances lead to operational problems that might result in decreased efficiency, high maintenance costs and unscheduled shutdowns. Bed agglomeration and de-fluidization are closely linked to the ash melting behaviour, and has been reported as one of the problematic issue prohibiting an economical and trouble-free operation. Hence, the key to unlocking fluidized bed biomass gasification as a viable route for biofuels production is by solving the challenges related to the ash.

This PhD thesis addresses the key issues related to bed agglomeration and de-fluidization in fluidized bed gasifiers. Experimental work and computational modelling were combined in order to achieve a fundamental understanding, and insight into the underlying mechanisms of the ash melting behavior and the bed agglomeration processes. The main objective was to develop effective and accurate methods and models to be used in prediction of the agglomeration tendency of different types of biomass during gasification in fluidized beds. The overall approach was divided into three sections: (i) CPFD simulations combined with fluidization and gasification experiments to gain necessary knowledge on the fluidization characteristics, (ii) fluidization experiments to generate new sets of data that could form the basis for (iii) a mathematical model for prediction of the critical amount of accumulated ash/bed material in the gasifier. The experiments were carried out in three different fluidized bed systems: (i) a cold flow model, (ii) a 20 kW laboratory scale model, and (iii) a micro-scale model. The commercial CPFD software package Barracuda Virtual Reactor was used for the computational part. The investigated biomass samples were grass, wood, straw and bark.

The results point out that the operating temperature and the composition of the major ash forming, in particular Si, K and Ca, are significant factors leading to ash melting problems in fluidized bed processes. Additionally, the findings show that the ratios between the major ash forming elements, K, Si and Ca, in the biomass play an important role in the agglomeration process, and that different combination of those elements are especially problematic when processing biomass fuels in fluidized bed systems. The results also indicate that bark tended to have the highest tolerance limit of accumulated ash in the bed for all the investigated temperatures. For example, the ash/bed material was measured to 7% by weight at 900°C, compared to grass (3%), straw (1%) and wood (1%).

A multiple regression was calculated to predict the mass ratio of accumulated ash/bed material based on the operation temperature (T) and the mass ratios of (Si/K) and (K/Ca). The final model expresses the amount of accumulated ash/bed material at the onset of bed agglomeration and de-fluidization:

Accumulated ash/bed material (wt %) = $17.06 - 0.02 \cdot T + 4.04 \cdot (Si/K) + 1.05 \cdot (K/Ca)$

The overall regression was statistically significant ($R^2 = 0.81$, $F(3, 30) = 38$, $p<0.0001$).

Key words: Biomass gasification, Fluidized beds, Bed agglomeration, De-fluidization.

List of papers

Paper 1

Furuvik, N.C.I.S., Jaiswal, R. and Moldestad, Britt M.E. (2019). *Flow behavior in an agglomerated fluidized bed gasifier*. International Journal of Energy and Environment 10(2) (2019), page 55-64.

Paper 2

Furuvik, N.C.I.S., Jaiswal, R., Thapa, R. K. and Moldestad, B.M.E. (2019). *CPFD Model for Prediction of Flow Behaviour in an agglomerated Fluidized Bed Gasifier*. International Journal of Energy Production and Management 4(2) (2019), page 105-114.
DOI: 10.2495/EQ-V4-N2-105-114

Paper 3

Furuvik, N.C.I.S., Jaiswal, Rajan, Thapa, Rajan K. and Moldestad, Britt M.E. (2019). *Study of agglomeration in fluidized bed gasification of biomass using CPFD simulations*. Linköping Conference proceedings, Volume 170 (2019), page 176-181.
DOI: 10.3384/ecp20170176

Paper 4

Jakobsen, K., Jaiswal, R., Furuvik, N.C.I.S and Moldestad, B.M.E. (2020). *Computational Modelling of Fluidized Bed behaviour with agglomerates*. Linköping Conference proceedings, Issue 176 (2020), page 421-427.
DOI: 10.3384/ecp20176421

Paper 5

Furuvik, Nora C.I.S., Jaiswal, Rajan and Moldestad, Britt M.E. (2020). *Comparison of Experimental and Computational study of Fluid Dynamics in Fluidized Beds with agglomerates.* Linköping Conference proceedings (2020), Issue 176, page 414-420.
DOI: 10.3384/ecp20176414

Paper 6

Furuvik, N.C.I.S., Jaiswal, R. and Moldestad, B.M.E. (2020). *Experimental study of agglomeration in Fluidized Bed Gasification of Grass pellets*. WIT Transactions on Ecology and the Environment, Volume 246 (2020) page 9-17.
DOI: 10.2495/EPM200021

Paper 7

Furuvik, Nora C.I.S., Jaiswal, Rajan, Eikeland, Marianne, Thapa, Rajan, Wang, Liang and Moldestad, B.M.E. *Experimental study and SEM-EDS analyses of agglomerates from gasification of biomass in fluidized beds.* Submitted for publication to the journal, Energy.

Paper 8

Furuvik, Nora C.I.S., Eikeland, Marianne and Moldestad, B.M.E. *Modelling of ash melts in fluidized bed gasification of biomass.* Submitted for publication to the journal, Chemical Engineering Science X.

Abbreviations

BFBG	Bubbling Fluidized Bed Gasifier
Ca(Mg)	Calcium (Ca) and/or Magnesium (Mg)
CFBG	Cold flow Bubbling Fluidized bed
CPFD	Computational Particle Fluid Dynamics
GHG	Greenhouse Gases
HHV	Higher Heating Value
K(Na)	Potassium (K) and/or Sodium (Na)
MBFB	Microscale Fluidized Bed
MSW	Municipal Solid Waste
SEM/EDS	Scanning Electron Microscope/Energy Dispersive X-ray
Si(P)	Silica (Si) and/or Phosphorous (P)
VR	Virtual Reactor

Nomenclature

Roman Symbol	**Description**	**Units**
$\Delta p/L$	Pressure drop per Length of unit	Pa/m
Re	Reynolds number	-
F	Variance ratio	-
R^2	Response variable variation	-
T	Temperature	°C
d	Diameter	m
m	Mass	kg
p	Probability value	-
t	Time	s
u	Velocity	m/s

Greek Symbol	**Description**	**Units**
ε	Porosity	-

θ	fraction	-
μ	Viscosity	Pa*s
ρ	Density	kg/m^3
ϕ	Sphericity	-

Subscript	**Description**
0	Superficial
f	Fluid
g	Gas
mf	Minimum fluidization
p	Particle

Table of contents

Preface I

Acknowledgements III

Abstract V

List of papers IX

Nomenclature XI

Part 1 1

1 Introduction 3

1.1 Background 3

1.2 Objectives 6

1.3 Scope 7

1.4 Main contribution 8

1.5 Outline 8

2 Literature study 11

2.1 Biomass-to-liquid transport fuels 11

2.2 Biomass gasification 15

2.3 Fluidization 19

2.4 Ash related challenges in fluidized bed systems during biomass gasification 22

2.4.1 Bed agglomeration 22

2.4.2 De-fluidization 26

3 Materials and methods 29

3.1 Materials 29

3.1.1 Biomass 29

3.1.2 Bed material 30

3.2 Experimental setups 31

3.2.1 Cold flow bubbling fluidized bed 31

3.2.2 Laboratory scale 20 kW bubbling fluidized bed gasifier 32

3.2.3 Micro-scale fluidized bed reactor 34

3.3 Analytical methods 35

3.3.1 Ash melting analyses 35
3.3.2 Ash sintering degree tests 36
3.3.3 SEM/EDS analyses 37
3.4 Modelling and simulations of ash melts and agglomeration in biomass fluidized bed processes 37
3.4.1 CPFD simulations 38
3.4.2 Mathematical modelling 38
3.5 Overview of research methods 39
4 Summary of the papers 41
4.1 Paper 1 - Flow behaviour in an agglomerated fluidized bed gasifier 41
4.2 Paper 2 - CPFD model for prediction of flow behaviour in an agglomerated fluidized bed gasifier 43
4.3 Paper 3 - Study of agglomeration in fluidized bed gasification of biomass using CPFD modelling 45
4.4 Paper 4 - Computational modelling of fluidized bed behaviour with agglomerates 47
4.5 Paper 5 - Comparison of experimental and computational study of the fluid dynamics in fluidized beds with agglomerates 51
4.6 Paper 6 - Experimental study of agglomeration of grass pellets in fluidized bed gasification 53
4.7 Paper 7 - Experimental study and SEM-EDS analyses of agglomerates from gasification of biomass in fluidized beds 55
4.8 Paper 8 - Modelling of ash melts in fluidized bed gasification of biomass . 58
4.9 Unpublished work 62
4.9.1 De-fluidized bed conditions during gasification of wood pellets in a laboratory scale bubbling fluidized bed gasifier 62
4.9.2 Ash sintering analyses 63
4.9.3 Ash Density measurements 64
5 Discussion of results 65
5.1 CPFD simulations of agglomeration and flow behaviour 65

5.2 Methods and models for determining the critical amount of ash 66
6 Conclusion and suggestions for further works 73
6.1 Conclusion 73
6.2 Suggestions for further works..74
References 77
Part 2 89
Paper 1 91
Paper 2 103
Paper 3 115
Paper 4 123
Paper 5 133
Paper 6 143
Paper 7 155
Paper 8 177

Part 1

Overview

1 Introduction

This chapter sets the overall background and the objectives of the PhD work.

1.1 Background

Climate changes are the most pressing environmental challenge the world faces today, and there is an urgent need to promote the use of renewable energy sources in order to ensure a sustainable future [1, 2]. The industrial revolution, along with the economic growth and the rising global population that have taken place in the past few centuries, have driven the energy demand upwards [3]. The increasing energy requirements needed to meet the modern way of life have resulted in a rapid increase in the global greenhouse gas (GHG) emissions. Consequently, the Earth's average surface temperature has experienced a sharp rise that causes a set of worrying changes to the Earth's climate [1]. The average surface temperature rose with roughly 1°C during the period from 1880 to 2020, and of this 0.7°C from 1980 to 2020. Thus, two-third of the global warming occurred in the last 40 years, meaning that the rate of temperature increase has nearly quintupled during these years. Without mitigating policies, the global average temperature is predicted to rise by 2°C - 6°C compared to pre-industrial levels by the end of 21st century [4]. Figure 1-1 shows the deviation in the Earth's average surface temperature in the period from 1880 to 2020. The temperature anomalies are calculated based on the average temperatures from 1951 to 1980 [4].

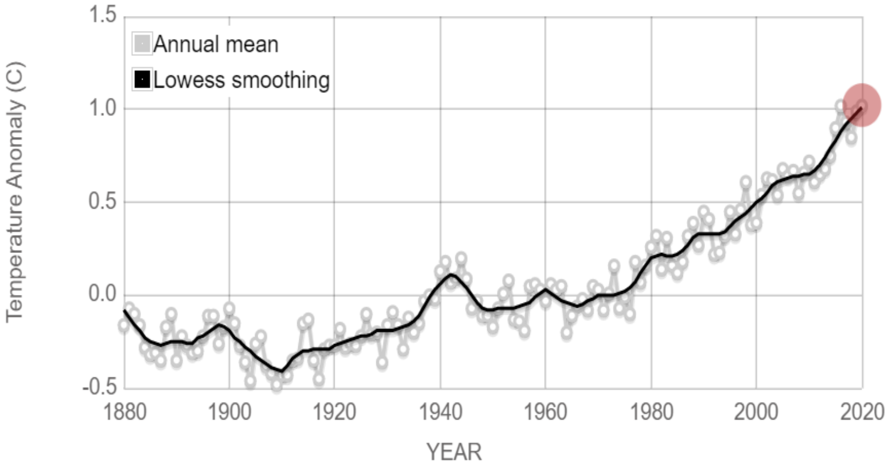

Figure 1-1. Global land-ocean temperature index [4].

The world emits around 50 billion tonnes CO_2 equivalents of GHG every year [5]. CO_2 comprises for 76% of the global GHG emissions, methane, nitrous oxides and hydrofluorocarbons contributes to 16%, 6% and 2%, respectively [6]. The primary emission source is the conversion of energy, which make up nearly three-quarters of the annual global GHG emissions. Within the energy sector, heat and electricity represents about 31% of the 2016 global GHG emissions, followed by the transport sector that stands for 16% [5]. Figure 1-2 shows the breakdown of global greenhouse gas emissions by sector in 2016.

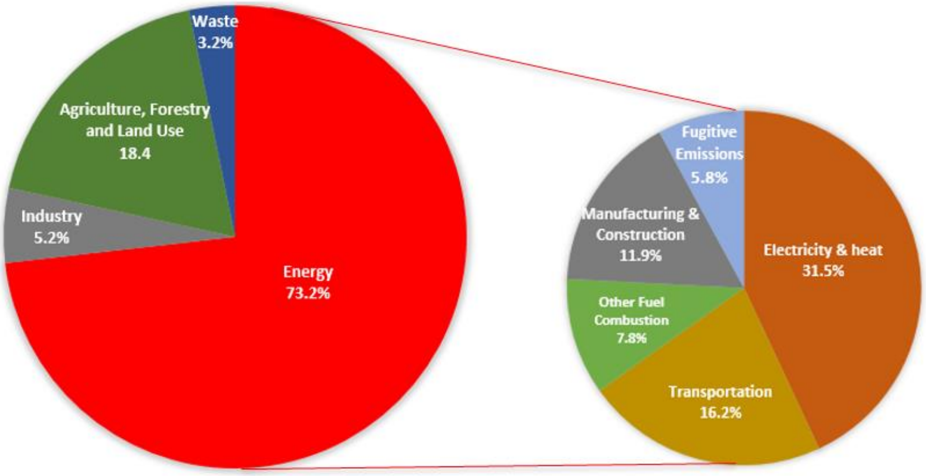

Figure 1-2. Global manmade Greenhouse Gas Emissions by sector in 2016. Based on data from [5].

Fighting the climate changes requires global action, and the importance of gathering global consensus and cooperation to tackle the ongoing crisis is essential. National and international climate policy guidelines include a global strategy to prevent the man-made climate changes by reducing the emissions and stabilizing the levels of GHG in the atmosphere. The global climate change mitigation is governed by commitments through the Paris Agreement, which aims to limit the average global surface temperature rise to well below 2°C above the pre-industrial levels by the end of the 21st century. In the long term, the goal is even further below 1.5°C [7, 8].

Although the climate change is a global issue, each country must play its part by drawing up comprehensive national climate action plans. Norway aims to be a driving force in the international climate work. The Norwegian government's goal is for Norway to become climate-neutral by 2030, and a low-emission society by 2050. One of the priority areas for actions is to reduce the emissions from the transport sector. The transport sector stands for 19% of the annual GHG emission in Norway, where the road transport is by far the biggest emitter accounting for more than 12% of the GHG emissions in 2016 [5]. One strategy is to reduce the sources of these gases by speeding up the introduction of low-emission alternative transport fuels, such as liquid transport biofuels [7, 9].

Liquid transport fuels are currently mainly produced from fossil fuels, which are non-renewable resources such as petroleum, natural gas and coal [2, 10]. The challenges with fossil fuels are, not only that the use of fossil fuels emits substantial amounts of GHG, but the stocks are finite and the availability of these resources is limited. The massive expansion in the transport sectors worldwide, and the rising fear over the effect of climate changes, have brought to life the search for a climate-friendly alternative to fossil fuels [11]. Biomass has become one of the key resources to reduce the dependence on fossil fuels in the transport sector, and at the same time provide energy in a more sustainable and climate-neutral manner [12]. Biomass refers to a broad variety of feedstock including harvested wood, forestry residues, energy crops, agricultural crops and residues as well as urban waste from commercial industry [13]. Unlike underground fossil reserves, biomass is abundantly available. It is considered a renewable energy source based on the concept that the plant material used can be replaced through re-growth. Biomass energy does not generate any net additional CO_2 into the atmosphere since the CO_2 emitted is already part of the biogenic carbon cycle. Thereby biomass offer immediate reductions in the greenhouse gas emission.

New and efficient technologies that make it possible to produce transport fuels from renewable sources, such as biomass, have lately become more popular. Fluidized bed gasification is a promising energy conversion technology, which converts the biomass into a high-quality syngas in presence of heat and a gasifying agent [14]. The syngas consists of mainly H_2 and CO, and can be processed into any gaseous and liquid transport fuels, as well as several other convenient chemical products [15]. However, processing biomass in fluidized bed is challenging due to the complex high-temperature chemistry of the biomass ash. The fluidized beds suffer from operational problems due to molten biomass ash that interacts with the bed material. The key to unlocking gasification as a viable route for biomass to transport biofuels is therefore by solving the ash related problems.

This PhD-work is part of project 280892 FLASH (Prediction of FLow behaviour of ASH mixtures for transport biofuels in the circular economy). The research is funded by the Research Council of Norway, program for Energy Research (EnergiX). The main objective of the FLASH-project is to accelerate the implementation of biomass to biofuels via gasification. The strategy is to mitigate the ash-related challenges, which still are the main barrier for a commercial breakthrough of thermo-chemical conversion of biomass. An important aspect is to discover the underlying ash mechanisms (ash behaviour and ash chemistry) that currently separates the two dominating gasification technologies (entrained flow and fluidized beds). The FLASH-project is divided into three work packages, WP1, WP2 and WP3, where this PhD-work is part of WP3. The main objective of WP1 is to increase the fundamental understanding of ash properties and ash behaviour in thermal systems, and particularly thermal systems under reducing conditions. The work package covers measured ash melting behaviour in correlation with ash viscosity, compared with calculated thermodynamic predictions of ash behaviour and viscosity (for ash speciation and phase distribution). WP2 proposes the development of methods and models for predicting ash behaviour through experimental investigation of ash viscosity. The viscosity data obtained are implemented to suggest and develop new methods for ash viscosity measurement. WP3 defines and tests strategies to mitigate ash-related challenges based on theoretical and experimental studies of ash melt in bubbling fluidized bed reactors. The FLASH-project group consists of partners from the University of South-Eastern Norway, SINTEF Energy Research, University of Natural Resources and Life Sciences, Austria and Aalto University, Finland.

1.2 Objectives

To improve the efficiency of biomass gasifiers, it is necessary to get a better knowledge of the ash properties and ash behaviour in the reactors. This PhD-work aims to increase the fundamental understanding of how the biomass ash characteristics influence on the bed agglomeration in fluidized bed systems. The flow behaviour was investigated at different bed conditions to mitigate the operational challenges caused by bed agglomeration. The main objectives of this research work were to:

1. Find a clear relationship between the biomass ash composition, high operating temperatures and bed agglomeration and de-fluidization during gasification in fluidized bed systems.
2. Develop methods and models to predict the agglomeration tendency for different biomass fuels based on experimental studies of the flow behaviour in fluidized beds.

1.3 Scope

The scope of this study is limited to investigation of biomass available in Norway. Other limitations are the selection bed material, particle size and fluidizing agent. In order to achieve the defined objectives, this work was planned with a combination of the following experimental and modelling studies:

- Experiments using a cold flow model of a bubbling fluidized bed to study the fluidization characteristics under different flow conditions.
- Experiments in a bubbling fluidized bed gasifier to study the fluidization characteristics and the onset of bed agglomeration under different hot flow conditions.
- CPFD simulations to fully understand the relationship between the flow behaviour and the agglomerated bed conditions.
- Experiments in a micro-scaled model of a bubbling fluidized bed to study the de-fluidized conditions and the agglomeration tendency for different biomass ashes.
- Measurements of the critical amount of ash in the bed at different gasification temperatures to develop a mathematical model for prediction of the onset of de-fluidization.

1.4 Main contribution

This work contributes to the field of biomass-to-liquid transport fuels and is related to the operational challenges with ash melting in fluidized beds. Based on this research, a more efficient and economical utilization of biomass can be obtained by adjusting the operational conditions.

The critical amount of ash in the bed has been studied both in laboratory scaled gasification experiments and in micro-scaled measurements. The experimental results generated new data and formed a good basis for development of a mathematical regression model. The model is capable of early detection of the formation of agglomerates and de-fluidized bed conditions during biomass gasification in bubbling fluidized bed. The developed method and model are new scientific tools that can be used to determine critical amount of ash analytically, and thus providing the necessary tools to accomplish a larger utilization of biomass in the future.

1.5 Outline

Including the introduction chapter, the thesis is divided into five chapters.

Chapter 2: Literature study

This chapter highlights the need for expanded research in advanced biofuel production within the framework of a global transition to a net-zero emission transport sector. It provides an insight into biomass gasification with particular focus on the fluidized bed technology. A general introduction to fluidization is given, briefly explaining the fundamental parameters that play an important role in the fluidization behaviour in the fluidized beds. The minimum fluidization velocity is discussed based on the Ergun equation. Furthermore, this chapter describes the bed agglomeration phenomenon during biomass gasification in fluidized beds. The biomass ash characteristics and the major ash forming elements that accelerate the agglomeration process in fluidized bed systems are described in more detail. The last section of this chapter shortly reviews the current status of available knowledge and the research studies of bed agglomeration due to ash melting.

Chapter 3: Materials and methods

This chapter presents the research methodology adopted in this work, including the experimental setups and analytical methods used to collect necessary data for the study of bed agglomeration in fluidized beds. The experimental results are used as input for CPFD simulations of flow behaviour in agglomerated fluidized beds and form the basis for a predictive mathematical model of the agglomeration phenomena.

Chapter 4: Summary of papers

This chapter presents a summary each of the scientific papers published through the present study. Additionally, some non-published results are presented.

Chapter 5: Discussion of results

This chapter discusses the main findings and results from this study.

Chapter 6: Conclusion and suggestions for further work

This chapter draw the conclusions from the present study and presents suggestions for future work.

2 Literature study

This chapter covers the most important theoretical topics that are relevant for this PhD-work. First, a brief overview of the current state of the global investment in advanced biofuels is provided. The role of biomass in a sustainable future is highlighted, followed by a short description of biomass gasification, with a major focus on bubbling fluidized bed systems. This chapter also looks into the basic fluidization theory necessary to follow this work. Finally, the chapter reviews literature, including important surveys and findings regarding the operational challenges related to the behaviour of the biomass ash at high temperatures.

2.1 Biomass-to-liquid transport fuels

In the light of the irreversible climate crisis, national and sectoral climate action plans have been derived from the 2015 Paris Agreement [8]. The Paris Agreement sets ambitious standards, requiring the signatory countries to take action in the fight against the climate changes, and underlines the need for a long-term strategy to achieve net-zero emissions. Among the action priorities are the development and rapid deployment of renewable energy technologies, specifically in the fossil fuel-dominated transport sector [8, 16]. The transport sector was the energy sector with the lowest share of renewable energy in 2016 [16], and is the only one in which the GHG emissions still are steadily rising [2]. There is an international scientific agreement that a shift from fossil-based fuels to electric vehicles and liquid and gaseous transport biofuels is crucial for achieving long-term net-zero emissions in the transport sector [2, 17, 18]. The electrification of light-duty vehicles such as cars and SUVs is growing, and has already started to transform the transport industry. However, some of the transport areas such as aviation, maritime/shipping, heavy goods vehicles and long-distance transport are dependent on high energy-density fuels and meet difficulties in converting to electrified solutions [2, 16-18]. Therefore, biomass-to-liquid transport fuel technologies have emerged as viable options for a more environmental friendly and clean energy transformation, which can contribute to immediate reduction in the GHG emission from the transport sector [11, 16, 17]. The biomass-to-liquid transport fuels are applied to fuels produced through a two-step thermochemical process. The first step is production of a high-quality syngas via biomass gasification, and the second step is typically a Fisher-Tropsch catalytic synthesis of the syngas into liquid biofuels [1, 19, 20].

Liquid biofuels are generally grouped into conventional biofuels (1st generation biofuels) and advanced biofuels (2nd and 3rd generation biofuels), depending on the origin of the biomass used [21]. The 1st generation biofuels are produced from crops that traditionally are used for food or animal feed production, such as vegetable oils, sugar and starch. Both 2nd and 3rd generation biofuels use advanced conversion technologies to produce biofuels from crops that do not directly compete with the food and animal feed. The 2nd generation biofuels take advantage of residues and wastes from forestry, agricultural and industry sectors, or energy crops grown using less productive and degraded land. The 3rd generation biofuels are algae-based biofuels derived from specially engineered energy crops [11, 17, 18]. Table 2-1 describes the biomass resources and the wide range of biomass sources that are available for advanced biofuel production.

Table 2-1. Classification of biomass resources for advanced biofuel production. Based on [22].

Biomass resource	Biomass source
Forestry waste and residues	*Biomass wood from industry:* Waste from sawmills and timber mills, e.g. sawdust and bark. *Forestry residues:* Logs, branches, leaves, needles and bark
Agricultural waste and residues	*Residues and waste from agricultural harvesting and processing:* Straws from cereals and pulses, seed coats, crop wastes like sugarcane, trash, rice husk, coconut shells etc.
Energy crops	*High yield crops and plants that are exclusively grown for energy conversion:* E.g., Rapeseed, Poplar and Red canary grass. *Algae.*
Industrial waste and residues	*Waste from industry:* Wastes from paper mills, pulp wastes from food processing units, textile fibre waste, food industry waste. *Municipal solid waste.*

The liquid transport fuel industries around the world have found a growing interest in biomass utilization. A contributing factor to the growing attention is that most industrial fossil fuel-fired gasifiers can easily process biomass in already existing infrastructures and facilities, without the need for costly modifications. However, the chemical properties of biomass differ significantly from fossil fuels, making it difficult to replace the fossil fuels in large-scale gasifiers without changing the operational conditions [1, 11, 12, 15, 23, 24]. One shortcoming with biomass is a modest reduction in the thermal efficiency of the gasifiers. Compared to fossil fuels, biomass has much higher ratios of O/C and H/C. Woody biomass typically contains around 50% C and 45% O by weight, while coal contains 70-95 wt % C and 5-20 wt % O depending on the coal rank [12]. The biomass is also characterized with relatively high moisture content as well as high fraction of volatile matters, and thus lower heating values than fossil fuels [22]. Another drawback with biomass is the operational challenges due to large variations in the ash characterization within the biomass sources. For example, the straw ash is typically rich in K and Si while woody ash has high Ca content. The composition of ash from fossil fuels varies within a broad range, but generally are the fossil fuel ashes characterized with high content of Si as well as high amount of impurities like nitrogen (N) and sulphur (S) [12]. The ash content of average biomass is lower than that of average coal. For example, coal will typically contain from 9-11% ash by weight while the ash content in woody biomass often is below 1 wt % [22]. However, some biomasses can have ash content up to 20 wt %, e.g. Straw-rice and Husk-rice [12]. Despite the relatively low ash content, the biomass ashes are generally more troublesome than ash from fossil fuels, especially those originating from biomass containing both alkali metals and Si. At high process temperatures, these types of biomass are more chemically reactive and particular susceptible to operational ash related problems that often lead to unscheduled plant-shutdowns [12]. In Table 2-2, the variations in the characteristics of average fossil fuel (Bituminous coal) and average biomass (forestry and agricultural residues) are presented.

Table 2-2. Variations in chemical properties of average fossil fuels and average biomass. Based on data compiled from multiple sources [12, 22, 25].

	Proximate analyses (wt %)				***Ultimate analyses (wt %)***						***Ash components (wt %)***		
	Moisture	*Volatiles*	*Ash*	*HHV*	*H*	*C*	*O*	*N*	*S*	*Cl*	*Si*	*Ca*	*K*
Coal													
Minimum	6	5	9	26	3	75	2	-	-	-	-	4	-
Maximum	10	40	11	30	5	90	12	<1.5	<3	<0.1	<3	12	< 0.03
Biomass													
Minimum	25	70	0.5	17	5	45	35		-	-	-	-	-
Maximum	60	85	7	20	7	55	45	<0.2	<0.2	<1	<1.5	<1.5	< 2

The potential for biomass-to-liquid transport fuels in a climate neutral future is promising. With the transport sector continuously growing, energy experts predict that the worldwide transport fuels demand will continue to rise [26]. This means that the current actions for limiting the climate impacts from the different transport areas are not sufficient. In order to achieve the global climate goals [8], the liquid transport fuel industries are pressed to step up their share of renewable solutions by phasing out fossil fuels already within the next decade [16]. This requires rapid and concerted actions that suggest strong growth in the use of alternative domestic sources of biomass [16]. European countries have committed themselves to follow the 2030 Climate target plan set by EU, which aims to ensure that all energy conversion from biomass has to be sustainable and that the environmental impacts should be minimized. European governments have implemented energy policies to ensure that biofuels are in line with the sustainability criteria of the 2018 EU Renewable Energy Directive (REDII) regulations [16]. The REDII also contains restrictions on the use of conventional biofuels, where the long-term vision is to completely phase out biofuels produced from 1st generation biomass. Consequently, the biofuels production must avoid competition with food production and preferably come from better use of biomass resources from wastes and residues [16, 27].

The development and deployment of biofuel technologies are limited by competing niches of other sustainable produced biofuels, as well as the access to renewable biomass sources. For the purposes of this PhD work, it was of interest to focus on the potential of biomass sources available for the biomass-to-liquid transport fuels for the Norwegian market. In the search for alternative biomass sources, locally available 2nd generation biomass is favoured to ensure that sustainability is preserved throughout the production chain. Norway has large areas with important biomass resources available from the forestry and agricultural sectors. Forestry residues are typically wastes from timber production and sawmills, and represent the main potential of biomass resources in Norway. While much of the agricultural residues such as straws, husks and grasses are used for animal feed a proportion of underutilized leftovers and side streams are still remained unused. However, it will always take energy to grow and harvest the biomass as well as processing and distributing the biofuels. In order to make the best possible use of the available biomass sources, the transport fuel industries should incorporate their technologies into today's Norwegian forestry and agricultural industries. Both agriculture and forestry generate large amounts of residues, waste products and by-products that are suitable for energy utilization through biomass-to-liquid transport fuel technologies. These technologies have the benefit to make use of the whole plant growth, rather than just the plant starches or sugars that are used for 1st generation biofuels. In this way, low-quality, low-cost and abundantly available biomass such as residues and wastes from agricultural and forestry sectors have great potential to supply significant shares for advanced biofuel production [18].

2.2 Biomass gasification

The biomass gasification process includes a set of complex thermochemical processes, which break the bonds of the organic materials and reform the intermediates into solids, liquids and an energy-rich producer gas [28]. The process involves pyrolysis and partial oxidation in a well-controlled oxidizing environment. The aim is to convert the biomass into a syngas by supplying a restricted amount of oxygen. The syngas is defined as the producer gas in which the main components is CO and H_2. However, CO_2 and gaseous H_2O as well as trace amounts of CH_4 and N_2 may also be present in the syngas [12, 19]. The generated syngas can be used directly as a fuel source for electricity and heat production, or it can be further processed into useful chemical feedstock and biofuels [12, 15].

A sequence of overlapping processes take place in the gasifier, these include drying, pyrolysis, combustion and gasification [1, 28]. Drying refers to the process by which the moisture content in the biomass is converted to water vapour. Pyrolysis involves thermal degradation in the absence of oxygen, where the dried biomass decomposes into solid carbon (char), long-chain liquid hydrocarbons (tars) and small fractions of a gaseous mixture. The combustion and gasification reactions include oxidation and partial-oxidation of the remaining char into heat and syngas. The heat produced from the combustion reactions provides most of the energy required to drive the endothermic gasification reactions. The by-products from the entire gasification process are tar and ash [1, 29, 30]. Figure 2-1 illustrates the overlapping stages in a general biomass gasification process.

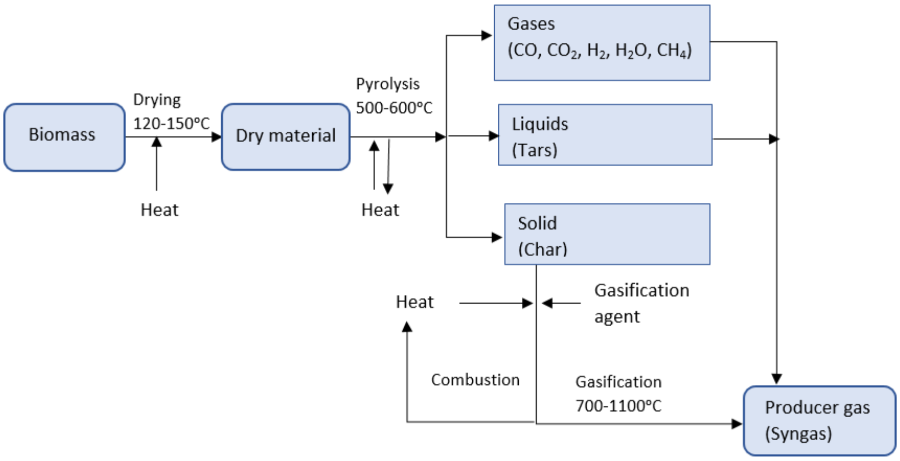
Gases
(CO, CO_2, H_2, H_2O, CH_4)
Biomass
Drying
120-150°C
Dry material
Pyrolysis
500-600°C
Liquids
(Tars)
Heat
Heat
Solid
(Char)
Heat
Gasification
agent
Combustion
Gasification
700-1100°C
Producer gas
(Syngas)

Figure 2-1. Shematic overwiev of a general biomass gasification process.

The overall biomass gasification efficiency is most likely addressed by the char conversion and the fraction of CO, H_2, CO_2, CH_4 and tar in the syngas, as well as the ratio between H_2 and CO [23]. The syngas composition depends on the biomass source and the operating process conditions such as the process temperature and the equivalence ratio. Furthermore, the choice of gasifying agent will affect the producer gas quality by controlling its heating value [31]. The gasifying agents are usually either air, pure O_2, steam, CO_2 or a mixture of these. Air is cheap and widely used as gasifying agent, but the high amount of N_2 in the air produces a dilute producer gas with low heating value. By using pure O_2 instead, a more concentrated producer gas with increased heating value is obtained. However, the operating costs by use of pure O_2 as gasifying agent are high due to the production of the O_2. Both CO_2 and steam gasification produces an almost inert-free (N_2-free) producer gas with high heating value. While steam gasification typically results in high fraction of H_2 in the producer gas, CO_2 (with a catalyst (Ni/Al)) can increase the H_2 and CO content by converting the char, tar and CH_4. Both steam and CO_2 require an external heating source for the endothermic reactions [1, 15, 31, 32].

The gasification technology has several alternatives to offer. Based on their mode of operation, three different gasifiers are currently available for processing biomass, namely fixed bed, fluidized bed and entrained flow gasifiers. The entrained-flow gasifiers are suitable for finely ground particles and large-capacity units (50-1000 MW). These gasifiers operate at very high temperature (1200 - 1500°C) and pressure (20 - 70 bar), and have the benefit of eliminating tar and condensable gases in the product gas. An important aspect in the design of entrained flow gasifiers is that the molten ash forms a glassy slag, which easily can be removed from the bottom of the reactor [12, 28, 32]. The fixed bed gasifiers are relatively inexpensive, easy to operate and are suitable for small and medium units (< 10 MW). These gasifiers typically produce a producer gas with a significant amount of CH_4, as well as high content of tar and/or unprocessed char due to the poor mixing and non-uniform heat transfer [15]. The fluidized bed gasifiers are appropriate for intermediate units (5 – 100 MW), and are more complicated than the fixed bed and more flexible than the entrained flow gasifiers. They operate at low temperatures (typically 700-1000°C) to avoid ash melting that can cause severe operational challenges [12, 15, 20, 28]. This work focuses on fluidized bed systems, and thus following a brief description of the main principles of the fluidized bed technology.

The advantages with the fluidized bed gasification systems have been widely studied and reported by several researchers [1, 15, 33]. These systems are well known for their uniform temperature distribution, high heat and mass transfer and excellent overall process efficiency [1, 15]. The fluidized beds consist of bed particles that are kept in a fluidized state by passing a proper gasifying medium through at a sufficient velocity [30]. Since moving particles transfer heat much more efficient than the fluid alone, the bed material acts as a heat transfer and storage medium providing the fluidized beds to operate under nearly isothermal conditions. Even for the most extreme exothermic reactions the fluidized beds are able to maintain an isothermal profile within a few degrees [10]. When the biomass enters the gasifier, it quickly mixes with the bed particles providing the drying and the pyrolysis to proceed immediately. Further tar-conversion and gasification reactions occur in the gas phase, while the remaining char is partially oxidized inside the bed [29]. The combination of intense mixing and bed material with large thermal capacity, ensure good distribution of fuel across the cross-section of the reactor and allow the fluidized beds to handle a wide range of biomasses [13]. These systems use back-mixing which leads to the efficient mixing between the biomass particles entering the gasifier and the particles already undergoing gasification [1]. The choice of bed material will influence on the optimization of the gasification process. The most commonly used bed material for fluidized bed systems are quartz sand (SiO_2) and olivine (Fe_2^+,$Mg_2^+(SiO_2)$). Quartz is the cheap alternative. The quartz sand is considered inert within the systems and does not have any influence on the quality of the produced gas. Olivine has the advantage of being chemical active and can improve both the gas composition and the rate of fuel conversion. Unfortunately, olivine contains heavy metals (Ni and Cr) which after use need to be disposed in line with environmental protection laws, which entails an additional cost. Other common catalytically active bed materials are dolomite ($CaMg(CO_3)_2$), calcite ($CaCO_3$), alumina (Al_2O_3), magnesite ($MgCO_3$) and feldspar ($KAlSi_3O_8$ – $NaAlSi_3O_8$ – $CaAl_2Si_2O_8$). However, each of these alternatives contribute a higher operating cost compared to quartz [1, 23, 34].

The fluidized beds are classified into two main types, bubbling fluidized bed (BFB) and circulating fluidized bed (CFB), that are illustrated in Figure 2-2 [12]. The major difference between the two fluidized bed systems is the velocity of the gasifying medium. BFB gasifiers are generally designed to operate at low velocity, typically below

1 m/s, so that the fluidized bed particles remain in the lower furnace. In a CFB, the velocity is higher (in the range 3-10 m/s) resulting in the hot particles circulating between the reactor vessel and a cyclone separator [28]. In this PhD-work, only the bubbling fluidized bed system has been studied.

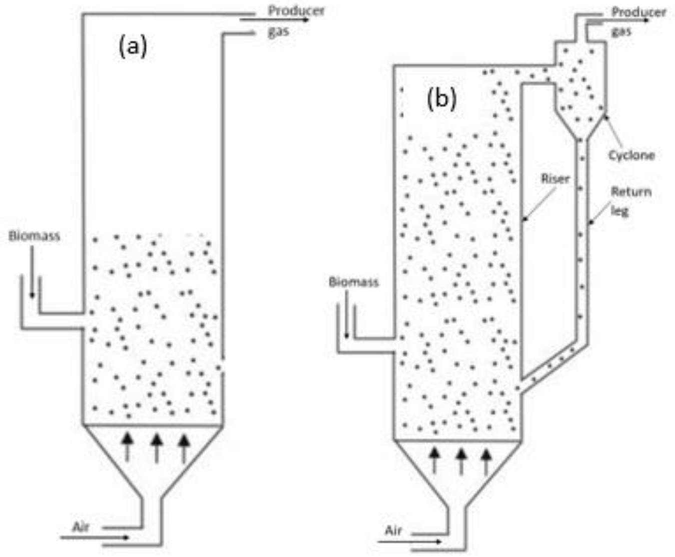

Figure 2-2. Schematic of (a) bubbling fluidized bed and (b) circulation fluidized bed.

2.3 Fluidization

Fluidization is the phenomenon in which particles are moved by an upward-flowing fluid that passes through a bed of particles (the fluidized bed) [35-37]. The fluid can be either gas or liquid. However, this work is solely focusing on gas-particle fluidization.

When the gas passes through the bed of particles, frictional forces (drag) from the gas act on the particles. At low superficial gas velocities, the drag is too weak to move the particles and the gas flows straight through the void spaces in the bed. In this regime, the particles remain stationary in a fixed bed. As the superficial gas velocity increases, the drag increases until the bed reaches a point where the gas fully suspends the particles in a fluidized bed. In this regime, the bed of particles acts like a boiling liquid where the particles move apart and float around. This fluid-like behaviour provides good gas-particle mixing as well as efficient heat and mass transfer rates, promoting uniform temperature distribution throughout all sections in the bed [33, 38]. The superficial gas velocity at which this phenomenon occurs is called the minimum fluidization velocity

(u_{mf}). Now, even with further increase in the superficial gas velocity, the bed pressure drop remains constant due to the upward drag being balanced by the weight of the suspended particles according to the following equation [38-40]:

$$\frac{\Delta p}{L} = \frac{m_p}{L} = g(1 - \varepsilon_{mf})(\rho_p - \rho_g) \tag{1}$$

where $(\frac{\Delta p}{L})$ is the pressure drop per unit length trough any section of the bed. ε_{mf} refers to the void fraction at minimum fluidization, ρ_g and ρ_p are the density of the gas and the particles respectively and m_p refers to the weight of the particles.

The minimum fluidization velocity is a useful indicator for the transition between fixed and fluidized bed conditions, and is thus a key parameter in process optimization of any fluidized bed. The minimum fluidization velocity can be found experimentally or theoretically. Experimentally, the minimum fluidization velocity is determined by reading the pressure drop in the bed at increasing superficial gas velocity. The results are plotted in a curve similar to Figure 2-3. The minimum fluidization velocity is detected as the exact point where the bed is transferred from a fixed to a fluidized regime. Once fluidization is achieved, the pressure drop flattens out and stabilizes as it is balanced by the total weight exerted by the particles [38, 39, 41].

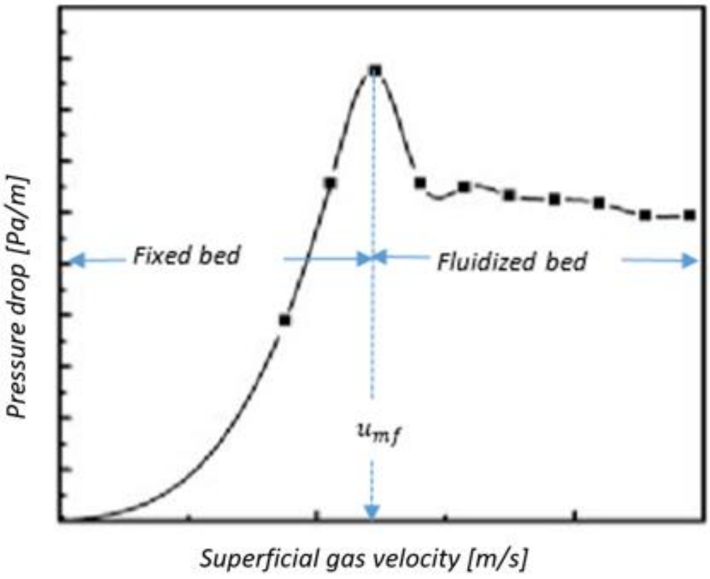

Figure 2-3. Pressure drop versus minimum fluidization velocity. Based on [41].

Theoretically, the minimum fluidization velocity can be determined by means of mathematical expressions (drag models). A number of drag models exist, which all provide approximations of the behaviour of a defined fluidized bed system. Common to all drag models are that they are sensitive to changes in flow conditions, and by that closely related to the bed porosity (ε) and the particles Reynolds number (Re) [42]. One of the frequently used drag models is the Ergun equation, which expresses the pressure drop characteristics as a function of the superficial gas velocity in packed beds according to [43]:

$$\frac{\Delta p}{L} = \frac{150 u_0 \mu_g (1-\varepsilon)^2}{\varepsilon^3 d_p^2} + \frac{1.75 \rho_g u_0^2 (1-\varepsilon)}{\varepsilon^3 d_p} \tag{2}$$

where d_p is the particles diameter, ε is the bed porosity, μ_g is gas viscosity and u_0 refers to the superficial gas velocity.

The Ergun equation is controlled by the particle volume fraction, and is based on a set of experimental observations covering a wide range of particle size and shapes [43]. The equation combines the terms for laminar and turbulent flow, and shows therefore good approximations for the bed pressure drop for both flow conditions, as well as the transient region [43]. By combining Equation (1) and Equation (2), the mathematical expression for the bed conditions at minimum fluidization takes the form [40]:

$$\underbrace{g(1-\varepsilon_{mf})(\rho_p-\rho_g)}_{\textit{Weight of particles}} = 150\underbrace{\frac{u_{mf}\mu_g}{(\varphi_p d_p)^2}\cdot\frac{(1-\varepsilon_{mf})^2}{\varepsilon_{mf}^3}+1.75\frac{\rho_g u_{mf}^2}{\varphi_p d_p}\cdot\frac{(1-\varepsilon_{mf})}{\varepsilon_{mf}^3}}_{\textit{Ergun equation/Drag by upward moving gas}} \tag{3}$$

Where u_{mf} is the minimum fluidization velocity and φ_p the particles sphericity.

In laminar flows, the gas density is unaffected by the drag and thus the drag shows a linearly dependency on the superficial gas velocity. The pressure drop in this region is approximated by the first term in the Ergun equation, while the second term can be ignored. In turbulent flow, the velocity drag kicks in and the second term of the Ergun equation dominates the flow conditions. In this region, the pressure drop increases with the square of the superficial gas velocity and the first term of the equation can be eliminated. For fluidized bed systems with small d_p, small ε_{mf} ($\varepsilon_{mf} < 0.5$) and low Reynold's number ($Re_{mf} < 20$), simplifications and rearrangement of Equation (3) gives the following equation for prediction of the minimum fluidization velocity [40]:

$$u_{mf} = \frac{d_p^2(\rho_p - \rho_g)g}{150\mu_g} \cdot \frac{\varepsilon_{mf}^3 \varphi_p^2}{1 - \varepsilon_{mf}} \tag{4}$$

Reynold's number at minimum fluidization is defined as:

$$Re_{mf} = \frac{\rho_g u_{mf} d_p}{\mu_g} \tag{5}$$

2.4 Ash related challenges in fluidized bed systems during biomass gasification

Ash related challenges have occurred in furnaces and boilers as long as solid fuels have been used for energy conversion. The problems have been studied for years, but most of the research within this field are related to coal. The growing interest in the use of climate-friendly and renewable alternatives to fossil fuels such as biomass, has introduced new kind of availability problems. Only a limited part of the coal-based research can be used for biomass, and there is still a need for expanded technical research within this field [44].

2.4.1 Bed agglomeration

During biomass gasification processes, high temperatures are preferred in order to increase the carbon conversion and reduce the amount of undesirable tar and other by-products. However, due to large fraction of alkali elements in the biomass ash, high process temperatures may lead to severe ash related problems in fluidized bed systems. These problems are generally associated with molten ash particles, which increase the risk for slagging, fouling and bed agglomeration [34, 44-47]. Slagging involves the creation of ash deposits on the surfaces of the reactor equipment and occurs mainly in the zones of the reactor that are directly exposed to flame irradiation. Fouling involves condensation and deposition of the tar, char and ash in the convective zones of the reactor [48]. Special attention has to be given to bed agglomeration, which can lead to fluidization problems causing operational challenges and reduced availabilities for the gasification plants. The process involves the growth of bigger particles (agglomerates) due to interactions between the ash-forming elements and the bed material [49]. The particle growth is highly coupled to the high temperature chemistry of the biomass ash, and is proven especially problematic when Si-based bed material is used [14, 34, 44, 45]. Visser et al. [50] described two key mechanisms responsible for agglomeration in fluidized beds, coating-induced agglomeration and melting-induced agglomeration. In both mechanisms, ash-melting behaviour plays an important role. Most dominant among the mechanisms is the coating-induced agglomeration. The coating-induced mechanism is initiated by chemical reactions between alkali-species from the biomass ash and Si from the bed material. When biomass ash particles deposit and melt on the surfaces of the bed particles, a sticky alkali-silica ash-layer will form and result in growth of agglomerates upon collision with other ash-coated bed particles [34, 51-55]. In some cases, especially when the biomass has high relative content of Si and K, melting-induced agglomeration can occur. Melting-induced agglomeration happens when the alkali-rich biomass ash melts without prior deposition and react with Si from the ash particles itself, before melting together with the bed material. In these cases, the agglomeration process is initiated by formation of low-melting alkali-silicates, which form hard bridges that glue the colliding bed particles together [14, 52, 56-58]. Under certain circumstances, a combination of these two mechanisms has been present. Figure 2-4 illustrates the two agglomeration mechanisms.

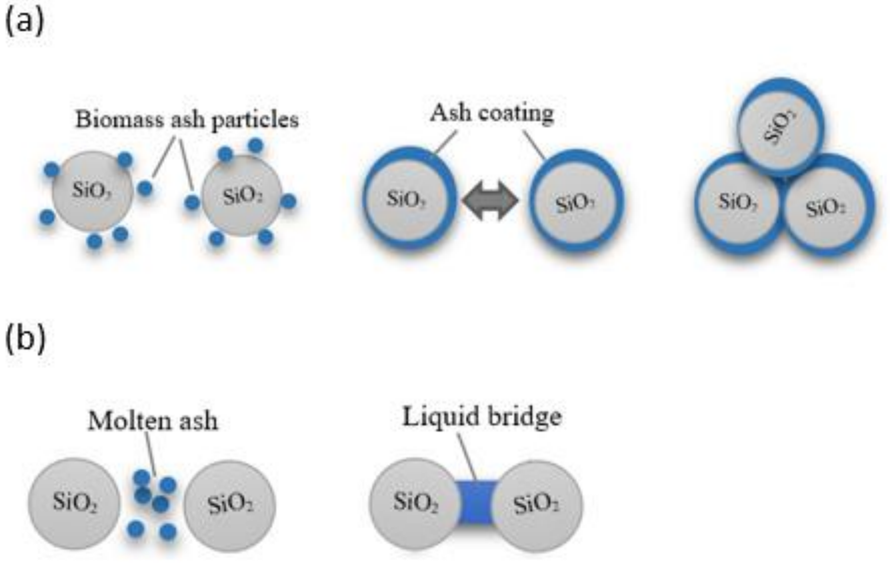

Figure 2-4. Coating-induced (a.) and melting-induced (b) agglomeration mechanism. Based on [50].

The ash melting behaviour is strongly dependent on the composition and concentration of the inorganic ash forming elements that are stored in enzymes, cell walls and membrane structures in the biomass. This means that the biomass ash composition varies widely between the different biomass types, as well as among species from the same biomass (depending on their stage of growth and their location) and within specific parts of the biomass (twigs, shoots, seeds etc.) [28, 45]. For example, young trees typically tend to have higher ash content than mature trees. In addition, agricultural biomass that die at the end of the growing season will generally have a higher ash content than forestry biomass, which is build up over years [14, 46, 59, 60]. Woody ashes typically have relatively large amounts of the alkali earth metals such as Ca and Mg and to a minor extent of K, compared to ashes from the agriculture that have a more diverse composition. Furthermore, straw ash tends to have relatively large fraction of Si and alkali metals such as K and Na, while other agricultural species can have large amounts of P, K or Mg depending on whether it is derived from seeds, grasses, shells or husks [61-64]. Although many studies have been conducted to gain more insight into the high-temperature ash chemistry of the biomass, the huge variations in the ash characteristics make it difficult to define a melting behaviour that applies to a general biomass ash [14, 23, 33, 34, 44]. Research focused on the various biomass resources has shown that the most critical ash forming elements leading to ash melting problems in fluidized beds are Ca, Mg, K, Na, Si and P [49, 58, 61, 65-67]. Once the organic materials in the biomass have been oxidized, the remaining mineral substances form oxides corresponding to the ash-forming elements. Due to their low ionization number (+1) in oxidized forms, the alkali metals are highly reactive and will preferably exist as gaseous compounds, which might condense in the colder areas of the reactor and then further interact with other ash-forming elements such as Si, Cl and S. The alkali earth metals, on the other hand, have high ionization numbers in oxidized forms and are preferably solid in all zones in the gasifier [65, 68].

Dzurenda & Pňakovič [69] and Vassilev et al. [62] have studied the major ash-forming elements and their impact on bed agglomeration in fluidized bed gasification processes. These studies concludes that the alkali earth elements Ca and Mg typically increase the ash-melting temperature, whereas Si, P and the alkali metals K and Na decrease the melting temperature. Vassilev et al. [62] also observed that the combination of high Si content and high K and/or Na (K(Na)) content are especially problematic for fluidized bed systems due to the formation of complex silicates (eutectics). These eutectics have structural formulas $K_2O{\cdot}nSiO_2$ and $Na_2O{\cdot}nSiO_2$ and are characterized by lower melting points than the individual components [40, 50]. For example, $K_2O{\cdot}2SiO_2$ is characterized with a melting point of 764°C and $Na_2O{\cdot}2SiO_2$ with a melting point of 874°C [70]. Other research studies associated with the critical elements in biomass ash came to the same conclusions, i.e. that biomass rich in K(Na) and Si(P) and low in Ca(Mg) typically give higher risk for bed agglomeration [34, 49, 71-73]. Furthermore, the same studies showed that biomass rich in K(Na) and Ca(Mg) and low in Si(P) favour the formation of oxides from Ca and Mg. CaO (s) and MgO (s) are less reactive oxides and are most likely to be released as fine particles during the gasification process. These particles will either flow out of the gasifier as a dry and non-sticky dust together with the producer gas (fly ash) or remain in the bed as bottom ash. High fraction of Ca(Mg) can outcompete K in the interaction with Si from the bed material and by that lower the risk for coating-induced agglomeration [49, 60, 71]. However, the portion of ash remaining in the bed decreases with less Ca(Mg) present, and thus the K/Ca ratio is decisive for the agglomeration tendency in these systems [49, 72]. On the other hand, high Si(P) in the biomass will always provide a risk for increased agglomeration tendency due to the condensed K-component interacting with Si from the biomass itself, causing a higher risk for melting-induced agglomeration. [59, 70].

Some of the ash forming elements that can contribute to reduced risk for agglomeration are Fe and Al. These elements can readily react with the alkali elements to form chemical compounds with increased melting point, for example $X_2Fe_2O_4$ (melting temperatures typically around 1135°C) and K_2O-Al_2O_3-SiO_2 (melting temperatures typically around 1800°C)) [45, 70, 74].

2.4.2 De-fluidization

One of the major challenges with bed agglomeration in fluidized bed processes is the issue of de-fluidization caused by sudden changes in the fluidization characteristics, i.e. the minimum fluidization velocity, the bubble size and the bubble frequency [75]. In such cases, the fluidized bed experiences flow disturbances that, without adjusting the operating bed parameters, make it difficult to maintain a smooth bubbling fluidized bed regime. The bed disturbances are represented by unevenly distributed bubble activity and/or by obstructed gas-flow leading to formation of gas channels in the bed [45, 58, 74].The de-fluidization phenomenon is illustrated in Figure 2-5.

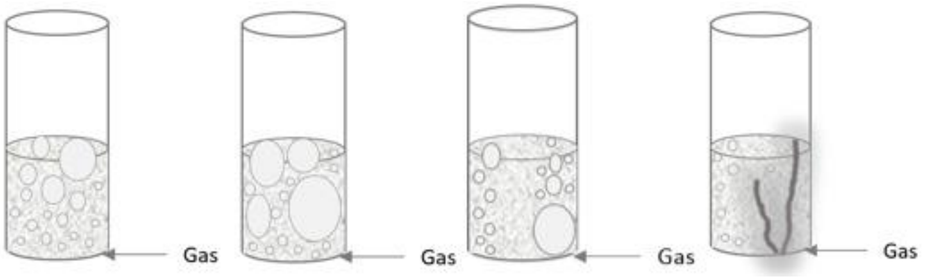

Figure 2-5. Comparison of smooth bubbling regime and de-fluidized regimes with uneven bubble distribution and channelling of gas.

In a study conducted by Montes et al. [76], the bubble activity was compared by measuring the bubble frequency in the different sections of normal and agglomerated fluidized beds. The study concluded that the bubbles were evenly distributed throughout the bed during normal fluidization. Agglomerated fluidization formed gas channels and de-fluidized zones where little or no bubble activity was detected.

Additional observations were that the agglomerated fluidized bed conditions experienced a rapid decrease in the bed pressure drop at the onset of de-fluidization [76]. Many research studies have showed that bed agglomeration leads to poor fluidization conditions, where large fractions of the hot gas flows straight through the bed in channels causing inefficient gas-particle mixing and reduced heat and mass transfer rates [50, 70, 74, 75, 77]. The point of de-fluidization is typically recognized by large fluctuations in the bed pressure drop, and subsequently loss of control of the important bed operating parameters. The agglomerates consist of numerous bed particles clustered together and appear in a large variety of shapes and size, as seen in Figure 2-6. In general, systems with larger particle sizes, irregularly shaped particles or heavy particles will require increased superficial velocity in order to achieve the efficient gas-particle mixing. For agglomerated fluidized beds the minimum fluidization velocity is no longer able to follow the theoretical value calculated by the initial drag equation [74]. If not counteracted, the consequence is a complete de-fluidization of the bed followed by total shutdown of the whole installation [50, 70, 75, 77].

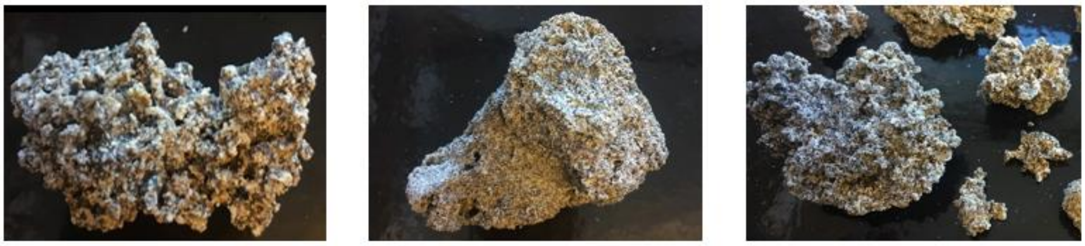

Figure 2-6. Agglomerated particles from biomass ash and silica sand particles formed during bubbling fluidized bed biomass gasification.

3 Materials and methods

This chapter provides descriptions of the materials, the experimental setups and the analytical and computational methods included in this work. Three different experimental setups were used for fluidization and agglomeration tests: (I) a cold flow model of a bubbling fluidized bed (CBFB), (II) a 20 kW laboratory-scaled bubbling fluidized bed gasifier (BFBG), and (III) a micro-scaled model of a bubbling fluidized bed (MBFB). All setups are located at the University of South-Eastern Norway. In addition, various analytical techniques such as ash melting microscope for ash melting behaviour, laboratory sintering tests for ash sintering degree and SEM/EDS for structure and morphology analysis were performed.

3.1 Materials

3.1.1 Biomass

The different biomass samples were selected to cover a wide range of variations in ash content and composition of the ash forming elements. The biomass used represented forestry residues from wood and bark, originated from Norwegian conifers, and agricultural residues from grass and straw. The straw was from barley and the grass samples were a mix of timothy, lucerne and clover. The biomass samples were analysed by Eurofins Norway AS. All analyses were carried out according to standardized methods. In all four biomass ashes, the dominating elements were Si, K and Ca. The woody biomass was rich in Ca, and the bark was rich Si and Ca, while the straw was rich in K and the grass samples was rich in Si and K. Figure 3-1 presents the ash content and the major ash forming elements in the different types of biomass ash.

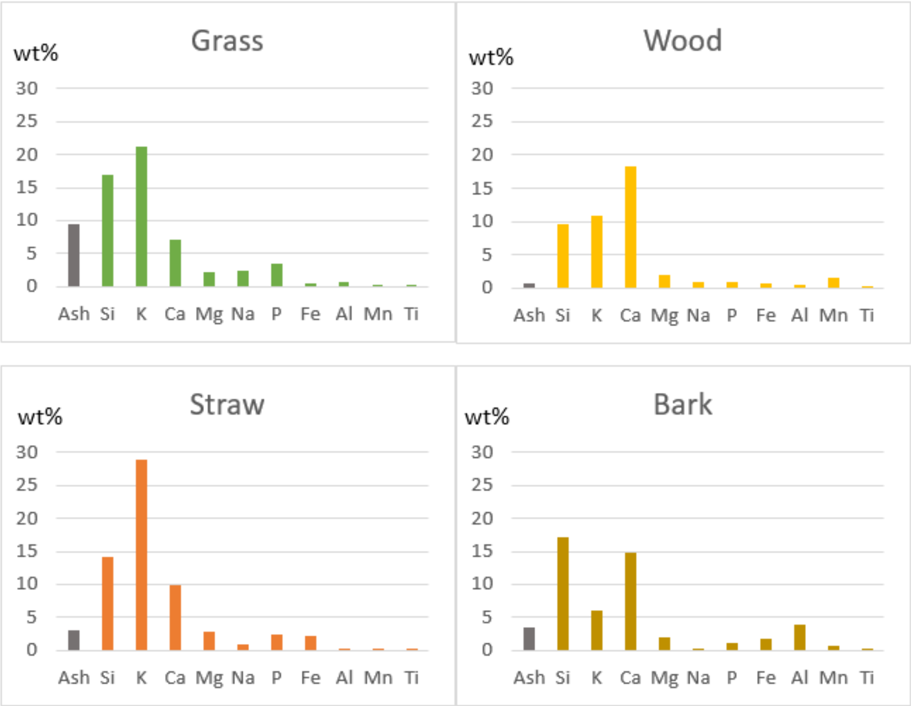

Figure 3-1. Ash content (black) and the compositions (wt % in ash) of the major ash forming elements for the grass, wood, straw and bark samples used in this study.

The experiments performed in the BFBG were carried out using pelletized wood and grass as feedstock. The pellets were sized with a length of 5 to 20 mm and a diameter of approximately 0.6 mm. The MBFB experiments used laboratory prepared ash samples from wood, bark, barley straw and grass. The biomass samples were grinded and ashed in a muffle furnace at 550°C.

3.1.2 Bed material

For all experiments, quartz with a solid particle density of 2650 kg/m^3 was used as bed material. The size of the sand particles varied in the different experiments, ranging from 175 µm to 600 µm. Prior to all the experiments, the particle size distribution was determined based on sieving analysis. The properties of the bed material are listed in Table 3-1.

Table 3-1. Properties and chemical composition (wt %) of bed material.

Sand	**Density [kg/m^3]**	**Particle size [µm]**	**Sphericity [-]**	**Shape [-]**	**SiO_2**	**Al_2O_3**	**K_2O**	**Na_2O**	**CaO**	**Fe_2O_3**	**MgO**	**TiO_2**
Quartz	2650	200-600	0.86	Angular	83.6	7.8	2.5	2.3	1.5	1.5	0.5	0.2

3.2 Experimental setups

3.2.1 Cold flow bubbling fluidized bed

The cold flow bubbling fluidized bed (CBFB) model was used to study the fluidization characteristics in the fluidized bed under different flow conditions. This setup was easy to control, and due to the cold operating environment, it was possible to add agglomerates and thus register how the agglomerated particles affected the important operating bed parameters, i.e. the minimum fluidization velocity (u_{mf}) and the bed pressure drop ($\Delta p/L$).

Figure 3-2 shows the CBFB system. The column is constructed with a transparent material and has a diameter of 8.4 cm and a height of 140 cm. The gasifying medium is compressed air at ambient temperature. The air flows into the column through a porous plate, which ensures even air distribution throughout the bed. Sierra mass-flow controllers are used to accurately adjust the airflow. Nine pressure transducers along the height of the column are constantly monitoring the pressure drop across the bed. The first pressure transducer is located 3.5 cm below the gas distributor and the second transducer is located 6.5 cm above the gas distributor. The distance between the each of the pressure transducers is 10 cm. The pressure transducers are connected to the LabVIEW software for data acquisition. The top of the column is open to the atmosphere.

The minimum fluidization velocity for the bed material in each experiment was determined based on the measured bed pressure drop at the selected superficial air velocities. The results were used for validation of CPFD models, which can simulate the flow behaviour in any bubbling fluidized bed.

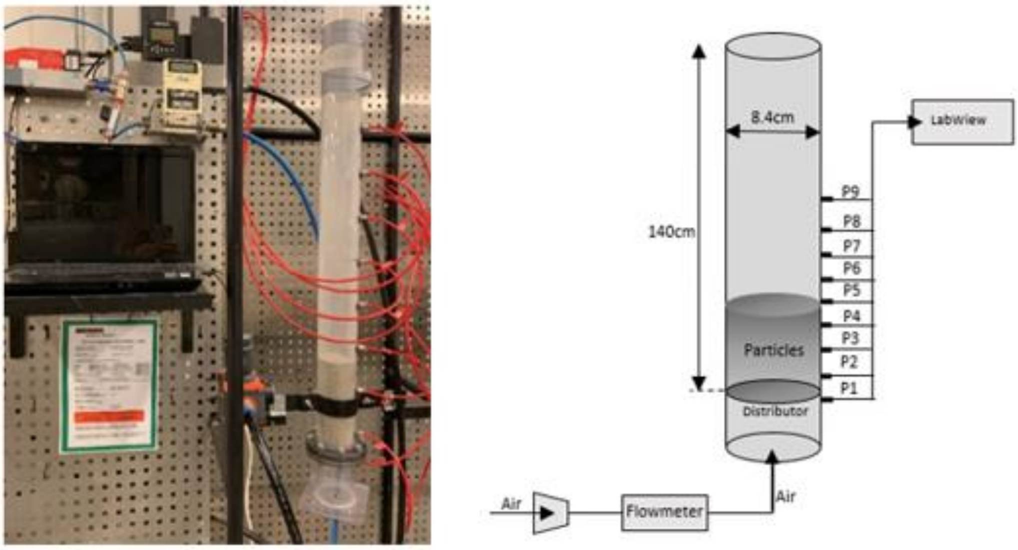

Figure 3-2. Cold flow model of a bubbling fluidized bed gasifier (CBFB).

3.2.2 Laboratory scale 20 kW bubbling fluidized bed gasifier

The bubbling fluidized bed gasifier (BFBG) model was used to study the fluidization characteristics under different hot flow conditions. By using the hot flow setup, it was possible to provoke the formation of agglomerates and with this examine the agglomeration tendency for different types of biomass. The flow behaviour and the agglomeration tendency were studied for three separate works: (I) Study of the bed conditions in agglomerated fluidized bed processes (II) study and comparison of agglomeration tendency for different types of biomass, and (III) study of agglomeration tendency for fluidized bed processes with different particle size of the bed material.

Figure 3-3 shows the 20 kW BFBG system. The gasification reactor is a cylindrical column built in stainless steel, insulated with a refractory material on the inside and a 200 mm thick fiberglass layer on the outside to minimize the heat losses. The inner diameter of the reactor is 10 cm and the height is 1.3 m. The gasifying medium is preheated air that flows into the gasifier through two 10 mm steel pipes placed 27.5 mm from the bottom of the reactor. The air mass flow rate is controlled with a Brook air flowmeter. A screw conveyor installed 21.2 cm above the air inlet, ensures a steady supply of biomass to the process. The BFBG is typically operated with temperatures ranging between 700°C and 900°C. Three electrical heating elements are coiled around the wall of the reactor and are used for external heating of the gasification process. The gasifier is heated to 400°C by the external heating source. Additional heating is obtained from the heat released from the combustion of the biomass. Five thermocouples and five pressure transducers placed along the height of the column are continuously monitoring the operating bed conditions. The distance between the temperature and pressure sensors are 10 cm, whereas the first sensor is at the same level as the air supply. Each pressure transducer measures the gauge pressure, i.e. the air pressure in excess of the atmospheric pressure, in the given position. The temperature and pressure sensors are connected to the LabWiew software for data acquisition. The producer gas leaves the reactor from the top.

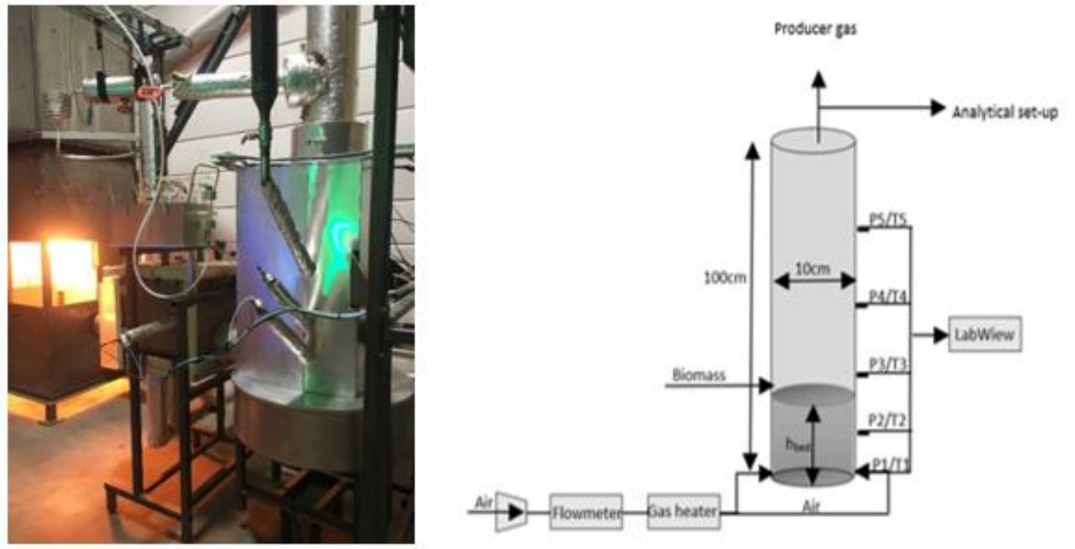

Figure 3-3. 20 kW bubbling fluidized bed gasification (BFBG).

The remaining bed particles, ash and any agglomerates were removed from the gasifier after each of the test runs. According to the different types of biomass and the relevant bed conditions, the morphologies and structures of the agglomerates were compared and examined. The results were combined with CPFD modelling in order to simulate the effect of bed agglomeration on bed de-fluidization, as well as to predict the critical amount of agglomerates in the bed.

3.2.3 Micro-scale fluidized bed reactor

The micro-scale fluidized bed (MBFB) model was designed to determine the onset of de-fluidization and the agglomeration tendency for different biomass ashes. The MBFB maintains stable operating conditions and provides relatively fast and flexible test runs for controlled bed agglomeration processes.

Figure 3-4 shows the MBFB system. The fluidized bed is a cylindrical column built in transparent quartz glass with an inner diameter of 43.6 mm and height 150 mm. The gasifying medium is air that flows in 7 mm thick pipe and enters the bed from the bottom of the column. The top of the bed is open to the atmosphere. The air flowrate is controlled with a Sierra mass-flow controller and flows into the bed through a 5 mm thick sintered disc distributor. The MBFB is placed in a Nabertherm muffle furnace to ensure stable and controllable temperature conditions in the bed. The muffle furnace is equipped with a quartz glass observation window that allows the user to see inside the chamber without disturbing the ongoing process. The experiments were carried out at temperatures of 700°C, 800°C, 850°C, 900°C, 950°C and 1000°C. The bed conditions were continuously observed throughout the experiments. The results were based on visual observations of changes in the fluidized conditions in the bed under different operating temperatures.

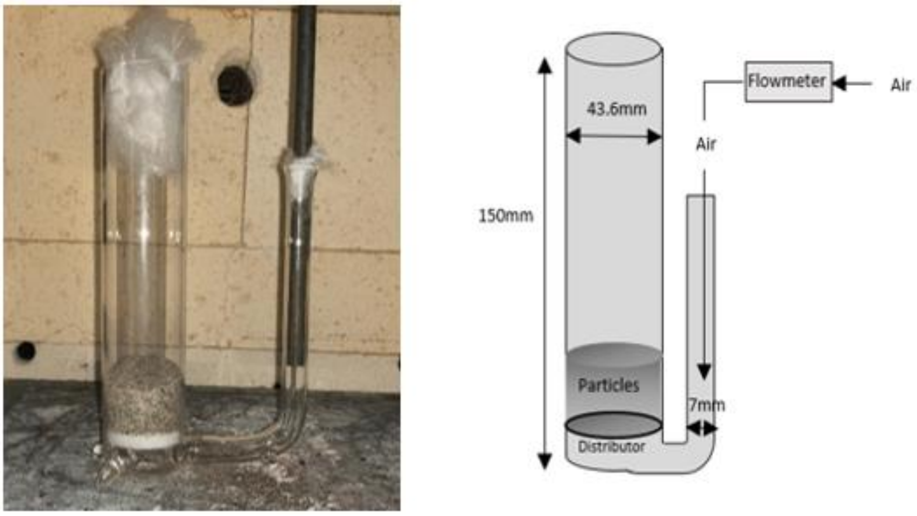

Figure 3-4. Micro-scaled fluidized bed reactor (MBFB).

The amount of accumulated ash in the bed was measured at the time of de-fluidization. The observations gave a multiple variable data set that formed the basis for a mathematical model for accurate predictions of de-fluidization and bed agglomeration for different types of biomass. Any agglomerates formed during the experiments were collected and examined with respect to their structural composition.

3.3 Analytical methods

3.3.1 Ash melting analyses

Ash melting analyses were carried out to provide indications of the ash melting temperatures for the different types of biomass. Two different ash melting microscopes have been used to determine the high temperature ash characteristic: Leco Ash Fusion Determinator AF700 and Hesse Heating Microscope EM201-15 with image analysis. The instruments have different design, but the principles of determination of the ash melting behaviour are quite similar. Figure 3-5 illustrates a schematic of the principles of the ash melting microscopy analysis. The ash melting behaviour is determined according to the international standards DIN CEN/TS 15730-1:2006 (analyses performed in the EM201) and ASTM D1857 (analyses performed in the AF700). The measurements are based on a thermo-optical analysis where a cylindrical ash test piece with specified dimensions is heated in a small tube furnace, at a defined heating rate. The analyses are mainly focusing on the geometric shapes and the volume change of the cylindrical ash test piece at four characteristic temperatures.

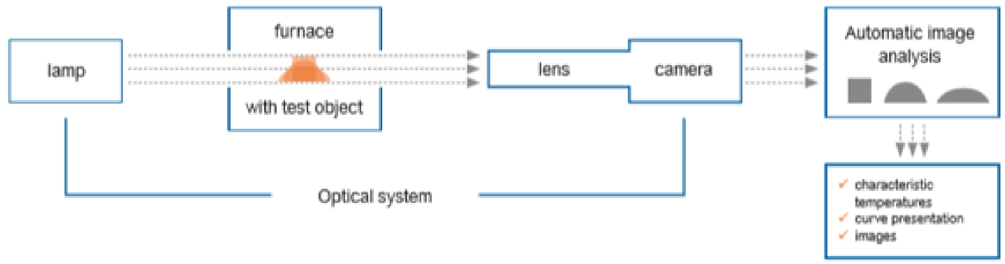

Figure 3-5. Principle schematic of determination of ash melting behaviour [78].

The four characteristic temperatures that describe the melting behaviour of the ash are presented in Figure 3-6 [78]. The ash melting behaviour was useful for the temperature settings in the experimental agglomeration and de-fluidization tests, as well as for the CPFD simulations.

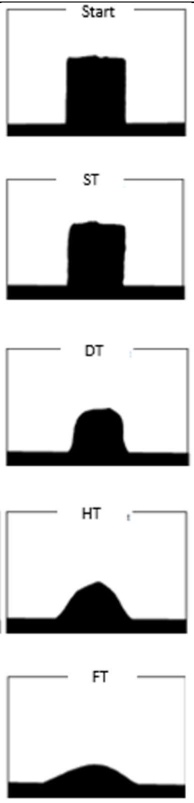

Shrinking starting temperature (ST):
Initial deformation.
First sign of shrinking of the cylinder.

Deformation temperature (DT):
Spherical appearance with original sample height.
First sign of rounding due to melting of the corners of the cylinder.
DT is often identified as the ash fusion temperature.

Hemispherical temperature (HT):
The cylindrical test piece forms a hemisphere with half the original sample weight.

Flow temperature (FT):
The cylindrical test piece has effectively melted and ash is spread over the tile in a layer.

Figure 3-6. Ash melting analysis of biomass ash from wood, performed in AF700.

3.3.2 Ash sintering degree tests

Laboratory sintering tests were carried out to study the sintering degree of the different biomass ashes. The chosen procedure was to heat the laboratory prepared ash samples in a muffle furnace at selected temperatures. Accurately 0.1000 g of the ash sample was transferred to an open alumina crucibles and placed in the preheated muffle furnace for 1 hour. The selected temperatures used for the sintering degree tests were 700°C, 800°C, 900°C, 1000°C, 1100°C and 1200°C. After heating, the weight loss was measured and the sintering degree of the ash residues remaining in the crucibles was evaluated. The evaluation was based on visual inspection of changes in the microstructure of the remaining ash samples. Any sintering of ash particles was detected as molten phases, either as spherical particles or as a shiny, glassy form. Five grades of sintering degrees were defined, as described in Table 3-2.

The ash sintering degree tests were used in combination with the ash melting analyses for prediction of the critical temperatures for the MBFB experiments. The remaining ash samples were examined by visual observations. The results from these observations are not published.

Table 3-2. Grades of sintering degree.

Sintering degree	Ash structure
0	Loose ash particles
1	Slightly sintered ash, porous and fragile structure that easily breaks
2	Sintered ash, partially melted ash particles
3	Hard sintered ash that does not break
4	Completely melted ash

3.3.3 SEM/EDS analyses

Scanning electron microscopy equipped with energy dispersive X-ray spectroscopy (SEM-EDS) was used to evaluate the morphology and elemental distribution of ash, bed material and agglomerates collected after the different experiments performed in the BFBG.

The equipment used was a Zeiss SUPRA 55-VP. The agglomerates were mounted on a carbon tape and directly scanned using the SEM. After scanning, the agglomerates were embedded in epoxy resin before being cut and polished for the SEM-EDS analyses of the cross-sectioned agglomerates. Backscattered images were taken from one sample to give a better view of the distribution of the chemical elements.

3.4 Modelling and simulations of ash melts and agglomeration in biomass fluidized bed processes

The data achieved from the experimental works together with the analytical results obtained from ash microscopy and ash sintering tests, were used for the computational studies. The CPFD software package Barracuda VR version 17.3.0 and 17.4.1, and Microsoft Excel 2016 were used to create the various prediction models.

3.4.1 CPFD simulations

CPFD is a powerful tool to help providing a realistic view inside a reactor. In this PhD-work, Barracuda VR was chosen as the CPFD platform for modelling and simulations of fluidization processes in bubbling fluidized beds. Barracuda VR is a commercial CPFD software package, specially designed for one single application: The Gas-Particle fluidized reactors. The software package is capable of modelling all fluid flows and all particulate-solid flows as well as thermal and chemically reacting behaviour inside fluidized reactors [79]. However, the producer gas composition and the gasification reactions are beyond the scope of this work. Reaction kinetics are not included in these simulations. The Barracuda software package includes several drag models. In order to find the most suitable model for the simulations, different drag models were tested during this work. Barracuda VR uses the three dimensional Multiphase Particle-in-Cell (3D-MP-PIC) based Eulerian-Lagrangian approach, where the Eulerian approach is used for solving the continuous fluid phase and the Lagrangian computational particle approach is used for solving the particle phase [80]. The output from the CPFD simulations are either 3D-model files or text-based data files. The 3D data provides insight into the flow behaviour in the bed, while the text-based data is useful for comparison with experimental data. The information and the data achieved from the fluidization experiments, the ash melting analyses and the agglomeration tests have been implemented in the work related to development and validation of the CPFD models.

3.4.2 Mathematical modelling

A mathematical model that can give approximate indications on the critical amount of ash in the bed during fluidized bed gasification of biomass was created. The chosen approach for the mathematical model was a multiple linear regression analysis, based on the experimental data sets obtained from the MBFB. The multiple regression analysis takes the number of independent variables into account at the same time, and can model the property of interest (the dependent variable) with a great precision. The dependent variable implemented in the regression model was the mass ratio of accumulated ash/bed material at de-fluidized bed conditions. The independent variables were the operation temperature and mass ratios of the major critical ash forming elements (Si/K and K/Ca). The regression coefficients were estimated using the method of least squares, which makes the sum of squared residuals a minimum. The residuals refer to the difference between the observed values and the predicted values of the accumulated ash/bed material ratio. With relatively small data sets, these coefficients are easy to calculate manually. In this study, however, the regression analysis was based on a larger data set. Thus, computing the least squares estimators relied on the use of matrix algebra. Microsoft Excel was used to model the linear relationship between the variables by fitting the observed data into a mathematical expression, but several other mathematical software could be applied for solving the matrix algebra.

The estimated regression model is reliable and valid as the key assumptions for multiple linear regression analysis were tested and proved to be true:

- There is a linear relationship between the dependent and the independent variables.
- There is a multivariate normality, meaning that the errors between the observed and the predicted variables are normally distributed.
- There is no multicollinearity in the data, meaning that there are no perfect or exact relationship between the independent variables.
- There is no homoscedasticity, meaning the error term is the same across all values of the independent variables.

The model describes a relationship between the accumulated ash in the bed at the onset of de-fluidization and the distribution of the major ash forming elements Si, K and Ca in the biomass.

3.5 Overview of research methods

The following delimitations and assumptions were made for this study:

- The experimental measurements are carried out with quartz sand as bed material. In terms of this research work, quarts sand has the advantage of being readily available and inexpensive.
- Grass, wood, straw and bark were investigated. The biomass samples were selected to represent a relatively broad area within Norwegian agriculture and forestry. However, the bark and straw samples caused mechanical challenges in the BFBG, as they tend to block the screw feeder. Therefore, these samples were not included in the BFBG experiments.
- Barracuda VR was used for the CPFD simulations. This software is very efficient and especially suitable for particle-gas simulations.
- The MBFB experiments were performed with relatively small bed particle size and a narrow particle size distribution. A small particle size was nesseccary to fit the size of the reactor, while a narrow particle size distribution prevented segregation of the bed particles.

The flow chart in Figure 3-7 shows a schematic overview of the research methods.

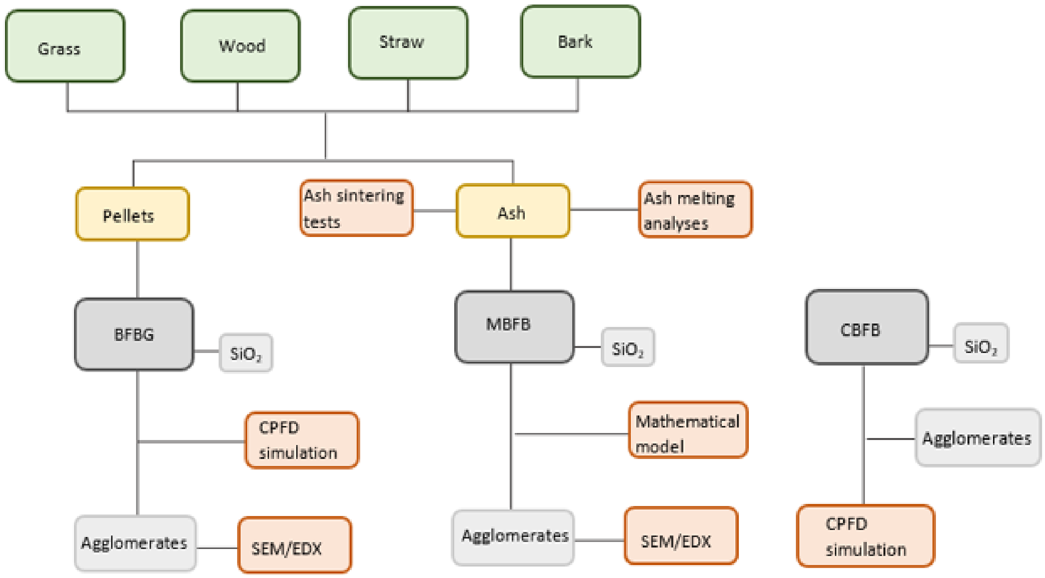
Grass
Wood
Straw
Bark
Pellets
Ash sintering tests
Ash
Ash melting analyses
BFBG
SiO₂
MBFB
SiO₂
CBFB
SiO₂
CPFD simulation
Mathematical model
Agglomerates
Agglomerates
SEM/EDX
Agglomerates
SEM/EDX
CPFD simulation

Figure 3-7. Overview of experimental and analytical studies carried out in the different experimental setups.

4 Summary of the papers

This chapter presents a summary of the scientific publications related to this study. The summaries highlight the methodologies and key findings of the theoretical and experimental results performed during this PhD-work. The papers are attached in Part 2.

4.1 Paper 1 - Flow behaviour in an agglomerated fluidized bed gasifier

This paper comprehensively discusses the challenges with bed agglomeration with respect to the flow behaviour in fluidized bed processes. Fluidization experiments were performed to compare the characteristics of normal fluidized bed conditions with agglomerated fluidized bed conditions. The experiments were carried out in the cold flow bubbling fluidized bed model. The flow conditions in three different cases were observed: (I) fluidization with only sand particles present in the fluidized bed, (II) fluidization with agglomerates located in the lower layer of the bed and (III) fluidization with agglomerates located in the upper layer of the bed. The agglomerates had been previously produced during gasification experiments of wood chips carried out in the 20 kW bubbling fluidized bed gasifier. Plots of the bed pressure drops vs the superficial air velocities for all the three experiments are shown in Figure 4-1.

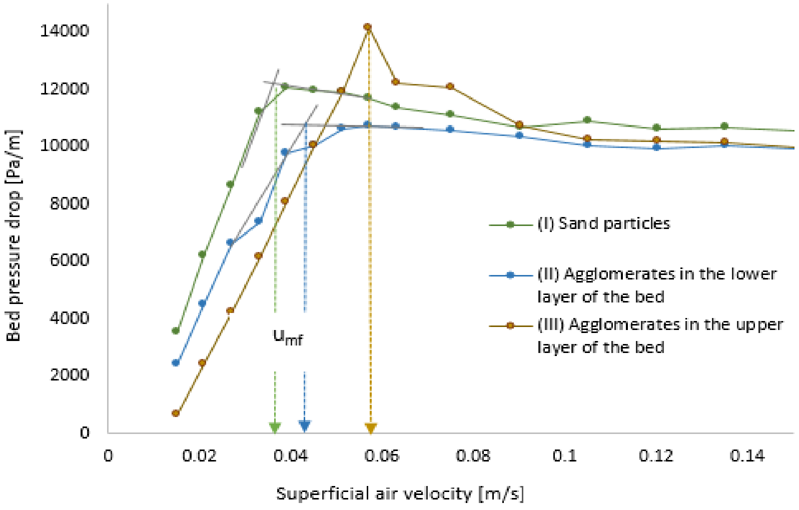

Figure 4-1. Experimental bed pressure drop vs superficial air velocity of fluidization in the cold flow bubbling fluidized bed model. u_{mf} indicates the minimum fluidization velocity.

The findings of this study reveal that in both of the agglomerated fluidization cases the bed pressure drop decreases and the minimum fluidization velocity (u_{mf}) increases, compared to the fluidization case where only sand particles are present. The agglomerates, which consist of a number of sand particles glued together by molten ash, are characterized by completely different physical properties than the original sand particles. They are larger in size, have a hollow surface, low sphericity and low particle density, all of which directly affect the operating bed parameters such as the pressure drop and the minimum fluidization velocity. Other findings made during this study are the visually observations of changes in the bubble distributions and activities in the different cases. While the normal fluidized bed condition shows well-distributed bubbling throughout the bed, both of the agglomerated cases experience disturbed fluidized bed conditions. These disturbances typically occur because the agglomerated particles tend to cause poor air distribution in specific zones of the bed, resulting in instabilities with uneven bubble distribution and/or channelling of air.

The results from this work are further used to develop and validate a CPFD model for investigation of the fluidization conditions of agglomerated beds. Additionally, the information received during the investigation of the flow behaviour and the associated bubbling regimes became useful in extended experimental studies related to de-fluidization due to ash melting and bed agglomeration in fluidized beds. Figure 4-2 presents a schematic overview of the way in which the results from this paper were useful to other studies related to this PhD-work.

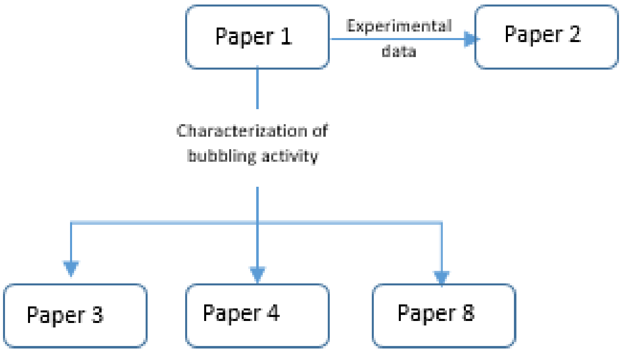

Figure 4-2. Schematic illustration of the link between Paper 1 and the works associated with Paper 2, 3, 4 and 8.

4.2 Paper 2 - CPFD model for prediction of flow behaviour in an agglomerated fluidized bed gasifier

In this paper, CPFD simulations are used to determine how the flow conditions are affected of bed agglomeration during fluidized bed processes. The commercial software package Barracuda VR, version 17.4.1, was applied for the CPFD modelling and simulations. The experimental data collected from the cold flow experiments presented in Paper 1 was used for development and validation of the CPFD model. The study compared the CPFD simulations for four different fluidization cases: (I) fluidization with only sand particles (II) fluidization with sand mixed with 5% by volume agglomerates (III) fluidization with sand mixed with 10% by volume agglomerates and (IV) fluidization with sand mixed with 15% by volume agglomerates. The simulated agglomerates were sized with a diameter from 0.5 to 1 cm, of which the limitations were set by the mesh size of the computational grid. Figure 4-3 shows the outputs from the CPFD simulations presented as plots of the pressure drops vs the superficial air velocities.

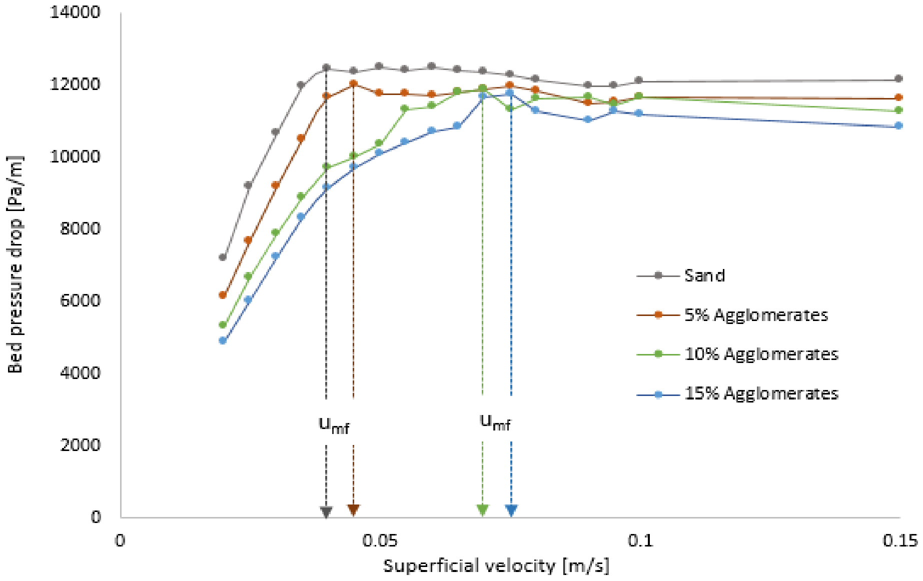

Figure 4-3. Simulated bed pressure drop vs superficvial air velocity of fluidization in the cold flow bubbling fluidized bed model. u_{mf} *indicates the minimum fluidization velocity.*

The verified CPFD model are used for simulations that predict the fluidized conditions in agglomerated fluidized bed processes. The simulated outputs from the different fluidization cases state that the agglomerates interfere with the fluidized bed conditions and consequently causes decreased bed pressure drop and increased minimum fluidization velocity. The experimental results presented in Paper 1 showed the same trend, which also support the validity of the developed CPFD model. Furthermore, CPFD simulations of the agglomerated fluidized conditions predict changes in the flow behaviour between the different cases. Notably, the minimum fluidization velocity increases with increasing amount of agglomerates. The results suggest that with 10% agglomerates by volume in the bed, the minimum fluidization velocity has almost doubled and the particles has already lost their ability to be fluidized by the initially defined superficial air velocity. With further bed agglomeration, the fluidized bed will eventually reach a critical point where complete de-fluidization is unavoidable. Table 4-1 presents the experimental and simulated values of the minimum fluidization velocities.

Table 4-1. Comparison of experimental and simulated minimum fluidization velocity.

Fluidization case	**Particle size [µm]**	**Agglomerate size [cm]**	**Minimum fluidization velocity [m/s]**
Experiment			
Sand	175	n/a	0.035
CPFD simulations			
(I) *Sand*	175	n/a	0.039
(II) *5% agglomerates*	175	0.5-1	0.045
(III) *10% agglomerates*	175	0.5-1	0.068
(IV) *15% agglomerates*	175	0.5-1	0.074

Snapshots taken of the particle distributions in the bed during the CPFD simulations show that the agglomerated particles are accumulated in the bottom layer of the bed, creating air channels and de-fluidized zones. Similar observations are made during the cold flow experiments, where the agglomerates prevent a proper fluidization of the particles. Figure 4-4 compares the post-process images of the particle distribution at (a) initial bed conditions and (b) fluidized conditions.

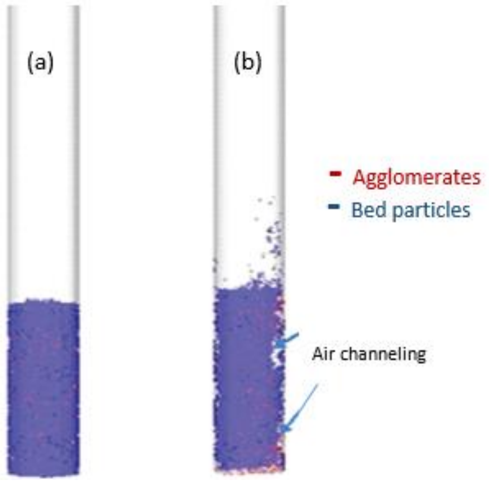
(a)
(b)
Agglomerates
Bed particles
Air channeling

Figure 4-4. Post process images of the simulation of particle distribution in the bed at (a) initial conditions and (b) fluidized conditions.

The developed CPFD model is used for further investigations of the fluidized and de-fluidized bed conditions during agglomerated bed processes. The link between the different studies are shown in Figure 4-5.

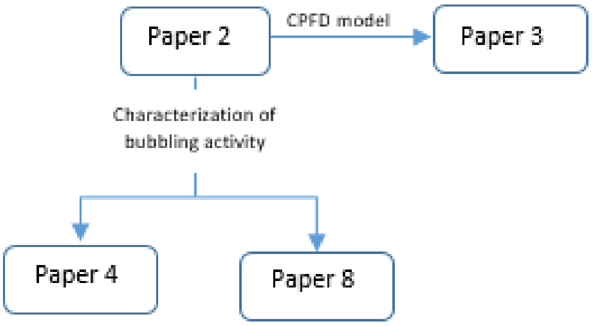
Paper 2
CPFD model
Paper 3
Characterization of bubbling activity
Paper 4
Paper 8

Figure 4-5. Schematic illustration of the link between Paper 2 and the works associated with Paper 3, 4 and 8.

4.3 Paper 3 - Study of agglomeration in fluidized bed gasification of biomass using CPFD modelling

This paper aims at obtaining a valuable insight into how different agglomerated conditions affect the flow behaviour in a bubbling fluidized bed gasifier. A computational study was carried out using the CPFD simulation software Barracuda VR, version 17.4.1. The previous developed and validated CPFD model, presented in Paper 2, was extended for use in simulations of hot flow fluidization processes in a full-scale bubbling fluidized bed gasifier. The CPFD model was scaled up using Glickman's scaling rules. The upscaling of the gasifier allowed the CPFD model to define agglomerates with larger size, which made it possible to simulate different and more realistic compositions of agglomerates in the bed. Three different fluidization temperatures were studied, of which two different combinations of amount and size of agglomerates were defined for each temperature. The amount of agglomerates added to the bed varied from 0% to 30% by volume, and the simulated agglomerates ranged from 1.0 to 4.0 cm in diameter. Figure 4-6 shows the simulated bed pressure drop as a function of the superficial air velocity for the two different fluidization processes at temperature 900°C.

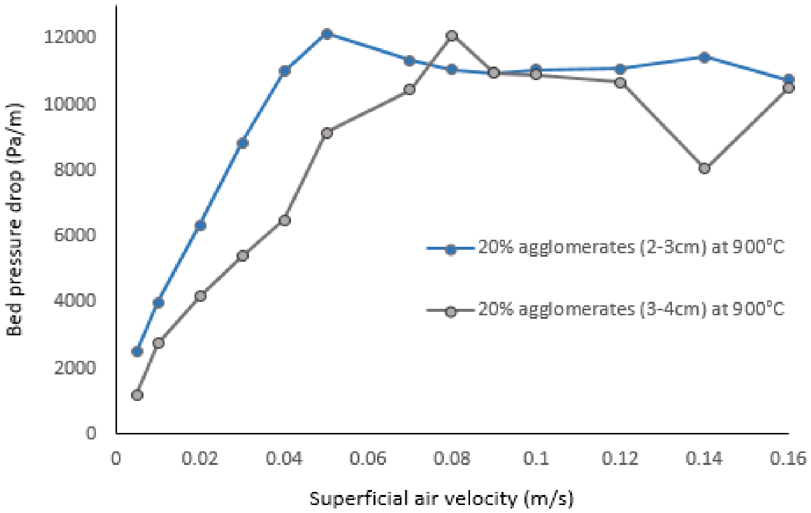

Figure 4-6. Simulated bed pressure drop vs superficial air velocity for the fluidization process at 900°C.

The simulation results support the previous findings that bed agglomeration leads to operational challenges in the fluidized bed processes. From the CPFD simulations, it is clear that the flow behaviour is affected by the size and amount of agglomerates, as well as the operation temperatures. The CPFD simulations show that the system is particularly sensitive to changes in the amount and size of agglomerates in the bed. The study reveals that when 20% agglomerates by volume with a mean diameter of 3-4 cm are present in the bed, the efficiency of bed operations is significantly reduced due to instabilities in the bed pressure drop. With further increase in agglomerated particles, the fluidized bed can no longer maintain proper bed control for an appropriate fluidized regime. With this, it can be assumed that the CPFD model can detect bed disturbances and indicate the critical point of de-fluidization. Table 4-2 summarizes the details of the simulation conditions, and the simulated minimum fluidization velocities and bed pressure drops for the different fluidization cases.

Table 4-2. Simulation results for fluidization at different temperatures and with various size and amount of agglomerates mixed with the bed particles.

Fluidization case	Temperature [°C]	Amount of agglomerates [volume %]	Size of agglomerates [cm]	Minimum fluidization velocity [m/s]	Bed pressure drop [Pa/m]
(I)	850	0	n/a	0.039	11900
(II)	850	15	1-2	0.042	11000
(III)	900	20	2-3	0.048	11050
(IV)	900	20	3-4	0.081	10500
(V)	1000	20	3-4	n/a	n/a
(VI)	1000	30	3-4	n/a	n/a

The simulation results illustrate the importance of optimizing the operating conditions. The findings provide useful information for further experimental works related to de-fluidization due to ash melting and bed agglomeration. The CPFD model is also used as a basis for a more accurate CPFD model modified for agglomerated fluidized bed processes. Figure 4-7 shows a schematic overview of other studies related to this PhD-work could make use of the findings of this study.

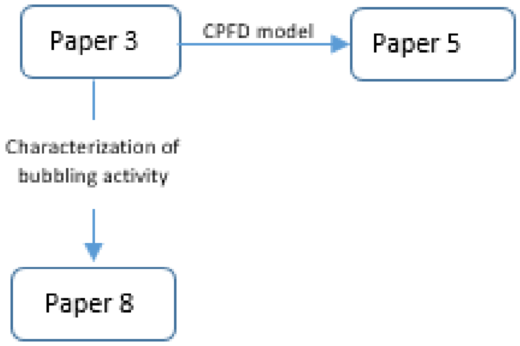

Figure 4-7. Schematic illustration of the links between Paper 3 and the works associated with Paper 5 and 8.

4.4 Paper 4 - Computational modelling of fluidized bed behaviour with agglomerates

In this paper, CPFD simulations are applied to calculate the critical amount of agglomerates in the bed, causing flow disturbances during fluidized bed processes. The commercial software package Barracuda VR, version 17.4.1 was implemented for the development of a CPFD model where the main objective was to provide valuable insights into the flow behaviour in agglomerated fluidized beds. The developed CPFD model was validated using data obtained from experiments performed in the cold flow bubbling fluidized bed. The CPFD simulations showed good agreement with the experimental data. However, this study aimed to focus on the agglomerated flow behaviour in a full-scale gasifier, operating at high temperatures. To accomplish the full-scale predictions, Glickman's scaling rules were applied to scale up the cold flow bed so that fluid-dynamic similarities were obtained between the fluidized bed systems. Further, the up-scaled CPFD model was validated against the pressure drop from experiments performed in the 20 kW bubbling fluidized bed gasifier. The validation showed a perfect fit to the gasification experiments, which confirmed that the model also could apply to extended studies related to hot-flow behaviour in a full-scale fluidized bed system. The CPFD simulations were run with a bed operating temperature of 735°C and with a constant superficial air velocity of 0.15 m/s. The mean bed particle size was 367 µm, with a calculated minimum fluidization velocity of 0.05 m/s. The chosen approach for the CPFD simulations was to continuously feed agglomerates to the bed during the fluidization process, and then use the calculated output to detect any flow disturbances. The mass flow rate of the agglomerates was 1.0 kg/s. Figure 4-8 compares of the simulation results of the normal fluidization process and the agglomerated fluidization processes in a full-scale fluidized bed system.

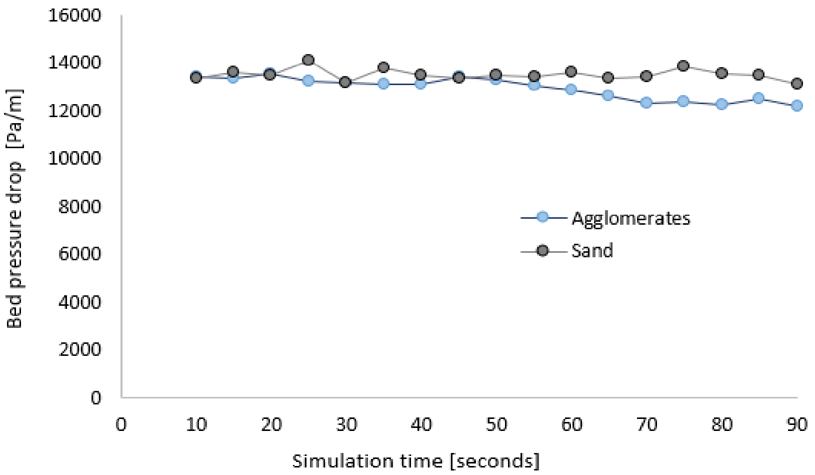

Figure 4-8. CPFD simulation of fluidization processes in full-scale fluidized bed gasifier.

The simulation results indicate that bed disturbances are detected already after 20 seconds, which correspond to 20 kg (7% by volume) agglomerates in the bed. This was in line with the simulations in Paper 2, where it was stated that 10% agglomerates by volume were sufficient to create destructive flow disturbances in the bed. The post-process images, which continuously depict the bed conditions during the fluidization process, reveal that the agglomerates tend to clump together and distribute unevenly inside the bed as the fraction of agglomerated particles increases. In addition, the same post-process images indicate that the bubble activity changes as the fraction of agglomerates in the bed increases. After 60 seconds of simulation, which corresponds to 60 kg (26 % by volume) of agglomerates in the bed, the fluidized bed shows clear signs that agglomerated particles have segregated at the bottom of the bed. This can also be confirmed by how the bubbles are getting more blurry, i.e. the particle fraction in the bubbles has increased. Figure 4-9 shows snapshot of the agglomerated fluidized bed at the time where the 26% agglomerates were present in the bed.

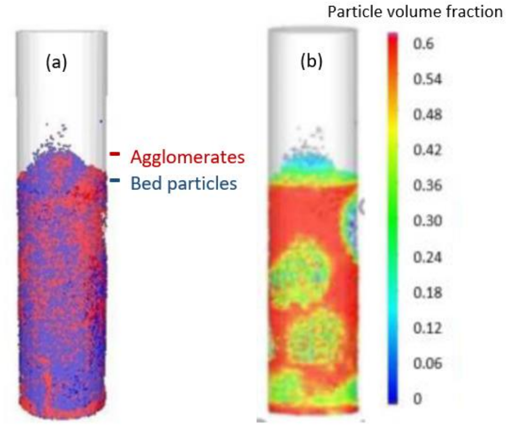

Figure 4-9. Snapshots of simulated (a) particle distribution and (b) particle volume fraction after 60 seconds of simulations, corresponding to 26% agglomerates in the bed.

To gain more insight into the flow behaviour during agglomerated fluidization processes, an additional CPFD simulation was performed in which 26% agglomerates by volume were mixed with the bed particles. The simulation results confirm that bed agglomeration poses significant challenges in maintaining an efficient fluidization in the bed. The post-process images picture that the agglomerated particles are uniformly distributed in the bed until the minimum fluidization velocity is reached. The minimum fluidization velocity of the mixed bed is calculated to 0.055 m/s based on the simulation results. However, as the velocity increases above this point, the agglomerated particles segregate in the bottom of the bed causing the air to flow in channels and result in poor fluidization conditions. Figure 4-10 shows the post-process images of (a) particle distribution at superficial air velocity of 0.085 m/s and (b) particle volume fraction at superficial air velocity of 0.101 m/s for the agglomerated fluidization process.

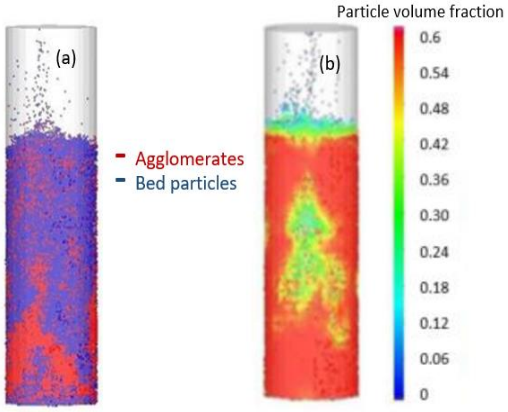
(a)
Agglomerates
Bed particles
(b)
Particle volume fraction
0.6
0.54
0.48
0.42
0.36
0.30
0.24
0.18
0.12
0.06
0

Figure 4-10. Snapshots of simulated (a) distribution of agglomerates in the bed at air velocity of 0.085 m/s and (b) particle volume fraction in the bed at air velocity of 0.101 m/s.

This study gives useful knowledge on the bubble distribution and activity in agglomerated fluidized beds. The observations are useful for further experimental study of bed agglomeration and the de-fluidized bed conditions. In Figure 4-11, a schematic diagram where the connection between this study and other studies related to this PhD-work is present.

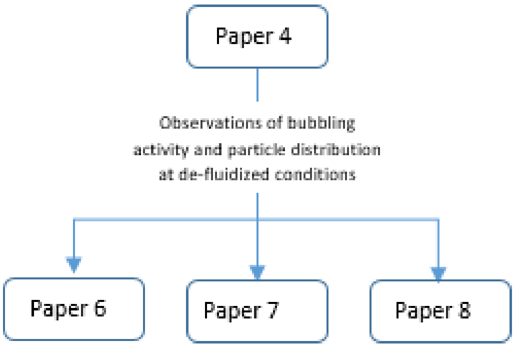
Paper 4
Observations of bubbling activity and particle distribution at de-fluidized conditions
Paper 6
Paper 7
Paper 8

Figure 4-11. Schematic illustration of the link between Paper 4 and the works associated with Paper 6, 7 and 8.

4.5 Paper 5 - Comparison of experimental and computational study of the fluid dynamics in fluidized beds with agglomerates

This paper uses a CPFD approach along with experimental data to evaluate the relationship between the fluid dynamic behaviour and bed agglomeration in fluidized bed processes. For the CPFD simulations, the commercial software package Barracuda VR version 17.4.1 was used. The experiments were carried out in the 20 kW bubbling fluidized bed gasifier. A number of fluidization experiments were performed using quartz sand as bed material: (I) fluidization of sand particles for each of the temperatures 300°C, 600°C, 700°C and 800°C and (II) fluidization of sand particles mixed with agglomerates for the temperatures 700°C and 800°C. The agglomerates had been previously produced during gasification experiments of grass pellets in the bubbling fluidized bed gasifier. The size of the agglomerates ranged from 1.0 to 3.0 cm in diameter. The amount of agglomerates added to the fluidization process was limited by the diameter of the gasifier. For the experiments, approximately 5% agglomerates by weight were mixed with the bed material. Figure 4-12 shows the experimental pressure drops obtained at different superficial velocities during fluidization experiments at 700°C and 800°C.

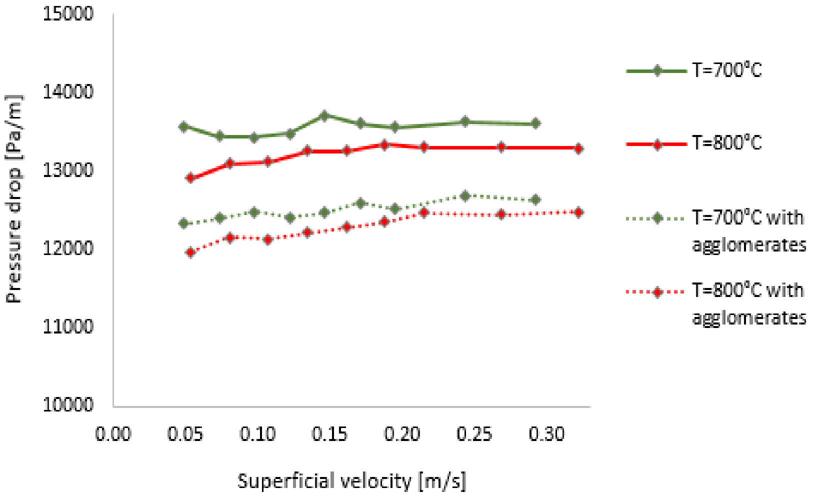

Figure 4-12. Experimental bed pressure drop vs superficial air velocity for fluidization of sand particles (solid lines) and sand particles mixed with agglomerates (dotted lines) at 700°C and 800°C.

The experimental measurements conclude that the bed pressure drop is closely related to the operating temperature. The experiments also indicate that even for a very small percentage of agglomerates in the bed, the fluidized bed conditions alter significantly. These findings are associated with the drag model equations, which have a complex dependency on both the Reynolds number and the void fraction. CPFD modelling is added to the study to provide a deeper understanding of the actual relationship between the fluid dynamics and the gas and particle properties. The CPFD simulation is able to describe the fluidized bed conditions quite accurate by taking the shape, size and density of the particles into consideration. The CPFD model is developed and verified against the experimental data. Figure 4-13 show the simulated bed pressure for fluidization with sand particles mixed with agglomerates at 700°C and 800°C.

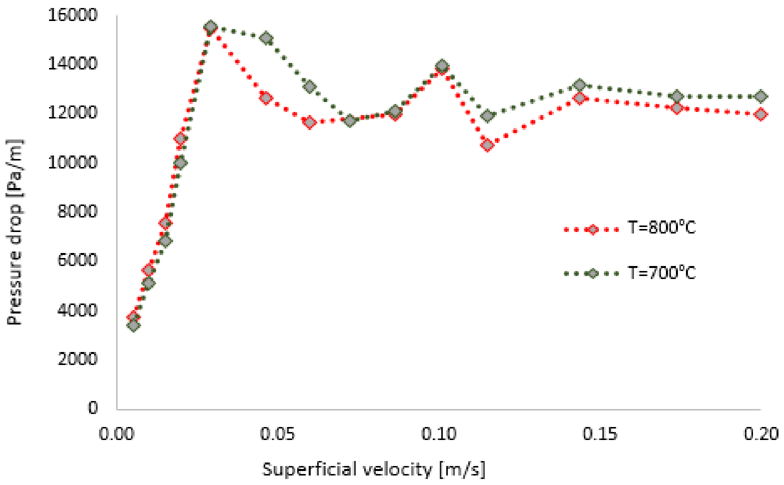

Figure 4-13. Simulated bed pressure drop vs superficial air velocity for fluidization of sand particles mixed with agglomerates at 700°C and 800°C.

The simulation results show that CPFD modelling is a reliable method that can be effectively used to predict the fluid dynamics in fluidized beds with very high accuracy. The observations obtained from this study give room for improving the operational fluidized bed conditions and are implemented in further experiments of agglomeration tendencies of different types of biomass, as illustrated in Figure 4-14.

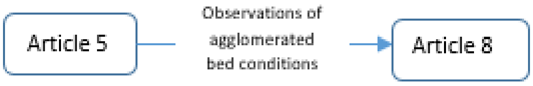

Figure 4-14. Illustration of the link between Paper 5 and the work associated with 8.

4.6 Paper 6 - Experimental study of agglomeration of grass pellets in fluidized bed gasification

In this paper, the phenomenon of bed agglomeration and the main agglomeration mechanisms are described. The study highlights varying degrees of bed agglomeration by comparing the agglomerated fluidized bed conditions during gasification of grass pellets at different air flow rates. An experimental method was conducted where controlled agglomeration tests were carried out in the 20 kW bubbling fluidized bed gasifier. The mean particle diameter of the bed material was 355 μm. The fluidization of three different air mass flow rates were investigated: (I) 2.0 kg/h, (II) 2.5 kg/h and (III) 3.0 kg/h. The gasifier was operated in the temperature range between 800°C and 900°C. The experimental run-time was 30 minutes, or until the experiments were interrupted due to bed agglomeration, observed as a total collapse of the fluidized bed. Table 4-3 summarizes the experimental bed conditions and the results obtained from the performed agglomeration tests.

Table 4-3. Experimental bed conditions and the results from agglomeration tests of grass pellets in a 20kW bubbling fluidized bed gasifier.

Agglomeration test	**Air mass flow rate [kg/h]**	**Equivalence ratio[1]**	**u_0/u_{mf}**	**De-fluidization temperature [°C]**	**Experimental run-time [minutes]**	**Onset of de-fluidization [minutes]**	**Theoretical ash/bed material ratio[2] [wt %]**
(I)	2	0.13	5.0	860	24	14	2.3
(II)	2.5	0.15	6.3	860	30	18	2.9
(III)	3	0.19	7.6	860	30	n/a	n/a

[1] Calculated based on a stoichiometric air/fuel ratio of 6.6.

[2] Assuming no ash and sand leaving the gasifier.

[2] Calculated based on initial mass of sand, m_{Sand} = 2.4 kg.

The results indicate that the air mass flow rate has a significant effect on the agglomeration tendency of the grass pellets. Comparisons of the bed conditions at the different air flow rates show that lower air flow gives higher risk for bed agglomeration and early de-fluidization of the bed. A useful and practical way of measuring the agglomeration tendency is by looking at the theoretical mass ratio between ash and bed material. Note that the theoretical amount of ash is calculated based on the onset of de-fluidization, in which the feeding of fresh grass pellets was stopped to prevent complete de-fluidization and avoid serious damage on the process equipment. Lower air flow rates result in reduced levels of ash/bed material ratio, suggesting that less grass is processed before the ash related challenges cause operational instabilities. On the other hand, with higher air flow rates, it is observed that more grass remained unprocessed and that small proportions of ash, char and sand particles have flown out of the reactor together with the produced gas.

After ended experiments, agglomerates were found in the bed for all three air flow rates. Visual examination of the produced agglomerates reveals that different agglomeration mechanisms are involved in the agglomeration processes. The agglomerates collected after fluidization with an air flow rate of 2.0 kg/h are clearly characterized by large proportions of sand particles bound together with hard bridges of molten ash. The agglomerates collected after fluidization with air flow of 2.5 kg/h are smaller, and have a more diverse composition of fused areas and porous areas where the particles are loosely bound together. The agglomerates found after fluidization with 3.0 kg/h are loosely bound particles that can be easily broken, and consist of large fractions of unreacted grass material. Figure 4-15 pictures some of the agglomerates that were removed from the gasifier after ended experiments.

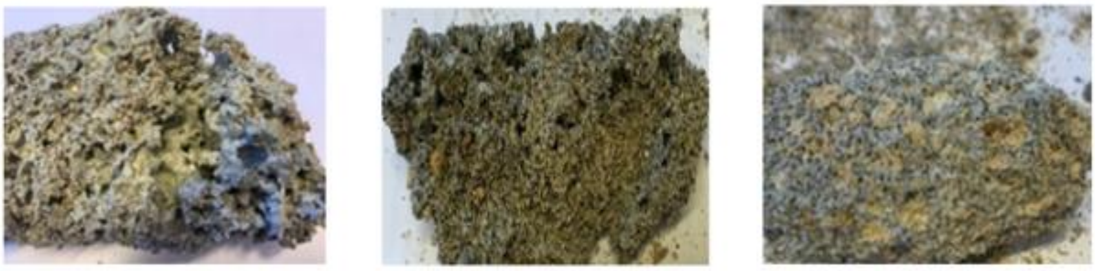

Figure 4-15. Agglomerates formed during gasification of grass pellets with air flow rate (I) 2.0 kg/h, (II) 2.5 kg/h and (III) 3.0 kg/h.

The findings of this study provide useful guidelines for further studies of the ash/bed material mass ratio and its effect on bed agglomeration and de-fluidization in fluidized beds. In Figure 4-16, a schematic diagram were the connection between this study and other studies related to this PhD-work is present.

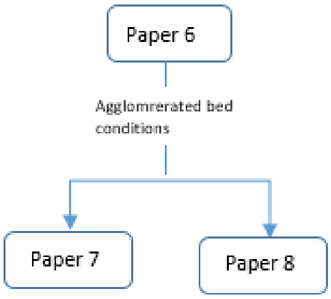

Figure 4-16. Schematic illustration of the link between Paper 6 and the works associated with Paper 7 and 8.

4.7 Paper 7 - Experimental study and SEM-EDS analyses of agglomerates from gasification of biomass in fluidized beds

This paper compares the agglomeration tendency of wood pellets and grass pellets under normal gasification conditions in a bubbling fluidized bed system. The study addresses a number of problematic challenges related to the high temperature chemistry of the major ash forming elements and their interaction with quartz sand bed particles. In addition, it points out how the composition of K, Si and Ca in the ashes plays an important role in the agglomeration process, and how different combinations of these elements are particularly problematic when processing biomass in fluidized bed systems. A series of gasification experiments were carried out for each of the two types of biomass. The 20 kW bubbling fluidized bed gasifier was used for the experiments, which aimed to provoke the formation of agglomerates. The fluidized bed gasifier was operated under normal gasification conditions where the operation temperatures were maintained in the range between 700°C and 900°C. The size of the bed particles varied from 200 µm to 600 µm. The operating bed conditions and experimental de-fluidization conditions are presented in Table 4-4.

The experimental findings concluded that that both grass and wood tended to form agglomerates under normal gasification conditions. For all test runs, the fluidized bed experienced de-fluidization where the onset of de-fluidization typically was detected as fluctuations in the bed pressure and temperature profiles. However, the de-fluidized bed conditions varied widely in the various test runs. For example, the agglomeration and de-fluidization processes for grass pellets took place after shorter time and at lower temperatures than for wood pellets at comparable bed conditions. Grass pellets were also the biomass that could withstand highest amount of ash in the bed before the fluidized bed collapsed. It was noticed that higher operating temperatures resulted in reduced levels of ash in the bed at the onset of de-fluidization, and thus expecting lower ash/bed material ratios.

Table 4-4. Operating bed parameters and results obtained from bed agglomeration during bubbling fluidized bed gasification.

Test run	Equivalence ratio[1]	u_0/u_{mf}	Operating temperature [°C]	De-fluidization temperature [°C]	Onset of de-fluidization [minutes]	Theoretical ash/bed material ratio[2] [wt %]
Grass						
(I)	0.13	> 2.5	< 750	698	56	10
(II)	0.13	> 2.5	700 – 800	750	29	5
(III)	0.13	> 2.5	800 - 900	898	14	3
Wood						
(I)	0.13	> 2.5	700 – 800	815	153	1.5
(II)	0.13	> 2.5	800 - 900	910	77	0.8

[1] Calculated based on a stoichiometric air/fuel ratio of 6.6 for the grass and 6.0 for the wood.
[2] Assuming no ash and sand leaving the gasifier.
[2] Calculated based on initial mass of sand, m_{Sand} = 2.4 kg

After each of the test runs, the agglomerates produced were collected and characterized using the scanning electron microscope with energy dispersive X-ray spectroscopy (SEM-EDS). Figure 4-17 and Figure 4-18 picture examples of SEM-images and the corresponding EDS-plots for agglomerates derived from gasification of grass pellets at operating temperatures < 750°C and wood pellets in the temperature range between 800°C and 900°C.

From the examination of the agglomerates, it is clear that large variations exist in the morphology and in the elemental composition of the agglomerates. The agglomerates from grass are mainly large in size, but have a relatively low weight. They are typically composed of loosely packed particles in a more porous structure, compared to the agglomerates from wood that are more dense and to a greater extent are characterized by molten ash-bridges. The morphology examination supports that grass and wood experiences different agglomeration mechanisms. It also appears that at increased temperatures a combination of different mechanisms is involved.

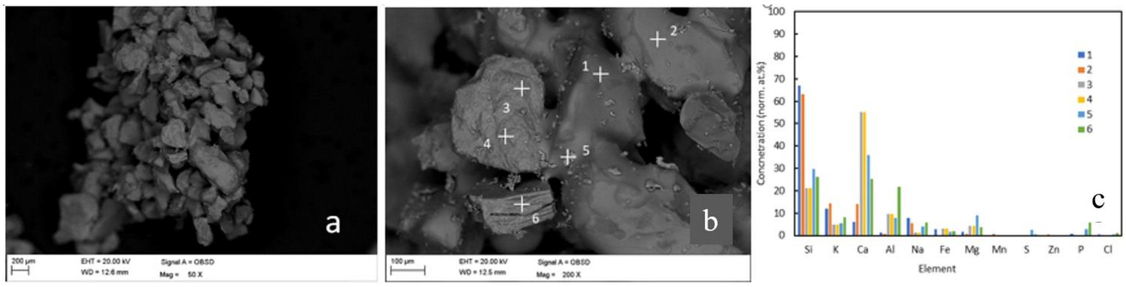

Figure 4-17. (a –b) SEM-images at different magnifications and (c) EDS-plot of an agglomerate derived from grass pellets during gasification at temperatures <750°C.

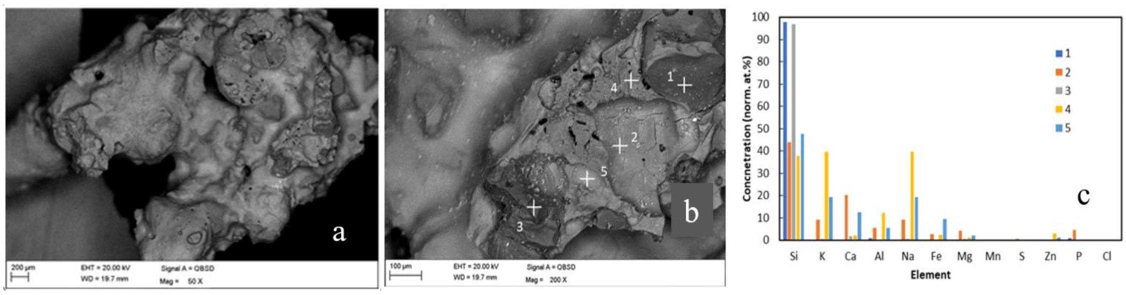

Figure 4-18. (a –b) SEM-images at different magnifications and (c) EDS-plot of an agglomerate derived from wood pellets during gasification in the temperature range between 800°C - 900°C.

The SEM-EDS analyses reveal that Si is the predominant element on the surface of the produced agglomerates from both types if biomass. Additionally, agglomerates from grass have large fractions of Ca and K on the surface. Other elements such as Na, Al, Fe and Mg exist in varying amounts on the surface of the agglomerates. The cross-sectional analyses of the agglomerates conclude that Si, Ca and K are the ash forming elements that play the most significant role in the agglomeration processes for both fuels. The high Al content in the agglomerates mainly derive from the quartz sand particles.

The results from the SEM/EDS- analyses provide the basis for decisive choices made for extended investigations of the relationship between the agglomeration tendency, the operation temperature and the major critical ash forming elements. Figure 4-19 shows a schematic illustration of the link between this study and the work related Paper 8.

Paper 7
Elemental composition of agglomerates
Paper 8

Figure 4-19. Schematic illustration of the link between Paper 7 and the work associated with Paper 8.

4.8 Paper 8 - Modelling of ash melts in fluidized bed gasification of biomass

This paper assesses the relationship between the major ash forming elements and the agglomeration tendency for grass, wood, straw and bark. The study focuses on visual observations of changes in the flow behaviour and the bubble activity as ash accumulates in the fluidized bed during high-temperature fluidization processes. The results and observations obtained from previous works (Paper 1 -7) were helpful in determining the bed conditions where the bed tended to de-fluidize. A number of fluidization experiments were carried out for laboratory prepared ashes from the selected biomass at specified gasification temperatures. The experiments aimed to collect data that could form the basis for a mathematical model that was able to predict the critical amount of accumulated ash in the bed at the onset of de-fluidization. The chosen approach for the mathematical model development was a multiple linear regression. The experimental method used the micro-scaled bubbling fluidized bed system (MBFB), and involved adding small portions of ash samples to the fluidized bed during the fluidization process. For each experiment the mass ratio of ash/bed material at the time of de-fluidized bed conditions was calculated. The investigated temperatures were 700°C, 800°C, 850°C, 900°C, 950°C and 1000°C. The critical mass ratios of accumulated ash/bed material obtained for all experimental test runs are presented in Figure 4-20.

Deviations in the de-fluidization characteristics were noticed, not only between the different types of biomass but variations were also seen in the different test runs of the same biomass. Common for all the four types of biomass is that they show the same trend, where the critical amount of ash in the bed decreases as the temperature increases. The results show that wood and straw experience quite similar agglomeration tendencies in that they can withstand approximately the same amount of accumulated ash in the bed at all investigated temperatures. Larger amount of accumulated ash in the bed are found for bark, apparently about twice the grass and five times the wood and straw.

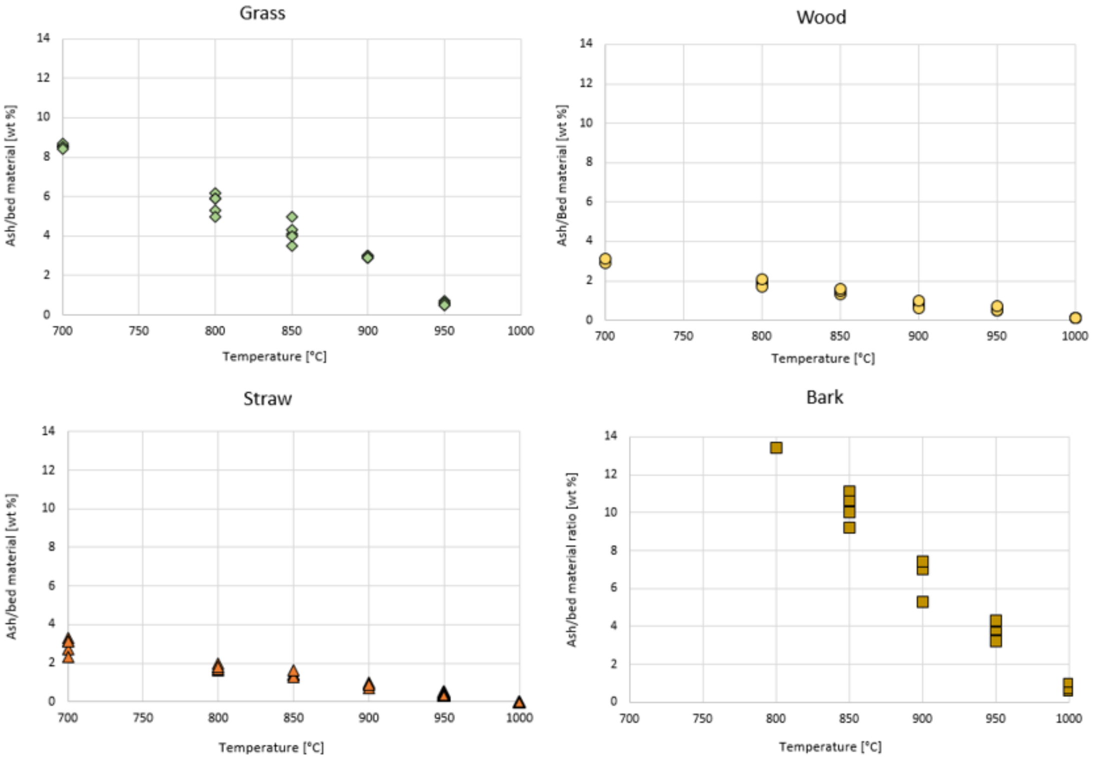

Figure 4-20. Mass ratio of the ash/Bed material vs temperature at the time of de-fluidization for fluidization experiments of grass (green), wood (yellow), straw (red) and bark (brown).

The observations confirm that the bubble activity experiences disturbances due to the accumulation of ash in the bed. The altered flow behaviour suggests that a melting process of the biomass ash has been initiated, and thus changed the fluidization characteristics of the quartz sand bed particles. The bed agglomeration and de-fluidization are detected as flow disturbances, which is seen as channelling of air and/or formation of air volumes in separated zones of the bed. The de-fluidized zones of the bed cause irregular bubble frequency where larger air bubbles typically erupt in the lower part of the column, instead of passing through the entire bed. Complete de-fluidization is determined when the fluidized state no longer can be maintained, even by increasing the air velocity. Figure 4-21 picture examples of de-fluidization characteristics observed during the fluidization experiments.

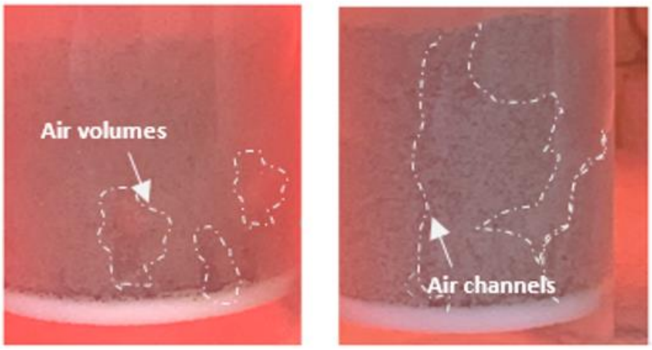

Figure 4-21. Examples of observed de-fluidization with de-fluidized air volumes (left) and channelling of air (right).

Bed agglomeration was detected in most of the experiments that showed de-fluidization. The agglomerates are identified as particles that are several times the size of the original bed particles. They either appear as enlarged particles mixed with the bed material, or as clusters of particles attached to the walls of the column. In Figure 4-22, a number of agglomerates collected after the performed fluidization experiments for grass, straw, wood and bark are pictured.

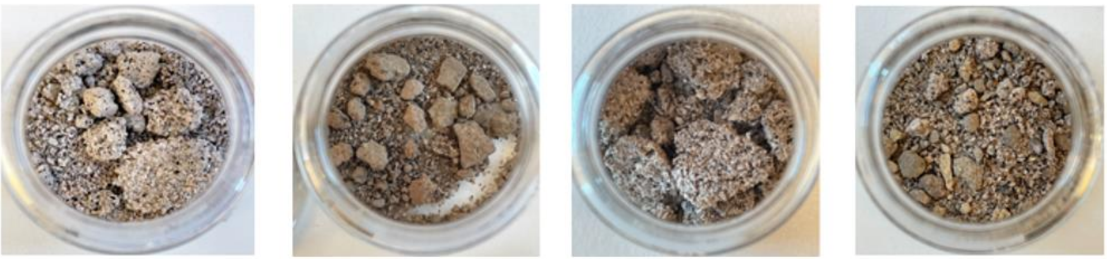

Figure 4-22. Agglomerates formed during the fluidization experiments with (a) grass, (b) wood (c) straw and (d) bark.

A multiple linear regression was carried out to determine if the operating temperature and the fractions of the major ash forming elements could predict the agglomeration tendency for different types of biomass during gasification in fluidized beds. The selected variables for the regression model are the mass ratio of accumulated ash/bed material (wt %), the gasification temperature in degree Celsius (T) and the mass ratios of Si/K and K/Ca. The final model is based on a total of 30 measurements, which represent average values of the results presented in Figure 4-20. The estimated regression coefficient and the calculated probability (p) for each of the independent variables are presented in Table 4-5, and the associated fitted regression model is showed in Equation ((*6*).

Table 4-5. Regression model coefficients.

Symbols	a	**b**	**c**	**d**	**R²**
Indication	Regression coefficients	Regression coefficients	Regression coefficients	Regression coefficients	R squared
Coefficient- value	- 0.02	4.04	1.05	17.06	0.814
Probability value (p)	< 0.0001	<0.0001	<0.01	<0.0001	

$$\frac{Accumulated\ ash}{Bed\ material}\ (wt\ \%) = \ 17.06 - 0.02 \cdot T + 4.04 \cdot \left({}^{Si}\!/_{K}\right) + 1.05 \cdot \left({}^{K}\!/_{Ca}\right) \tag{6}$$

The regression model expresses that the critical amount of ash in the bed decreases with 2% by weight for each 100°C increase in temperature, and decreases with 4.04% by weight and 1.05% by weight for each unit increase in Si/K and K/Ca, respectively. Both T, Si/K and K/Ca are significant predictors ($p < 0.05$) for the mass ratio of accumulated ash/bed material (wt %) at the onset of bed agglomeration and de-fluidization. The squared R (R^2) explains the strength of the predicted model. $R^2 = 0.81$ indicates that the three independent variables (T, Si/K and K/Ca) explain 81% of the variance in the critical amount of accumulated ash/bed material. The overall regression was statistically significant ($R^2 = 0.81$, F (3, 30) =38, $p<0.0001$).

The model was validated against the complete set of 95 observations presented in Figure 4-20. In Figure 4-23, the predicted values of the critical accumulated ash/bed material are compared with the experimental values obtained from the MBFB experiments. The R^2 of 0.72 indicates that the developed model fits the experimental data well.

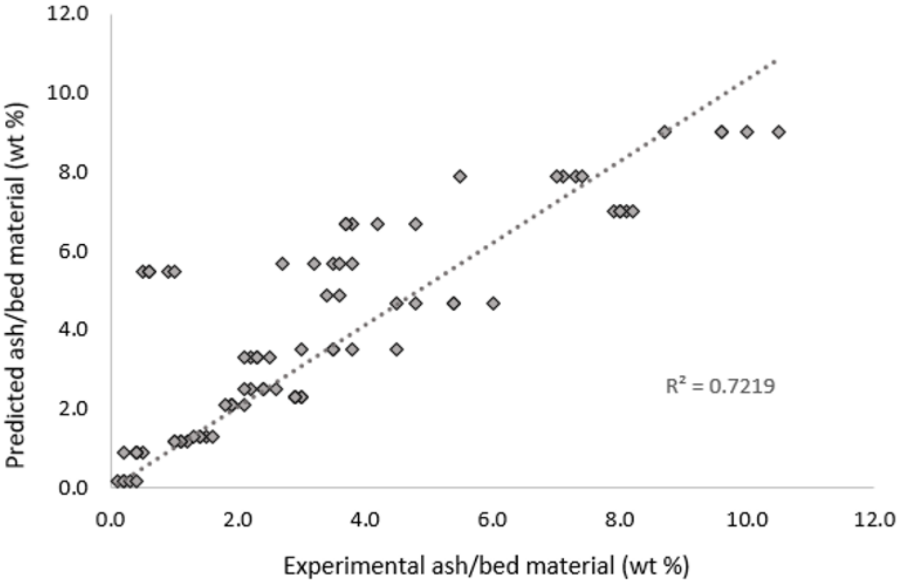

Figure 4-23. Predicted values vs experimental values.

4.9 Unpublished work

This section presents works that are not published in the papers.

4.9.1 De-fluidized bed conditions during gasification of wood pellets in a laboratory scale bubbling fluidized bed gasifier

Table 4-6 presents the operating bed conditions and experimental de-fluidized conditions during a gasification experiment of wood pellets carried out in the 20 kW bubbling fluidized bed. The results are part of the investigations performed related to Paper 7. However, these results were not included in the publication. More details on the experimental method and procedures are presented in Paper 7.

Table 4-6. Operating bed parameters and results obtained from bed agglomeration during bubbling fluidized bed gasification.

	u_0/u_{mf}	**Operation temperature [°C]**	**De-fluidization temperature [°C]**	**Onset of de-fluidization [minutes]**	**Theoretical ash/bed material ratio[1] [wt %]**
Wood	> 2.5	900-1000	951	58	0.7

[2] Assuming no ash and sand leaving the gasifier.

[2] Calculated based on initial mass of sand, m_{Sand} = 2.4 kg.

4.9.2 Ash sintering analyses

Table 4-7 and Table 4-8 present the result of the ash sintering degree tests described in Chapter 3.3.2. The results are part of a planned publication that will focus on melting and sintering behaviour of ash from different types of biomass. In addition to the presented results, the paper will include SEM-EDS analyses of the sintered ash and agglomerates from micro-scales reactor, in combination with FactSage calculations of the sintered biomass ash samples.

Table 4-7. Ash sintering analyses of grass, wood, straw and bark at different temperatures.

Grass	**550°C**	**700°C**	**800°C**	**900°C**	**1000°C**	**1100°C**	**1200°C**
	Sintering:0	*Sintering:1*	*Sintering:2*	*Sintering:3*	*Sintering:4*	*Sintering:n/a*	*Sintering:n/a*
	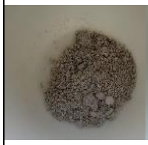	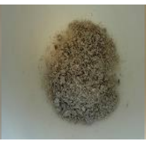	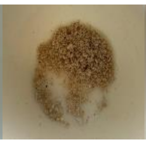	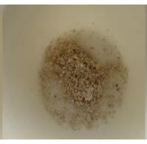	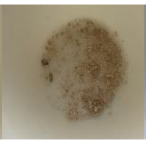	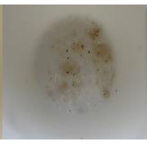	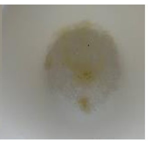
Wood	**550°C**	**700°C**	**800°C**	**900°C**	**1000°C**	**1100°C**	**1200°C**
	Sintering:0	*Sintering:1*	*Sintering:1*	*Sintering:2*	*Sintering:2*	*Sintering:3*	*Sintering:4*
	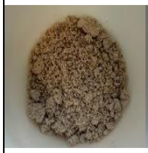	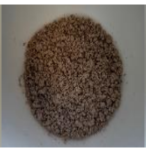	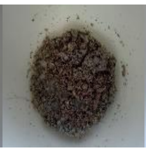	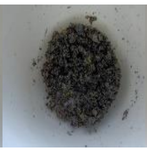	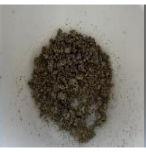	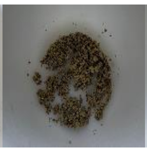	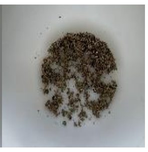
Straw	**550°C**	**700°C**	**800°C**	**900°C**	**1000°C**	**1100°C**	**1200°C**
	Sintering:0	*Sintering:1*	*Sintering:2*	*Sintering:3*	*Sintering:3*	*Sintering:4*	*Sintering:n/a*
	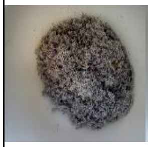	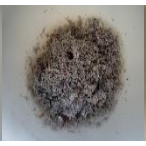	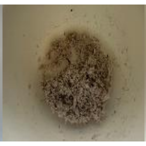	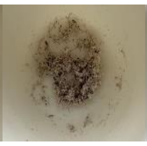	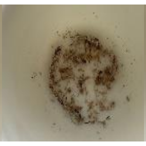	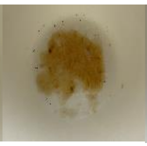	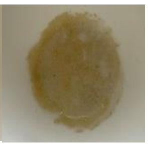
Bark	**550°C**	**700°C**	**800°C**	**900°C**	**1000°C**	**1100°C**	**1200°C**
	Sintering:0	*Sintering:0*	*Sintering:1*	*Sintering:1*	*Sintering:2*	*Sintering:3*	*Sintering:4*
	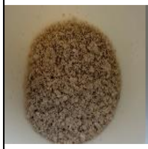	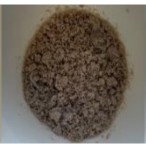	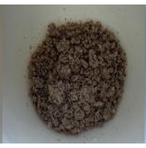	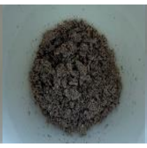	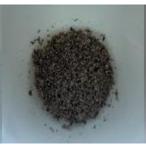	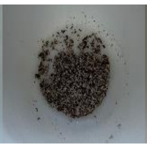	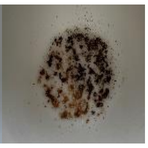

Table 4-8. Weight loss of ash from grass, wood, straw and bark at different temperatures.

Biomass ash	700°C	800°C	900°C	1000°C	1100°C	1200°C
Grass	5.3	15.7	21.3	21.9	22.3	25.4
Wood	14.7	19.9	22	23.5	27.2	40.6
Straw	9.8	18.8	25	25	30	30
Bark	7.4	9	9.3	12.4	13.1	14.7

4.9.3 Ash Density measurements

Table 4-9 presents the results of ash density measurements carried out for grass, wood, straw and bark. The analyses were performed in a Micrometrics Autopyconometer, model 1320. The results are used as a part of the investigations performed related to Paper 8. However, these results were not included in the present publication.

Table 4-9. Ash density measurements of samples from grass, wood, straw and bark.

	Ash Density [kg/m^3]			
	1	**2**	**3**	**Average**
Grass	2 844	2 749	2 773	2 789
Wood	3 110	3 086	2905	3 033
Straw	2 898	2 833	2 909	2 880
Bark	3 990	4 979	4 356	4 442

5 Discussion of results

In this chapter, the main results from the theoretical and experimental works presented in Chapter 4 are discussed. The experimental observations and developed models lead to a better understanding of the flow behaviour in fluidized bed systems. Additionally, the findings provide increased knowledge and competence within the field of bed agglomeration and de-fluidization due to biomass ash accumulation during high-temperature processes in bubbling fluidized beds. The developed predictive methods and models contribute to improved efficiency of the biomass gasifiers in order to accelerate the implementation of biomass-to-liquid transport fuel technology.

5.1 CPFD simulations of agglomeration and flow behaviour

The CPFD models simulate the flow behaviour in bubbling fluidized bed gasifiers, and describe the presence of agglomerates as disturbances in the operating bed conditions. The decreased bed pressure drop due to agglomeration is explained by the drag models, which describe how the size, shape and density of the particles indirectly influence on the fluidization characteristics in the bed. The agglomerated fluidized bed conditions substantially differ from the normal fluidized bed conditions in terms of bubble distribution and activity. This is in line with conclusions drawn from other research studies related to the flow behaviour and the operational problems due to bed agglomeration in fluidized beds [50, 70, 74, 75, 77]. The findings are also supported by the visual observations made in the fluidization experiments in both the cold flow and the micro-scale fluidized bed systems. However, the time when the bed disturbances become irreversible and result in complete de-fluidization depends on the amount and structure of the agglomerates, as well as their location in the bed. The simulation results show that the fluidized beds can operate with small fractions of agglomerates in the bed without significant changes in the flow conditions. This is also seen in other parts of this study that conclude that by increasing the gas velocity or changing the fuel feed conditions in the fluidized bed system, the onset of de-fluidization can be delayed. More specifically, the intensive bed mixing allows the fluidization to continue due to breakage of brittle and loosely bound agglomerates. Note that the equivalence ratio and the ratio between the superficial air velocity (u_0) and the minimum fluidization velocity (u_{mf}) are critical process parameters that should always be controlled within specified ranges during the fluidized bed processes. Both parameters are closely related to the air flow rate, and play important roles for both the quality of the gasification process and the quality of the syngas. If the equivalence ratio and the u_0/u_{mf} ratio are not controlled correctly, the risk of poor gasification conditions with reduced energy conversion and production of gases with low heating values increases.

The overall findings suggest that CPFD models can be effectively used to predict the flow behaviour in fluidized beds with very high accuracy. The CPFD modelling and simulations provide increased knowledge on the basic theory and terms used in the fluid dynamics. This knowledge is necessary to fully understand the influence of agglomerates on the fluidization characteristics, and thus be able to design and operate the fluidized bed gasifiers properly. However, the progress in modelling and simulating ash melting and bed agglomeration in biomass gasification processes is still lacking. The simulation results pinpoint a significant challenge in using the CPFD models for the investigations of the relationship between agglomeration and flow behaviour in unspecified systems. The challenge involves the existence of agglomerates that comes in all size, shapes and structures, which makes it difficult to identify a standard way of defining the particles appropriately. Although, the Barracuda software is specifically designed to simulate gas-particle flow in fluidized beds, it has no specification for merging particles during the fluidization process. It is therefore not possible to model the ash behaviour nor the formation process of agglomerates in a reasonable way. Thus, new methods and models were developed that can predict the onset of bed agglomeration and de-fluidization based on ash composition and operating temperature.

5.2 Methods and models for determining the critical amount of ash

The gasification and fluidization experiments show that there is a clear relationship between the mass ratio of accumulated biomass ash/bed material and the onset of bed agglomeration and de-fluidization in fluidized beds. The observations from the micro-scale fluidized bed (MBFB) experiments conclude that the agglomeration tendency for the different biomasses show similar trend where the mass ratio of accumulated ash/bed material decreases with increasing operating temperature. On the other hand, the investigated biomasses suggest large individual differences in the agglomeration and de-fluidization characteristics, which explains the effects of the biomass ash melting behaviour on the agglomeration tendency. Theoretical and experimental studies conducted during this PhD-work point out that high temperature is a significant factor leading to biomass ash melting problems and following bed agglomeration in fluidized bed processes. The SEM-EDS study reveal that bed agglomeration also is closely associated with the ash forming elements Si, K and Ca. These findings are consistent with the results presented by several other researchers that have investigated the cause of bed agglomeration during thermochemical conversion in fluidized beds [49, 58, 61, 65-67]. Based on the ash composition, in particular the Si, K and Ca content, the grass and straw are expected to form complex chemical compounds that increase the risk for formation of agglomerates during high-temperature gasification processes in fluidized bed reactors where quartz sand is used as bed material. On the other hand, the gasification of wood and bark is expected to preferably result in bottom ash with high proportion of stable and unreactive oxides, which prevent rather than favour the bed agglomeration process. Somewhat surprisingly, the wood and straw behave quite similarly in terms of the amount of critical accumulated ash/bed material in the fluidized bed. This is clearly shown in the block diagram in Figure 5-1, which summarize an average of the experimental results presented in Paper 8. The findings give indications that additional determining factors, other than the ash compositions and the operating temperatures, contribute to the bed agglomeration processes. The agglomeration processes, as well as the mechanisms by which the agglomerates are formed, are obviously controlled by an ongoing competition between physical and chemical mechanisms and reactions. The examinations of agglomerates derived from the various experimental studies clearly indicate that the agglomerates may be the result of either coating-induced or melting-induced agglomeration mechanism, or in some cases even a combination of these two mechanisms are present. There are therefore good reasons to believe that the mass ratios of Si/K and K/Ca play major roles and are of great importance in the bed agglomeration processes. This has also been highlighted in a research study conducted at the Royal Institute of Technology in Stockholm (KTH) where the formation of ash from different fuels during combustion was discussed [73]. They found that the risk for agglomeration depends highly on the ratio between Si and K, and suggested that increased Si content contributes to greater agglomeration tendency due to an increased risk of involvement of more than one agglomeration mechanism.

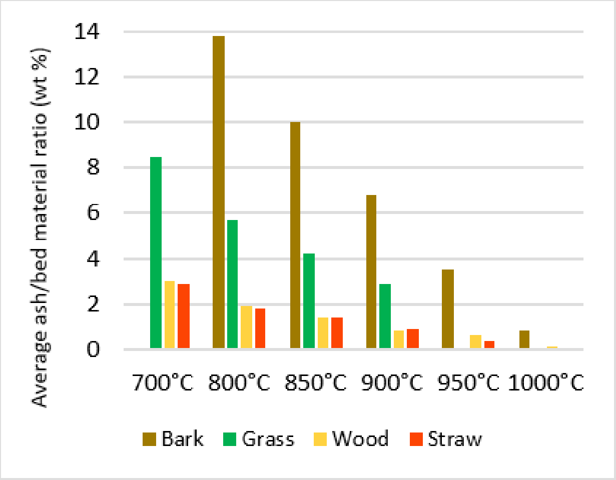

Figure 5-1. Critical amount of ash in the bed resulting from experiments in micro-scale fluidized bed.

Although the agglomeration phenomenon in fluidized beds has been widely studied, there is still work remaining for the development of tools for reliable predictions of the ash melting behaviour in biomass gasification processes. Valuable outcomes from this PhD-work are the identification of the different de-fluidized bed characteristics and the definition of the critical accumulated ash/bed material. The information obtained formed the basis for a mathematical model capable of predicting the agglomeration tendency at given temperatures, based on chemical analyses of the raw biomass. The model provides reliable predicted values that can be easily adapted to industrial facilities in order to estimate the onset of bed agglomeration and de-fluidization in a manageable, fast and inexpensive way. By introducing the dependent variable in terms of the mass ratio of ash/bed material, it is possible to adapt the model to other fluidized bed systems. The predicted results are validated against measured values from experiments performed in the laboratory scale bubbling fluidized bed gasifier and the micro-scale bubbling fluidized bed. Figure 5-2 compares the predicted mass ratios of accumulated ash/bed material with the experimental mass ratios of accumulated ash/bed material for grass, wood, straw and bark. Note that the value presented for wood from the bubbling fluidized bed gasifier in the temperature range from 900°C to 1000°C is not part of any publication, and is therefore presented as unpublished works in chapter 4.9.1.

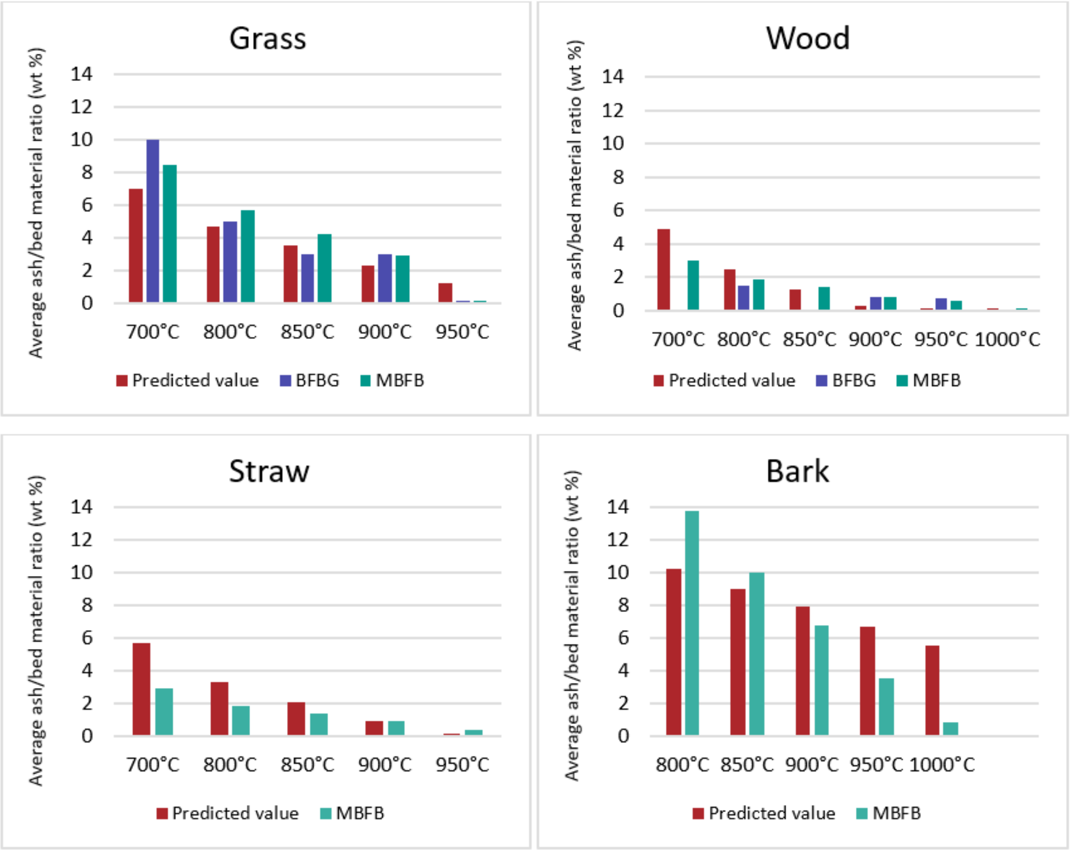

Figure 5-2. Predicted and experimental values of accumulated ash/bed material for grass, wood, straw and bark. The experiments are performed in a laboratory scaled (BFBG) and a micro-scaled (MBFB) fluidized bed system.

The diagrams show that the predictive model estimates the amount of critical ash with an acceptable accuracy. Although the samples from which data are gathered are relatively small, they represent a wide variety of the biomass available for liquid transport biofuel production in Norway. The experimental results can therefore provide meaningful information that cover the main determining factors related to problems with ash melting in biomass gasification. However, the model does not consider the relevant physical mechanisms that must be included to fully explain the ash melting behaviour. As a consequence, the model poses challenges with unidentifiable parameters that were initially omitted from the model development. This may be one reason for the systematic errors that cause the model to fail to provide good fit to the data in specific measuring areas. Furthermore, which determining factors that are relevant or irrelevant may vary among the different biomass ashes, based on their elemental composition as well as the operating bed conditions. The model shows best fit in the temperature range between 800°C and 900°C. On the other hand, the model turns out to be less predictive in the measuring areas with high systematic errors. It is most likely to believe that this is caused by increasing complexity due to the un-identifying parameters and underlying mechanisms that control the ash behaviour. The measurements carried out in these areas were characterized by the need to add very large amounts of ash, which made it difficult to determine the exact time of de-fluidization due to increased particle size distribution that interfere with the fluidization condition. This is especially prominent for the measurements at 700°C and samples with low K/Ca ratio.

More information is needed to create a predictive model that can be generalized to cover a broader range of biomasses. To improve the model, it is of great importance to add more information on new ash compositions that can explore the limit of accurate estimations in the regimes with high systematic error. Although the study conducted a thorough survey, it is not sufficient to claim that the model can be extrapolated. This gives the model certain limitations in terms of its validity outside the validated measuring ranges. In addition, it should always be taken into account that the model does not calculate the exact values but gives an estimated value with an accepted inaccuracy. Thus, the model has the following limitations:

- $700°C < T < 1000°C$
- $0.5 < Si/K < 2.9$
- $0.4 < K/Ca < 3.0$
- Inaccuracy

This PhD-work has applied experimental methods to develop a mathematical model that gives a valuable contribution to improve the gasification efficiency and accelerate the implementation of biomass-to-liquid transport biofuels in the future. Predicting the onset of bed agglomeration and de-fluidization based on the ash composition provides the opportunity to mitigate the operational problems caused by molten biomass ash in the fluidized bed systems. The main goal is to avoid unscheduled, costly and resource-intensive shutdowns of the large-scale industrial gasifiers. Although the mathematical model has limitations, the predictions give approximate estimates that are acceptable for the purpose of this model. The modelling results are useful for selecting a gasification process with optimal process design and operation based on the calculated critical amount of ash/bed material. The predicted value can be combined with specified operating bed conditions to calculate the time limit for ash removal and/or recirculation of bed material in fluidized bed systems. In addition, plant operators can be able to differentiate promising alternative biomasses from biomass that potentially cause large operational problems.

In order to meet the international climate goals of becoming a society with net-zero emissions by 2050, the future biofuels have to depend on feedstock including the use of low-quality feedstock, with diverse ash contents and ash compositions. A solution for the poor quality might be blending of different biomasses. Consequently, the fluidized bed gasification systems must handle larger ranges of biomasses, not only woody biomass nor only agricultural biomasses, but a mix of biomasses that are dependent on seasonal variations or other factors determining availabilities. The blending of biomasses is demanding from an availability point of view, and new methods and models based on good knowledge of the biomass and the ash melting behaviour are needed for an optimal selection of biomass.

Optimal blending of different biomasses not only to avoid problems, but also to give essential clean energy effect which can boost both the lifetime for existing equipment and give useful guidelines for an environmental friendly design and operation.

6 Conclusion and suggestions for further works

This chapter include the main conclusions drawn in the published scientific papers related to this PhD-work, and the suggestions for further works.

6.1 Conclusion

The aim of this work was to assess the ash related challenges leading to bed agglomeration and de-fluidization during gasification of biomass in fluidized beds. Experimental work and computational modelling were combined in order to gain a fundamental understanding and a deeper insight into the physical and chemical mechanisms involved in the bed agglomeration processes. The agglomeration tendencies for different biomasses were studied, where the main focus was on the ash melting behaviour and the major ash forming elements Si, K and Ca. Grass, wood, straw and bark were selected to represent general biomass samples with large compositional variations, which cover a wide range of the biomass available for liquid biofuel production in Norway.

For the experimental part, three different bubbling fluidized bed systems were used: (i) A cold flow model, (ii) a 20 kW laboratory scale model, and (iii) a micro-scale model. The commercial CPFD software package Barracuda Virtual Reactor was used for the computational part. The results highlight the challenges with biomass ash melting and subsequently formation of agglomerates during fluidized bed gasification. The agglomerated particles change the fluidization characteristics, causing poor gasification conditions due to bed instabilities with disturbed bubble activity and channeling of air. The experimental results show that bed agglomeration is closely associated with high operating temperature and the biomass ash composition. It is also revealed that the ratios between the major ash forming elements K, Si and Ca in the biomass play an important role in the agglomeration process, and that different combination of those elements are especially problematic when processing biomass fuels in fluidized bed systems.

A micro-scaled fluidized bed was designed to perform accurate agglomeration and de-fluidization experiments in an effective and controlled manner. The observations gave accurate measurements of the amount of accumulated ash in the bed at the onset of bed agglomeration and de-fluidization. The results indicate that bark tends to have the highest tolerance limit of accumulated ash in the bed for all the investigated temperatures. For example, the ash/bed material was measured to 7 % by weight at 900°C, compared to grass (3 %), straw (1 %) and wood (1 %).

The combination of basic knowledge about the fluidization characteristics and the key findings from the experimental studies provided a good basis for development and validation of a mathematical model capable of predicting the agglomeration tendency of different types of biomass during gasification processes in fluidized bed systems. The chosen approach for the model development was a multiple regression analysis that resulted in a predictive model that estimates the critical amount of accumulated ash/bed material (wt %) based on the operation temperature and the composition of the ash forming elements Si, K and Ca. A significant regression equation was found ($F(3, 30) = 38$, $p < 0.0001$), with an $R^2 = 0.814$. The weight percentage of accumulated ash/bed material is equal to $17.63 - 0.02 \cdot T + 4.04 \cdot (Si/K) + 1.05 \cdot (K/Ca)$, where the T is the operating temperature measured in degree Celsius and (Si/K) and (K/Ca) are the mass ratios.

6.2 Suggestions for further works

This PhD-work has contributed to the field of biomass-to-liquid transport biofuels, and has provided methods and models that can improve the biomass gasification efficiency and accelerate the implementation of biofuels. Although, the objectives of this thesis have been fulfilled, other research questions have emerged during the course of this study. The mathematical model are based on results and findings obtained from investigations of four different biomasses, using one type of bed material and one particle size distribution. More information is needed to create a predictive model that can be generalized to fully cover a broader range of biomasses, and be adapted to use in all types of industrial fluidized bed systems. The following extended studies are suggested for further research and development of a comprehensive and reliable model that can help reduce the ash-related challenges in fluidized bed:

- Experiments with different particle sizes and distribution of bed particles.
- Experiments using steam or other types of gasifying medium.
- Experiments using Olivine as bed material.
- Investigations of biomass with ash compositions that can explore the limit of accurate estimations in the regimes with high systematic error to make the model more robust.
- Investigating blending of different feedstock for utilizing difficult and troublesome types of waste material.

References

[1] S. K. Sansaniwal, K. Pal, M. A. Rosen, S. K. Tyagi. Recent advances in the development of biomass gasification technology: A comprehensive review, Renewable and Sustainable Energy Reviews 72 (2017), 363-384.
DOI: 10.1016/j.rser.2017.01.038.

[2] International Energy Agency (IEA), Net Zero by 2050 - A Roadmap for the Global Energy Sector, IEA Publications (2021). Report retrieved from: https://www.iea.org/events/net-zero-by-2050-a-roadmap-for-the-global-energy-system. [Cited 2021 19/10/2021].

[3] J. Zalasiewics, M. Williams, P. J. Crutzen, W. Steffen. The New World of the Anthropocene, Environmental Science and Technology 44 (7) (2010), 2228-2231. DOI: 10.1021/es903118j.

[4] NASA's Jet Propulsion Laboratory, Global Temperature: Vital Signs - Climate Change - Vital Signs of the Planet, California Institute of Technology (October 13, 2021). Retrieved from: https://climate.nasa.gov/vital-signs/global-temperature. [Cited 2021 19/10/2021].

[5] H. Ritchie, M. Roser. CO_2 and Greenhouse Gas Emissions. (August 2020). Published online at OurWorldInData.org. Retrieved from: https://ourworldindata.org/co2-and-other-greenhouse-gas-emissions.
[Cited 2021 19/10/2021].

[6] International Panel on Climate Change (IPCC). Climate Change 2014: Mitigation of Climate Change, Contribution of Working group III to the Fifth Assessment Report of the Intergovernmental Panel on Climate Change, Cambridge University Press, Cambridge, United Kingdom and New York, NY, USA (2014).

[7] Political Platform for the Norwegian Government, formed by the Conservative Party, the Progress party and the Liberal party, (January 14, 2018). Retrieved from:

https://www.regjeringen.no/contentassets/e4c3cfd7e4d4458fa8d3d2bb1e43bcbb/plattform.pdf. [Cited 2021 19/10/2021].

[8] The United Nations Framework Convention on Climate Change (UNFCCC). The Paris Agreement (December 2015). Retrieved from: https://unfccc.int/process-and-meetings/the-paris-agreement/the-paris-agreement. [Cited 2021 19/10/2021].

[9] Norwegian Parliament. Norway's long-term low-emission strategy for 2050 – An innovative society with attractive towns and communities (February 2020): https://unfccc.int/sites/default/files/resource/LTS1_Norway_Oct2020.pdf. [Cited 2021 19/10/2021].

[10] S. K. Sansaniwal, M. A. Rosen, S. K. Tyagi. Global challenges in the sustainable development of biomass gasification: An overview, Renewable and Sustainable Energy Reviews 80 (2017), 23-43. DOI: 10.1016/j.rser.2017.05.215.

[11] A. J. K. Pols, A. Spahn. Biofuels: ethical issues. Biofuels: Ethical Aspects, Encyclopedia of Food and Agricultural Ethics, edited by Paul B. Thompson and David M. Kaplan, Springer Netherlands (2014) 1-10. DOI: 10.1007/978-94-007-0929-4_343.

[12] P. Basu. Biomass Gasificaion, Prolysis and Torrefaction, Second Edition, Academic Pess, UK (2013). ISBN: 978-0-12-396488-5.

[13] S. C. Capareda. Introduction to Biomass Energy Conversions, CRC Press, Boca Raton, US (2014). ISBN: 978-1-4665-1334-1.

[14] M. Öhman, A. Nordin, B. J. Skrifvars, R. Backman, M. Hupa. Bed Agglomeration Characteristics during Fluidized Bed Combustion of Biomass Fuels, Energy & Fuels 14 (1) (2000), 169-178. DOI: 10.1021/ef990107b.

[15] L. Wang, C. L. Weller, D. D. Jones, M. A. Hanna. Contemporary Issues in Thermal Gasification of Biomass and Its Application to Electricity and Fuel Production, Biomass and Bioenergy 32 (7) (2008), 573-58.
DOI: 10.1016/j.biombioe.2007.12.007.

[16] European Commission. Communication from the Commission to the European Parliament, the Council, the European Economic and Social Committee and the Committee of Regions. Stepping up Europe's 2030 Climate Ambition Investing in a climate-neutral future for the benefit of our people (2020).
Report: COM (2020) 562 final (2020).

[17] F. Bergk, W. Knörr, U. Lambrecht. Climate Protection in Transport - Need for Action in the Wake of the Paris Climate Agreement, Report as part of the project: "Climate Change Mitigation in Transport until 2050", Environmental Research of the Federal Ministry for the Environment, Nature Conservation, Building and Nuclear Safety (June 2017). http://www.umweltbundesamt.de/publikationen. [Cited 2021 19/10/2021].

[18] International Renewable Energy Agency (IRENA). Advanced biofuels. What holds them back? International Renewable Energy Agency, Abu Dhabi (November, 2019). ISBN: 978-92-9260-158-4.

[19] S. S. Ail, S. Dasappa S. Biomass to liquid transportation fuel via Fisher-Tropcsh synthesis - Technology review and current scenario, Renewable and Sustainable Energy Reviews 58 (C) (2016), 267-286. DOI: 0.1016/j.rser.2015.12.143.

[20] E. Kurkela, M. Kurkela, I. Hiltunen. Pilot-scale development of pressurized fixed-bed gasification for synthesis gas production from biomass residues, Biomass Conversion and Biorefinery, page 1-22. (2021).
DOI: 10.1007/s13399-021-01554-2.

[21] Nuffield Council on Bioethics Biofuels: Ethical Issues, Nuffield Press, Oxfordshire, UK (2011). ISBN: 978-1-904384-22-9.

[22] J. S. Tumuluru, S. Sokhansanj, C. T. Wright, R. D. Boardman, N. A. Yancey. A Review on Biomass Classification and Composition, Co-Firing Issues and Pre-treatment Methods, (2011). Presentation at the 2011 American Society of Agricultural and Biological Engineers (ASABE) Annual International Meeting, Paper Number: 1110458, Louisville, Kentucky (7-10 August 2011). DOI: 10.13031/2013.37191.

[23] K. Fursatz, J. Fuchs, F. Benedict, M. Kuba, H. Hofbauer. Effect of biomass fuel ash and bed material on the product gas composition in DFB steam gasification. Energy 219 (C) (2021), 119650. DOI: 10.1016/j.energy.2020.119650.

[24] M. J. Prins, K. J. Ptasinski, F. J. J. G. Janssen. From coal to biomass gasification: Comparison of thermodynamic efficiency. Energy 32 (7) (2007), page 1248-1259. DOI: 10.1016/j.energy.2006.07.017.

[25] D. A. Tillman. Wood as an energy resource, Elsevier Science (2012). ISBN (e-book): 978-03-2315-855-8.

[26] C. C. Hsieh, C. Felby. Biofuels for the marine shipping sector - An overview and analysis of sector infrastructure, fuel technologies and regulations, IEA Bioenergy, Task 39, Paris (October, 2017). Report retrieved from: http://task39.sites.olt.ubc.ca/files/2013/05/Marine-biofuel-report-final-Oct-2017.pdf. [Cited 2021 19/10/2021].

[27] European Commission. Renewable Energy - Recast to 2030 (REDII) (2016). Retrieved from: https://ec.europa.eu/jrc/en/jec/renewable-energy-recast-2030-red-ii. [Cited 2021 19/10/2021].

[28] E. Dahlquist. Technologies for Converting Biomass to Useful Energy; Combustion, gasification, pyrolysis, torrefaction and fermentation, CRC Press, London, UK (2013). ISBN: 978-0-415-62088-8.

[29] M. J. Taherzadeh, T. Richards. Resource Recovery to Approach Zero Municipal Waste, CRC Press, Boca Raton, US (2016). ISBN: 978-1-4822-4036-8.

[30] T. Kittivech and S. Fukunda. Investigating Agglomeration Tendency of Co-Gasification between High Alkali Biomass and Woody Biomass in a Bubbling Fluidized Bed System, Energies 13 (1) (56) (2019), page 1-15.
DOI: 10.3390/en13010056.

[31] S. Valin, S. Ravel, P. Pons de Vincent, S. Thiery, H. Miller, F. Defoort and M. Grateau. Fluidized Bed Gasification of Diverse Biomass Feedstock and Blends - An overall Performance Study, Energies 13 (14) (2020), 3706.
DOI: 10.3390/en13143706.

[32] A. V. Bridgwater. Renewable fuels and chemicals by thermal processing of biomass, Chemical Engineering Journal (91) (2-3) (2003), page 87-102.
DOI: 10.1016/S1385-8947(02)00142-0.

[33] M. Balland, K. Froment, G. Ratel, S. Valin, J. Roussely, R. Michel, J. Poirier, Y. Kara and A. Galnares. Biomass Ash Fluidized-Bed Agglomeration: Hydrodynamic Investigations, Waste and Biomass Valorization 8 (2017), page 2823-2841.
DOI: 10.1007/s12649-017-9853-9.

[34] H. A. Alabdrabalameer, M. J. Taylor, J. Kauppinen, T. Soini, T. Pikkarainer and V. Skoulou. Big problem, little answer: Overcoming Bed Agglomeration and Rector Slagging during the Gasification of Barley Straw under Continuous Operation. Sustainable Energy and Fuels 4 (7) (2020), page 3764-3772.
DOI: 10.1039/d0se00155d.

[35] J. Van Caneghem, A. Brems, P. Lievens, C. Block, P. Billen, I. Vermeulen, R. Dewil, J. Baeyens and C. Vandecasteele. Fluidized bed waste incinerators: Design, operational and environmental issues. Progress in Energy and Combustion Science 38 (4) (2012), page 551-582. DOI: 10.1016/j.pecs.2012.03.001.

[36] B. Leckner. Process aspects in combustion and gasification Waste-to-Energy (WtE) units, Waste Management 37 (2015), page 13-25.
DOI: 10.1016/j.wasman.2014.04.019.

[37] B. G. Miller, S. F. Miller, B. G. Miller and D. A. Tillman. Combustion Engineering Issues for Solid Fuel Systems, Chapter 8 - Fluidized-Bed Firing Systems, Academic Press, Burlington (2008), page 275-340. ISBN: 978-0-12-373611-6.

[38] R. Cocco, S. B. Reddy Karri and T. Knowlton. Introduction to Fluidization. Chemical Engineering Progress 110 (11) (2014), page 21-29.

[39] S. J. Pickering. Management, Recycling and Reuse of Waste Composites, Chapter 4 -Thermal methods for recycling waste composites, Woodhead Publishing Series in Composites Science and Engineering (2010), page 65-101.
DOI: 10.1533/9781845697662.2.65.

[40] D. Kunii and O. Levespiel. Fluidization Engineering, Second Edition. Butterworth-Heinemann, USA (1994). ISBN: 978-0-40-990233-4.

[41] H. Sutar and C. Das Kumar. Mixing and Segregation Characteristics of Binary Granular Material in Tapered Fluidized Bed: A CFD Study. Engineering 04 (04) (2012), page 215-227. DOI: 10.4236/eng.2012.44029.

[42] F. Marchelli, Q. Hou, B. Bosio, E. Arato, A. Yu, Comparison of different drag models in CFD-DEM simulations of spouted beds. Powder Technology 360 (2020), page 1253- 1270. DOI: 10.1016/j.powtec.2019.10.058.

[43] S. Ergun. Fluid flow through packed columns. Journal of Chemical Engineering Progress 48 (2) (1952), page 89-94.

[44] J. Capablo, P. A. Jensen, K. H. Pedersen, K. Hjuler, R. Nikolaisen, R. Backman and F. Frandsen. Ash Properties of Alternative Biomass, Energy & Fuels 23 (4) (2009), page 1965-1976. DOI: 10.1021/ef8008426.

[45] M. Bartles, W. Lin, J. Nijenhuis, F. Kapteijn and R. Ommen. Agglomeration in fluidized beds at high temperatures: Mechanisms, detection and prevention. Progress in Energy and Combustion Science: An international review journal 34 (5) (2008), page 633-666. DOI: 10.1016/j.pecs.2008.04.002.

[46] L. C. Williams, T. L. Westover, R. M. Emerson, J. S. Tumuluru and C. Li. Sources of Biomass Feedstock Variability and the Potential Impact on Biofuels Production. Bioenergy Research 9 (1) (2016), page 1-14. DOI: 10.1007/s12155-015-9694-y.

[47] N. B. K. Rasmussen and N. Aryal. Syngas production using straw pellet gasification in fluidized bed allothermal reactor under different temperature conditions. Fuel 263 (2020), 116706. DOI: 10.1016/j.fuel.2019.116706.

[48] D. J. Vega-Nieva, A. Garcia-Maraver and L. Ortiz. Slagging and Fouling Risks Derived from the Combustion of Solid Biofuels. WIT Transactions on State-of-the-art in Science and Engineering 85 (2015), page 137-147.
DOI: 10.2495/978-1-84566-062-8/008.

[49] Y. Niu Y, H. Tan and S. Hui. Ash-related issues during biomass combustion: Alkali-induced slagging, silicate melt-induced slagging (ash fusion), agglomeration, corrosion, ash utilization, and related counter measure, Progress in Energy and Combustion Science 52 (2016), page 1-61. DOI: 10.1016/j.pecs.2015.09.003.

[50] H. J. M. Visser, S. C. van Lindt and J. H. A. Kiel. Biomass Ash - Bed Material Interactions Leading to Agglomeration in FBC. Journal of Energy Resources Technology 130 (1) (2008), page 1-6. DOI: 10.1115/1.2824247.

[51] J. D. Morris, S. S. Daood, S. Chilton and W. Nimmo. Mechanisms and Mitigation of Agglomeration during Fluidized Bed Combustion of Biomass: A Review, Fuel 230 (2018), page 452-473. DOI: 10.1016/j.fuel.2018.04.098.

[52] M. Kuba, N. Skoglund, M. Öhman and H. Hofbauer. A review on bed material particle layer formation and its positive influence on the performance of thermo-

chemical biomass conversion in fluidized beds. Fuel 291 (2021) 120214. DOI: 10.1016/j.fuel.2021.120214.

[53] E. Brus, M. Öhman and A. Nordin. Mechanisms of bed agglomeration during fluidized-bed combustion of biomass fuels, Energy Fuels 19 (3) (2005), page 825–832. DOI: 10.1021/ef0400868.

[54] M. Öhman, L. Pommer and A. Nordin. Bed agglomeration characteristics and mechanisms during gasification and combustion of biomass fuels, Energy Fuels 19 (4) (2005), page 1742–1748. DOI: 10.1021/ef040093w.

[55] E. Natarajan, M. Öhman, M. Gabra, A. Nordin, T. Liliedahl and A. N. Rao. Experimental determination of bed agglomeration tendencies of some common agricultural residues in fluidized bed combustion and gasification, Biomass and Bioenergy, 15 (2) (1998), page 163-169. DOI: 10.1016/S0961-9534(98)00015-4.

[56] B. Gatternig and J. Karl. Prediction of ash-induced agglomeration in biomass-fired fluidized beds by an advanced regression-based approach, Fuel 161 (2015), page 157-167. DOI: 10.1016/j.fuel.2015.08.040.

[57] R. Chirone, F. Miccio and F. Scala. Mechanism and prediction of bed agglomeration during fluidized bed combustion of a biomass fuel: effect of the scale, Chemical Engineering Journal, 123 (3) (2006), page 71-80. DOI: 10.1016/j.cej.2006.07.004.

[58] W. Lin, K. D. Johansen and F. Frandsen. Agglomeration in bio-fuel fires fluidized bed combustors, Chemical Engineering Journal, 96 (1-3) (2003), page 171-185. DOI: 10.1016/j.cej.2003.08.008.

[59] E. Tiffault, S. Sokhansanj, M. Ebadian, H. Rezaei, E. O. B Ghiasi, F. Yazdanpanah, A. Asikainen and J. Routa. Biomass pre-treatment for bioenergy - Case study 2: Moisture, physical property, ash and density management as pre-treatment practices in Canadian forest biomass supply chains, IEA Bioenergy (2018). Report retrieved from:

https://www.ieabioenergy.com/wp-content/uploads/2018/10/CS2-Forest-biomass-pre-treatment.pdf. [Cited 2021 19/10/2021].

[60] M. Chen, X. Hou, J. Chen and B. Zhao. Phase Equilibria Studies in the SiO2-K2O-CaO System, Metallurgical and Materials Transactions B 47 (3) (2016). DOI: 10.1007/s11663-016-0623-z.

[61] S. V. Vassilev, D. Baxter, L. K. Andersen and C. G. Vassileva. An Overview of the Chemical Composition of Biomass, Fuel 89 (2010), page 913–933. DOI: 10.1016/j.fuel.2009.10.022.

[62] S. V. Vassilev, D. Baxter, L. K. Andersen and C. G. Vassileva. An overview of the composition and application of biomass ash.: Part 2. Potential utilization, technological and ecological advantages and challenges, Fuel 105 (2013), page 19-39. DOI: 10.1016/j.fuel.2012.10.001.

[63] D. Boström, M. Broström, N. Skoglund, C. Boman, R. Backman, M. Öhman and A. Grimm. Ash transformation chemistry during energy conversion of biomass, (2012). In: Impacts of Fuel Quality on Power Production & Environment, Finland (August 29 – September 3, 2010).

[64] S. V. Vassilev, C. G. Vassileva, Y. C. Song, W. Y. Li and J. Feng. Ash contents and ash-forming elements of biomass and their significance for solid biofuel combustion, Fuel, 208 (2017), page 377-409. DOI: 10.1016/j.fuel.2017.07.036.

[65] D. Boström, N. Skoglund, A. Grimm, C. Boman, M. Öhman, M. Broström and R. Backman. Ash Transformation Chemistry during Combustion of Biomass, Energy & Fuels 26 (1) (2012), page 85-93. DOI: 10.1021/ef201205b.

[66] S. Li, Q. Lu and H. Teng. Agglomeration during fluidized-bed combustion of biomass. The 13th international conference on fluidization - New paradigm in fluidization engineering, Art.36, Korea (2010).

[67] J. Werkelin, B. J. Skrifvars and M. Hupa. Ash-forming elements in four Scandinavian wood species. Part 1: Summer harvest, Biomass and Bioenergy 29 (6) (2005), page 451-466. DOI: 10.1016/j.biombioe.2005.06.005.

[68] A. Mlonka-Medrala, A. Magdziarz, M. Gajek, K. Nowinska and W. Nowak. Alkali metals association in biomass and their impact on ash melting behavior, Fuel 261 (2020), 116421. DOI: 10.1016/j.fuel.2019.116421.

[69] L. Dzurenda and L. Pňakovič. Influence of the burning temperature of the non-volatile combustible content of wood and bark of plantation-grown, fast-growing tree species upon ash production, and its properties in terms of fusibility, BioResources 11 (3) (2016), page 6464-6476.
DOI: 10.15376/BIORES.11.3.6464-6476.

[70] J. Werther, M. Saenger, E. U. Hartge, T. Ogada and Z. Siagi. Combustion of agricultural residues, Progress in Energy and Combustion Science 26 (1) (2000), page 1-27. DOI: 10.1016/S0360-1285(99)00005-2.

[71] Y. Shao, W. Jinsheng, F. Preto, J. Zhu and C. Xu. Ash Deposition in Biomass Combustion or Co-Firing for Power/Heat Generation, Energies 5 (12) (2012), page 5171-5189. DOI: 10.3390/en5125171.

[72] Y. Iqbal Y and I. Lewandowski. Biomass composition and ash melting behaviour of selected miscanthus genotypes in Southern Germany, Fuel 180 (2016), page 606-612. DOI: 10.1016/j.fuel.2016.04.073.

[73] S. Andersson and E. Hamedi. Biomass as fuel for reheating furnaces - focusing on impurities. KTH, Royal Institute of Technology, Stockholm, Sweden (2014).

[74] Y. Zhong, J. Gao, Z. Guo and Z. Wang. Mechanism and Prevention of Agglomeration/Defluidization during Fluidized-Bed Reduction of Iron Ore, From the Edited Volume: Iron Ore and Iron Oxide Materials, IntechOpen, UK, (2018). DOI: 10:5772/intechopen.68488.

[75] G. Tardos and R. Pfeffer. Chemical reaction induced agglomeration and defluidization of fluidized beds, Powder Technology 85 (1) (1995), page 29-35. DOI: 10.1016/0032-5910(95)03002-Q.

[76] A. Montes, M. Hamidi, C. Briens, F. Berruti, H. Tran and C. Xu. Study on the critical amount of liquid for bed materials agglomeration in a bubbling fluidized bed, Powder Technology 284 (2015), page 437-442.
DOI: 10.1016/j.powtec.2015.07.017.

[77] L. E. Fryda, K. D. Panopoulos and E. Karakaras. Agglomeration in fluidized bed gasification of biomass, Powder Technology 181 (3) (2008), page 307-320.
DOI: 10.1016/j.powtec.2007.05.022.

[78] Hesse Instruments. The Heating Microscope and EMII Software, (2016): https://www.hesse-instruments.de/fileadmin/downloads/Prospekt/BRO_EM301_EN_160608.pdf.
[Cited 2021 19/10/2021].

[79] CPFD Software LLC. Barracuda VR Solutions, (2020). Retrieved from:
https://cpfd-software.com/barracuda-vr-solutions/barracuda-vr
[Cited 2021 19/10/2021]

[80] Thapa R.K. and Halvorsen B.M. Study of Flow Behavior in Bubbling Fluidized Bed Biomass Gasification Reactor using CFD simulation. The 14th International Conference on Fluidization - From Fundamentals to Products, Eds, ECI Symposium Series, Volume (2013).

Part 2

Scientific papers

Paper 1

Flow behaviour in an agglomerated fluidized bed gasifier

This paper is published in the International Journal of Energy and Environment 10 (2) (2019), page 55-64.

INTERNATIONAL JOURNAL OF
ENERGY AND ENVIRONMENT

Volume 10, Issue 2, 2019 pp.55-64
Journal homepage: www.IJEE.IEEFoundation.org

Flow behavior in an agglomerated fluidized bed gasifier

Nora C I S Furuvik, Rajan Jaiswal, Britt M E Moldestad

Department of Process, Energy and Environmental Technology, Faculty of Technology, Natural Sciences and Maritime Sciences, University of South-Eastern Norway, Kjølnes Ring 56, 3901 Porsgrunn, Norway.

Received 4 Feb. 2019; Received in revised form 25 Mar. 2019; Accepted 27 Mar. 2019; Available online 31 March 2019

Abstract
The global energy demand has increased over the last decades and the need for utilization of energy produced from sustainable sources is stressed. Fluidized bed gasification of biomass is a thermochemical conversion process that involves heating and converting of biomass into a gaseous mixture of syngas. The syngas can be used for sustainable production of heat, power and biofuels for useful applications. Agglomeration of bed material due to ash melting is one of the biggest challenges associated with fluidized bed gasification of biomass. Inorganic alkali components from the biomass cause problems as they can form a sticky layer on the surface of the bed particles and make them grow towards larger agglomerates that will interfere with the fluidization process. The aim of this work was to study the effect of agglomerates on the flow behavior in a fluidized bed gasifier. The experiments were performed in a cold-flow model of a bubbling fluidized bed at ambient temperature. Three different experiments were carried out: (I) with sand particles as bed material, (II) with agglomerates located at the bottom of the bed and (III) with agglomerates located at the top of the bed. The results show that agglomerates lead to decreased pressure drop and increased minimum fluidization velocity. The minimum fluidization velocity increased from 0.035 m/s in the normal fluidized bed to 0.041 m/s in the agglomerated fluidized bed where the agglomerates were placed at the bottom of the bed. The minimum fluidization velocity increased further to 0.057 m/s in the agglomerated fluidized bed where the agglomerates where added from the top of the bed. This study also found that bed agglomeration causes channeling and poor fluidization conditions.
Copyright © 2019 International Energy and Environment Foundation - All rights reserved.

Keywords: Biomass gasification; Fluidized bed gasification; Fluidization, Agglomeration.

1. Introduction

In order to limit the earth's global warming due to increased CO_2-emissions, there is an urgent need to promote the use of sustainable alternatives to fossil fuels. Among all the renewable resources, biomass is considered the most important source for sustainable energy production [1]. One of the promising energy conversion technologies for biomass is fluidized bed gasification, which converts the biomass into a gaseous mixture of syngas in presence of heat and a gasifying agent [2]. The syngas consists of mainly hydrogen (H_2) and carbon monoxide (CO), which can be further converted into biofuels [3]. Fluidized bed conversion is the leading technology for utilization of a broad variety of solid fuels, and is proved particularly advantageous for biomass gasification technology [4]. In addition to their fuel flexibility, fluidized bed gasifiers are noted for their uniform heating, excellent heat transfer, high efficiency and low environmental impact. Despite the advantages with fluidized bed technology, some difficulties appear during the thermochemical conversion of biomass-derived fuels. Ash-related problems are the main obstacles for successful applications of fluidized bed gasification of biomass [3]. The major challenge associated with the ash produced in the gasification reactor is the formation of melted ash, which forms agglomerates that deposit at high temperatures. Bed agglomeration decreases both the heat transfer in the bed and the fluidization quality, resulting in poor conversion efficiencies and loss of control of the bed operation parameters. In the most severe cases, bed agglomeration can lead to total de-fluidization of the bed material [2]. The objective of this work is to study the effect of bed agglomeration on the flow behavior in fluidized bed gasification of biomass. In the present study, sand particles with a mean diameter of 175 µm are used as bed material. The experiments are carried out in a cold flow model of a bubbling fluidized bed. The minimum fluidization velocity is measured from the pressure drop in the bed at different superficial velocities. Bubble behavior in the bed is observed to study the fluidization characteristics of the bed material in an agglomerated fluidized bed.

2. Theory

2.1 Fluidization theory

Fluidization is the phenomenon in which solid particles are kept in a fluidized state by passing a gasifying medium through at an appropriate temperature. The gasifying medium can be steam, air or oxygen [6]. At a very low superficial velocity, the frictional force (drag) between the particles and the gasifying medium is too weak to suspend the particles, and the fluid passes straight through the void spaces between the particles. In this condition, the bed essentially remains fixed and the pressure drop in the bed is given by Ergun's equation [7]. As the superficial velocity is steadily increased, the bed expands slightly. The drag increases and at some point the particles begin to move. At a certain velocity, the upward-flowing fluid will suspend the particles [8]. This state is referred to as the minimum fluidization and the corresponding superficial velocity is the minimum fluidization velocity. The minimum fluidization velocity is useful as a rough indication of the quality of the fluidization, and is an important parameter required for the design and operation of a fluidized bed.

In fluidized state, the pressure drop through any section of the fluidized bed is equivalent to the weight of the solid particles per unit area. In this condition, the suspended particles exhibit fluid-like properties. The minimum fluidization velocity can be found both theoretically and experimentally. Theoretically, the minimum fluidization velocity is determined based on [8].

$$\underbrace{g(1-\varepsilon_{mf})(\rho_s-\rho_f)}_{\textit{Weight of particles}} = \underbrace{150\frac{u_{mf}\mu_f}{(\varphi_s d_p)^2}\cdot\frac{(1-\varepsilon_{mf})^2}{{\varepsilon_{mf}}^3} + 1.75\frac{u_f^2\rho_f}{\varphi_s d_p}\cdot\frac{(1-\varepsilon_{mf})}{{\varepsilon_{mf}}^3}}_{\textit{Drag force by upward moving fluid}} \tag{1}$$

Where ε_{mf} indicates the bed voids at minimum fluidization condition, ρ_f is the density of the fluid and ρ_s is the density of the bed material. u_{mf} is the superficial velocity at minimum fluidization, μ_f is the viscosity of the fluid, φ_s is the sphericity of the solid particles and d_p is the particle diameter.

For fluidization of small particles and Reynolds number less than 20, the viscous drag force dominate the process. The minimum fluidization velocity is then calculated by the mathematically expression [8].

$$u_{mf} = \frac{d_p^2(\rho_p-\rho_f)g}{150\mu_f}\cdot\frac{\varepsilon_{mf}^3\varphi_s^2}{1-\varepsilon_{mf}}\ ,\ Re_{mf} < 20 \tag{2}$$

Where Re_{mf} refers to Reynolds number.

Experimentally, the minimum fluidization velocity is determined by measuring the pressure drop in the bed at different superficial velocities. The data are plotted in a curve similar to Figure 1. At u_{mf}, the bed is at the boundary between fixed and fluidized conditions. As the velocity increases above u_{mf}, bubbles begin to form and the bed becomes fluidized.

The formation of bubbles in the fluidized bed depends on properties of the particles such as size, size distribution and density [9, 11]. Geldart classified particles into four types: A, B, C and D based on their fluidization behavior and mapped the particle types by its size and density in a diagram [12].

In the present study Group B particles are investigated, they are characterized by fluidizing easily due to good mixing of the particles in the bed. At the onset of fluidization, bubbles are formed. [8, 12].

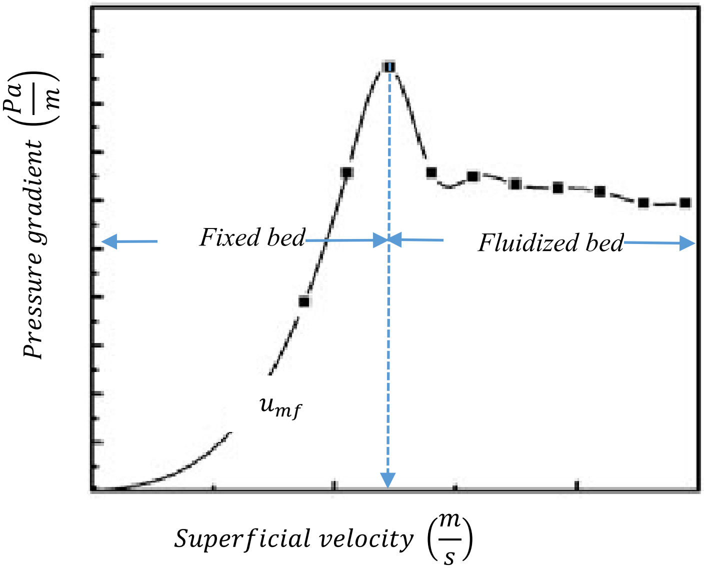

Figure 1. Pressure drop versus minimum fluidization velocity [10].

2.2 Bed agglomeration

Despite the widespread use of fluidized beds, the gasification process of biomass still has some difficulties [5]. The main problem is the melting or the partial melting of ash components that forms agglomerates, meaning the ash components adhere to each other to form larger entities [12].

During biomass gasification, inorganic alkaline components from the fuel can interact with silica from the bed material to form low-melting silicates that coat the bed particles [12]. If the alkali content is high enough, the coating melts and binds the bed particles together. Figure 2 illustrates how alkali-melt compounds contributes to the agglomeration process in a bubbling fluidized bed. The phenomenon occurs due to chemical reactions and physical collisions between the bed materials and the alkaline ash components. A consequence of the collisions is attachment of ash particles on the bed particles, resulting in formation of an adhesive and porous ash layer on the surface of the bed materials. As the ash particles and the bed materials continue to collide, the ash coating grow thicker. Eventually, the bed particles grow towards larger agglomerates that will interfere with the fluidization process. The agglomerates will become too large to be fluidized, and consequently they will stick to the walls or sink to the bottom of the bed and prevent the fluid to pass freely through. [12, 13].

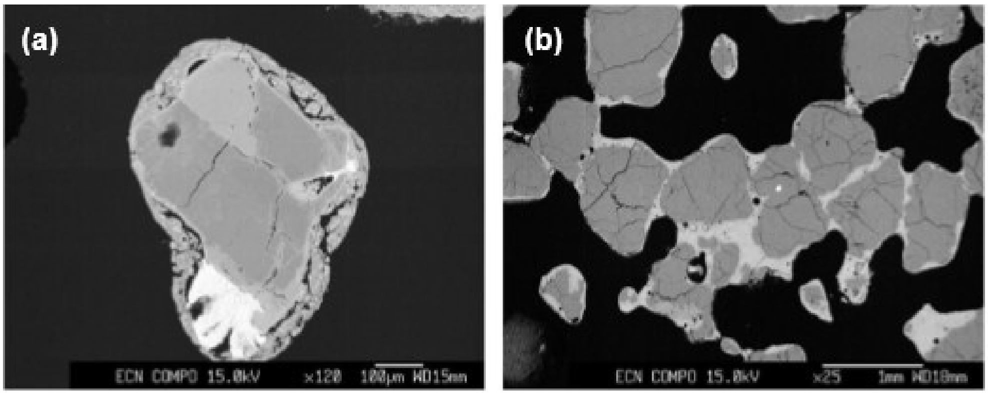
(a)
ECN COMPO 15.0kV ×120 100μm WD15mm
(b)
ECN COMPO 15.0kV ×25 1mm WD18mm

Figure 2. (a) silica sand particle surrounded by an alkali layer, (b) agglomerate formation [12].

Smooth fluidization is essential for efficient and effective operation as it ensures good contact between the particles, hence optimal heat transfer in the bed. Due to the distinctive shapes, sizes and densities, agglomerates are difficult to fluidize adequately. Figure 3 pictures the irregularity in structures and compositions of agglomerates. The sticky and cohesive particles forms small volumes in the bed that are not completely fluidized. These de-fluidized volumes will have decreased heat transfer leading to overall increased temperatures in the bed. Moreover, higher temperatures will increase the stickiness of the particle surfaces resulting in increased de-fluidized volume in the bed. Eventually, the bed takes a sluggish appearance. The unwanted collapse of the fluidized bed is rarely recognized until sudden de-fluidization occurs and often leads to shutdown of the whole installation [12].

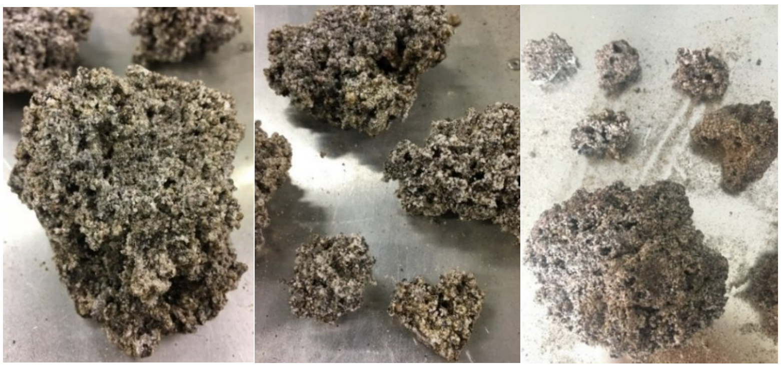

Figure 3. Agglomeration of silica sand particles.

Agglomeration of bed material and ash sintering during fluidized bed gasification of biomass has been reported frequently in the literature. Pietsch [14] defined agglomeration as *"the formation of larger entities from particulate solids by sticking particles together by short range physical forces between the particles themselves, or through substances that adhere chemically or physically to the solid surface and form a material bridge between the particles"*.

Bartles et al. [12] presented an overview of research in the area of the mechanism of agglomeration. According to this review paper, there is agreement among researchers that the agglomeration process in fluidized bed gasifiers is a result of stickiness or adhesiveness of bed material produced by alkali compounds derived from the biomass ash. Siegill [15] and Squires [16] describe the de-fluidization phenomena as a direct consequence of stickiness. They also claim that stickiness of bed material can be caused by changed properties of bed material at a certain temperature or due to presence of a liquid phase (melt) that deposit on the surface of the particles [17].

Visser et al. [18] proposed two different routes for the initiation of the bed agglomeration: 1) 'melt-induced' agglomeration and 2) 'coating-induced' agglomeration. The 'melt-induced mechanism is direct adhesion of the bed particles caused by alkali compounds (molten ash) that acts as a glue, forming hard bridges between the particles. The 'coating-induced' mechanism refers to the formation of sticky uniform coating layers on the surface of the bed particles due to chemical reactions between the bed materials and the fluid phase.

Extensive studies performed on agglomeration in fluidized beds indicate that agglomeration and deposition leads to decreased pressure drop and instabilities with bubbling and channeling of gas [8]. Tardos and Pfeiffer [19] stated that bed material agglomeration dramatically changes the fluidization behavior of a BFB, thus the fluidization characteristics of the bed such as the minimum fluidization velocity, the pressure drop across the bed and the bubble behavior. Therefore, changes in bubble properties can be useful as an indication of agglomeration in BFBs [5]. The bubble frequency are defined as the number of bubbles passing through a specific area of the bed in a certain period of time. Under normal conditions, the bubble frequency through different sections along the bed are similar. When agglomeration occurs, the fluidization behavior changes and the bubble frequency through the different sections within the bed becomes different. During an experimental study of standard deviation of bubble frequency (STDBF), Montes [5] observed that the bed was channeling in some locations as illustrated in Figure 4 [5].

One widely used and more appropriate experimental method to study the status of a bubbling fluidized bed is to measure the differential pressure. Under fluidized conditions, the pressure drop through the bed are equal to the total hydrostatic pressure of the bed. Due to channeling and agglomerated zones, agglomerated fluidized beds are characterized by lower pressure drop [5].

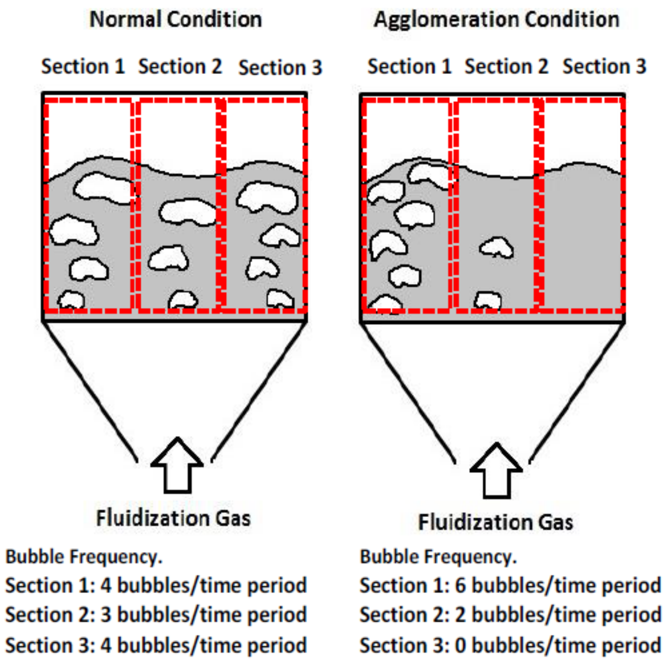
Normal Condition
Section 1
Section 2
Section 3
Agglomeration Condition
Section 1
Section 2
Section 3
Fluidization Gas
Fluidization Gas
Bubble Frequency.
Section 1: 4 bubbles/time period
Section 2: 3 bubbles/time period
Section 3: 4 bubbles/time period
Bubble Frequency.
Section 1: 6 bubbles/time period
Section 2: 2 bubbles/time period
Section 3: 0 bubbles/time period

Figure 4. Bubble frequency in a fluidized bed [5].

3. Material and methods

The experiments were performed in the cold flow bubbling fluidized bed shown in Figure 5. The fluidized bed system consists of a cylindrical transparent column with height 140 cm and a diameter of 8.4 cm. The static bed height was approximately 21 cm. The gasifying medium was ambient air introduced into the bed through a porous plate distributor installed at the bottom of the column. The distributor ensures uniform air supply. The top of the column was open to the atmosphere. Nine pressure transducers along the height of the column were constantly monitoring the pressure drop across the bed. The pressure transducers were connected to the systems engineering software LabWiew for data acquisition.

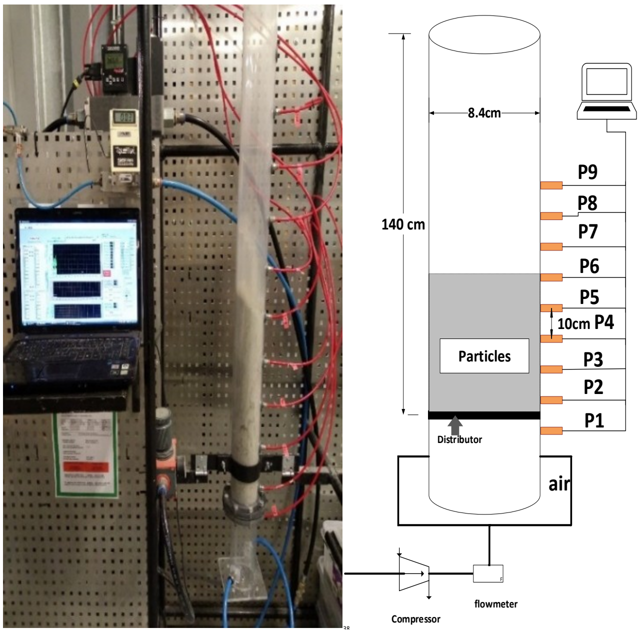
8.4cm
140 cm
P9
P8
P7
P6
P5
10cm P4
P3
P2
P1
Particles
Distributor
air
Compressor
flowmeter

Figure 5. Cold flow model of bubbling fluidized bed.

The bed material used in the experiments were sand particles with a mean diameter of 175 µm and a bulk density of 1431 kg/m^3. According to Geldart fluidization diagram, the bed material corresponds to group B particles. The agglomerates are porous, which give them low density. As they consists of a large amount of primary particles clustered together, the agglomerates have completely random shapes and sizes and are therefore difficult to classify by Geldart diagram. [12] In the present experiments, the agglomerates varied from approximately 2 cm to 8 cm and density approximately equal to 1510 kg/m^3, as pictured in Figure 6. The agglomerates were weighed and the density was calculated based on mass and volume. The volumes of the agglomerates was found using a graduated cylinder. A precisely measured volume of sand particles was poured into the cylinder. The agglomerate was submerged in the sand, and the volume of sand displaced by the submerged agglomerate equals the volume of the agglomerate.

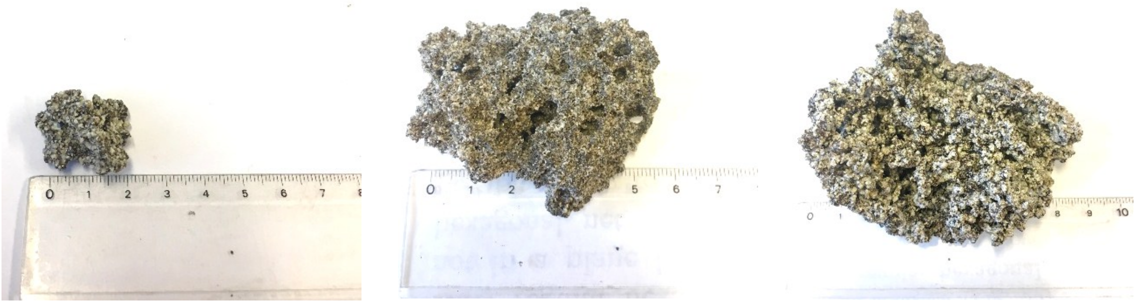

Figure 6. Agglomerates from fluidized bed gasification of biomass.

Prior to the experiments, a sieving analysis of the sand particles was carried out and the mean diameter was determined from the mass fraction [20]. The bed material was weighed and the bulk density was calculated based on the mass and volume. The agglomerates were introduced to the bed together with the bed material and the superficial velocity (u_f) was gradually increased. The pressure drop in the bed (Δp_{bed}) was measured at different u_f, and the bubble behavior was observed during the whole fluidization process. The experiments continued until slugging of the bed was observed. Three different cases of fluidization processes were carried out: (I) with bed material (II) with agglomerates added at the bottom of the bed and (III) with agglomerates added from the top of the bed. Detailed specifications for the experiments are listed in Table 1.

Table 1. Details for the performed experiments.

Experiment	Description	Particle size	Particle weight	Particle density
I	Bed material	175 µm	-	ρ_{Bulk} = 1431 kg/m^3
II	Agglomerates located at the bottom of the bed	Smallest ~2 cm Largest ~ 8 cm	Smallest: 2.9020 g Largest: 75.4766 g	$\rho_{Agglomerate}$ = 1510 kg/m^3
III	Agglomerates located in the upper layer of the bed	Smallest ~2 cm Largest ~ 8 cm	Smallest: 2.9020 g Largest: 75.4766 g	$\rho_{Agglomerate}$ = 1510 kg/m^3

4. Results and discussion

Smooth fluidization is essential for efficient and effective operation as it ensures good contact between the particles, hence optimal heat transfer in the bed. Smooth fluidization is a result of hydrodynamic, gravitational and inter-particle forces, and due to of the balance of forces bed agglomeration will interfere with the fluidization process. When agglomerates are present, the inter-particle forces are considerable and hence they will take control over the bed behavior.

In the present study of flow behavior in the fluidized beds, it was observed that with the presence of agglomerates, the bed was only partially fluidized. Figure 7 shows how Δp_{bed} varies with u_f for experiment (I) and experiment (II). Experiment (I) represents the flow behavior in a fluidized bed during normal fluidization, and experiment (II) represent the flow behavior in an agglomerated fluidized bed. For the agglomerated fluidized bed, Δp_{bed} was decreased and u_{mf} was increased. Decreased Δp_{bed} is a result of the bed particles growing into larger entities. These agglomerates are too large to be fluidized, and thus they will remain in the lower part of the bed and prevent the air from being evenly distributed. Moreover, bed agglomeration causes channeling and low particle-fluid contact, as the air tends to flow into the openings between the agglomerates. The poor air distribution might lead to de-fluidized volumes in the bed followed by complete de-fluidization.

The increase in u_{mf} is a result of the increased void fraction causing decreased drag forces. u_{mf} increases from 0.035 m/s in normal fluidization to 0.041 m/s in agglomerated fluidization. Lower u_{mf} means little gas bypassing and is beneficial for good mixing and high rates of heat and mass transfer. A consequence of the high u_{mf} is that the gasification process will be characterized by instabilities, with bubbling and channeling of air. Higher u_{mf} means higher air flow and thereby more oxygen mixed in the bed, which in turn may cause that the process will go towards combustion instead of gasification.

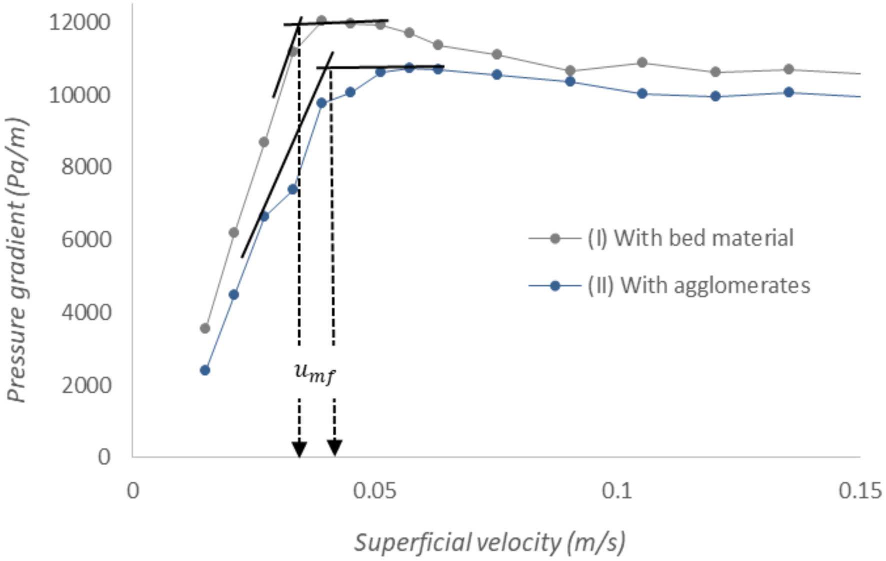

Figure 7. Fluidization in a normal and an agglomerated fluidized bed.

Figure 8 shows the variation in Δp_{bed} when u_f increases for experiment (II) and experiment (III). Experiment (II) represent the flow behavior when agglomerates are placed at the bottom of the bed, and experiment (III) represent the flow behavior when the agglomerates are placed at the top of the bed. It is seen that the different location of the agglomerates lead to different fluidization processes. Agglomerates that either stick to the wall of the bed or are located in the upper layer of the bed, entail higher u_{mf} and higher Δp_{max} than agglomerates that are located at the bottom or in the lower part of the bed. u_{mf} increases from 0.041 m/s in experiment (II) to 0.057 m/s in experiment (III). The increase in u_{mf} and Δp_{max} is a result of the bed expanding causing rise in bed porosity. Increase in void fraction decreases the overall drag until it is balanced by the total weight exerted by the solid particles.

As u_f increases beyond u_{mf}, the bubble formation increases. Figure 9 shows snapshots obtained of the bubbling behavior in the agglomerated fluidized bed during the fluidization experiments. When agglomerates were present, it was observed that the bed was not fully fluidized. In the agglomerated fluidized beds most of the bubbles collapsed at the bottom of the bed instead of passing through the entire bed (Figure 9-a). Visual observation also revealed that the bed material was in motion at the top of the bed, while the larger agglomerates remained at the bottom causing the gas to flow in channels between them (Figure 9-b). The agglomerated beds showed almost no expansion, and as the measured pressure drop was less than the bed weight indicating that the bed was not fully fluidized. In biomass gasification, this phenomenon causes improper circulation of the biomass and non-uniform temperature distribution in the bed. The non-uniform temperature distribution forms zones with de-fluidized volumes and increased temperatures. Higher temperatures increase the stickiness of the particle surfaces and might result in enhanced formation of agglomerates. Eventually, the bed takes a sluggish appearance.

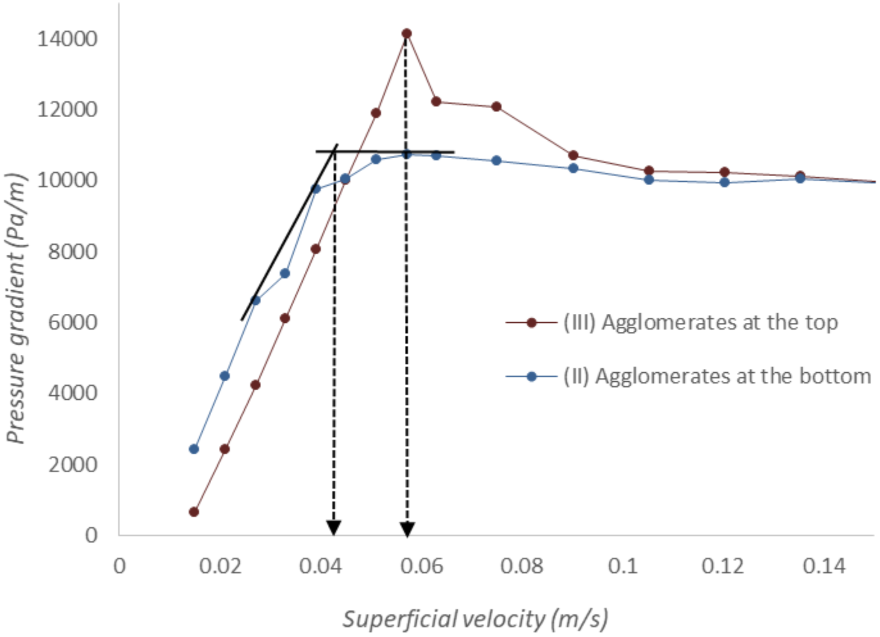

Figure 8. Fluidization in a normal and an agglomerated bed.

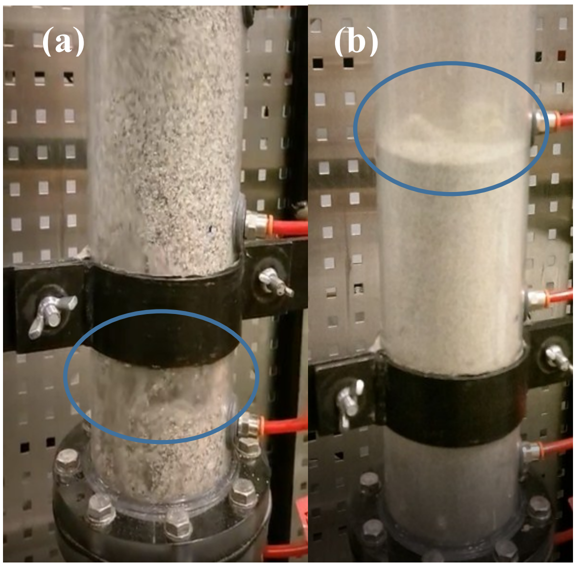

Figure 9. (a) Bubbles collapse at the bottom of the bed (b) air flows in channels of the bed.

5. Conclusion

The objective of this work was to study how agglomerates affect the flow behavior in fluidized bed gasification of biomass. The study included experiments performed in a cold flow model of a bubbling fluidized bed. The experiments were carried out with 175 µm sand particles as bed material. A mix of agglomerates of different sizes was introduced to the bed. The pressure drop across the bed and the minimum fluidization velocity were determined and the bubbling behavior was observed.

The formation of low-melting ash components such as alkali silicates creates problems in fluidized bed reactors, as the formation of sticky glassy melt causes bed particle agglomeration. This can happen when the ash particles on the bed particle surface stick together and sinter to form hard bridges between the particles. Agglomerates have peculiar shapes, sizes and densities, which make them difficult to fluidize and handle adequately. The formation of agglomerates cause instabilities with bubbling and channeling in the bed, resulting in loss of fluidization. When channeling occurs in the bed, the particle-gas contact becomes low and any heat and mass transfer operation is weakened. Consequently, de-fluidized volumes occur in the bed, which often lead to complete de-fluidization of the bed, followed by unscheduled shutdowns of the whole installation.

The experiments indicate that bed agglomeration changes the flow behavior in fluidized beds. The minimum fluidization velocity increased from 0.035 m/s in the normal fluidized bed to 0.041 m/s in the agglomerated fluidized bed where the agglomerates were placed at the bottom of the bed. The minimum fluidization velocity increased further to 0.057 m/s in the agglomerated fluidized bed where the agglomerates were added from the top of the bed. During the experiments, it was observed that the pressure drop decreased and the minimum fluidization velocity increased with the presence of agglomerates in the bed. Additionally, channeling was observed in the bed, and the bubble formation and bubbles growth in the bed was interrupted.

Acknowledgements

This study is funded by The Research Council of Norway, Programme for Energy Research (ENERGIX).

References

[1] A. Bridgewater. Biomass fast pyrolysis. Thermal Science 2 (2004), page 21-49.

[2] M. Öhman and A. Nordin. The Role of Kaolin in Prevention of Bed Agglomeration during Fluidized Bed Combustion of Biomass Fuels. Energy & Fuels 14 (2000), page 618-624.

[3] L. Wang, C.L. Weller, D.D. Jones & M.A. Hanna. Contemporary issues in thermal gasification of biomass and its application to electricity and fuel production. Biomass and Bioenergy 32 (2008), page 573-581.

[4] P. Basu. Biomass Gasification, Pyrolysis and Torrefaction, Second Edition. Academic Press, UK, 2013.

[5] A. Montes. Factors Affecting Bed Agglomeration in Bubbling Fluidized Bed Biomass Boilers. September 2014. Electronic Thesis and Dissertation Repository. 2320 (htps://ir.lib.owo.ca/etd/2325).

[6] F. Moradian. Ash Behavior in Fluidized-Bed Combustion and Gasification of Biomass and Waste Fuels. 2016. Thesis for the Degree of Doctor of Philosophy, University of Borås, Sweden. (http://urn.kb.se/resolve?urn=urn:nbn:se:diva-9563).

[7] S. Ergun. Fluid flow through packed columns. Chemical Engineering Progress 48(89) (1952)

[8] D. Kunii and O. Levenspiel. Fluidization Engineering, Second Edition. Butterworth-Heinemann, USA, 1994.

[9] R. Cocco, S.B. Reddy Karry and T. Knowlton. Introduction to Fluidization. American Institute of Chemical Engineering (AIChE) (November 2014).

[10] H. Sutar and C. Das Kumar. Mixing and Segregation Characteristics of Binary Granular Material in Tapered Fluidized Bed: A CFD Study. Engineering 04 (04) (2012).

[11] D. Gidaspow. Multiphase Flow and Fluidization. Academic Press Inc., USA, 1994.

[12] M. Bartles, W. Lin, J. Nijenhuis, F. Kapteijn and R. Ommen. Agglomeration in fluidized beds at high temperaures: Mechanisms, detection and prevention. Progress in Energy and Combustion Science 34 (2008), page 633-666.

[13] T. Lind. Ash formation in circulating fluidized bed combustion of coal and solid biomass. 1999. Dissertation for the Degree of Doctor of Technology, Helsinki University of Technology, Finland. (https://www.vtt.fi/inf/pdf/publications/1999/P378.pdf).

[14] W. Pietsch. Agglomeration Process: Phenomena, Technologies, Equipment, First Edition. Weinheim:Wiley-VCH.

[15] J.H. Siegill. Defluidization phenomena in fluidized bed of sticky particles at high temperatures. 1976. Dissertation for the degree of Doctor of Philosophy, The City University of New York, USA.

[16] A.M. Squires. Behavior of mineral matter in a fluidized bed-gasifying cone; the ignifluid process. Trans. Brit. Ceram. Soc. 75 (1976), page 85-91.

[17] N. Padban, S. Kiuru and A.L. Hallgren. Bed material agglomeration in PFB biomass gasification. Department of Chem. Eng. II. Chemical Center, University of Lund, Sweden.

[18] S. Visser, S. van Lith and J. Kiel. Biomass Ash-Bed Material Interactions Leading to Agglomeration in FBC. Journal of Energy Resources Technology (2008).

[19] G. Tardos and R. Pfeiffer. Chemical reaction induced agglomeration and de-fluidization of fluidized beds. Powder Technology 85 (1995), page 28-35.

[20] C.T. Crowe, J.D. Schwarzkopf, M. Sommerfield and Y. Tsuji. Multiphase Flows with Droplets and Particles, Second Edition. Taylor & Francis Group, USA, 2012.

Nora C. I. S. Furuvik has completed master’s degree in Energy and Environmental Technology from Telemark University College. At present she is working with her PhD degree in the field “Modelling of ash melts in gasification of biomass” at University of South-Eastern Norway.
E-mail address: nora.c.i.furuvik@usn.no

R. Jaiswal has completed master’s degree in Process Technology from University of South-Eastern Norway in the year 2018. He is working as a Research Assistant at the University of South-Eastern Norway under supervision of Prof. Britt M. E. Moldestad in the field of Biomass gasification.
E-mail address: rajanjaiswal357@outlook.com

Britt. M. E. Moldestad has her Master in Process Technology from Telemark University College. The PhD degree is from Norwegian University of Science and Technology and is in the field “Flow behavior in fluidized beds”. Her research work includes both experimental and computational multiphase studies. She has worked within the field of fluidization since 2000. She is employed as Professor in Process Technology at the University of South-Eastern Norway.
E-mail address: britt.moldestad@usn.no

Paper 2

CPFD Model for Prediction of Flow Behaviour in an agglomerated Fluidized Bed Gasifier

This paper was presented in the 10th International Conference on Computational & Experimental Methods in Multiphase & Complex Flow in Lisbon, Portugal on May 2019. The paper is published in International Journal of Energy Production and Management 4(2) (2019), page 105-114. DOI: 10.2495/EQ-V4-N2-105-114.

N. C. I. S. Furuvik, et al., Int. J. of Energy Prod. & Mgmt., Vol. 4, No. 2 (2019) 105-114

CPFD MODEL FOR PREDICTION OF FLOW BEHAVIOR IN AN AGGLOMERATED FLUIDIZED BED GASIFIER

NORA C.I.S. FURUVIK, RAJAN JAISWAL, RAJAN K. THAPA & BRITT M.E.MOLDESTAD
Department of Process, Energy and Environmental Technology, Faculty of Technology, Natural Science and Maritime Science, University of South-Eastern Norway, Norway.

ABSTRACT

Renewable energy sources have significant potential for limiting climate change and reducing greenhouse gas emissions due to the increased global energy demand. Fluidized bed gasification of biomass is a substantial contribution to meeting the global energy demand in a sustainable way. However, ash-related problems are the biggest challenge in fluidized bed gasification of biomass. Bed agglomeration is a result of interaction between the bed material and alkali metals present in the biomass ash. The agglomerates interfere with the fluidization process and might result in total de-fluidization of the bed. The study focuses on ash challenges related to the fluidization behavior in gasification of biomass. A model is developed and verified against results from previous performed experiments in a cold flow model of a bubbling fluidized bed. The commercial computational particle fluid dynamics (CPFD) software Barracuda Virtual Reactor is used for the computational study. The simulations show that the CPFD model can predict the fluidization process of an agglomerated fluidized bed gasifier.

Keywords: agglomeration, Barracuda VR, bubbling fluidized bed, CPFD simulation, flow behavior.

1 INTRODUCTION

Global warming is perhaps the most pressing environmental challenge in our time, and there is an urgent need to promote the use of renewable energy sources in order to ensure a sustainable future. The massive expansion in the use of fossil fuels and the rising fears over the effects of the increased CO_2 emissions have forced the countries to search for climate-friendly alternatives to fossil fuels [1]. Biomass-based energy is presently the largest contributor of renewable energy, and according to World Bioenergy Association, biomass annually accounts for 10.3% of the global energy supply [2]. The leading energy conversion technology for utilization of biomass fuels is fluidized bed gasification, which converts biomass into a gaseous mixture in the presence of heat and a gasifying medium [3].

Fluidized beds are noted for their high heat transfer, uniform heating and high productivity. Despite being a promising technology for sustainable heat and power generation, biomass gasification has operational problems that can restrict its commercialization [1]. Interactions between the bed material and the molten ash components cause formation of agglomerates, resulting in the ash components adhering to each other to form larger entities [4]. Bed agglomeration is the main obstacle for successful applications of biomass gasification [5]. Presence of agglomerates in the bed alters the flow behavior in the gasifier, causing changes in the fluidization properties and consequently loss of control of important operating parameters such as pressure drop, minimum fluidization velocity and bubble behavior. In the most severe cases, bed agglomeration can lead to total de-fluidization of the bed [6].

Due to the operational problems caused by bed agglomeration, extensive studies have been performed to gain more insight into the ash-related issues in biomass gasification. These research activities have provided important knowledge about ash from biomass, and the relation between ash composition and the ash melting temperatures. However, only few data are available on the ash melting and agglomeration, and its relation to the fluidization behavior

© 2019 WIT Press, www.witpress.com
ISSN: 2056-3272 (paper format), ISSN: 2056-3280 (online), http://www.witpress.com/journals
DOI: 10.2495/EQ-V4-N2-105-114

in a biomass gasification reactor. Understanding the phenomenon of agglomeration is crucial to optimizing the design and the operation conditions of a bubbling fluidized bed gasification reactor. The objective of this work is to develop a computational particle fluid dynamics (CPFD) model that describes how the agglomerates affect the fluidization process in a bubbling fluidized bed reactor.

The model is based on theoretical and experimental studies. The commercial CPFD software package, Barracuda Virtual Reactor (VR) 17.1.0 is used for the computational study. The CPFD model is validated against previous performed experimental results carried out in a cold flow model of a bubbling fluidized bed [7].

2 BED AGGLOMERATION

Ash melting and subsequently formation of agglomerates is one of the major challenges in fluidized bed gasification of biomass [4]. Bed agglomeration occurs due to chemical reactions and physical collisions between the bed material and biomass ash with high content of alkali species. The phenomenon is illustrated in Fig. 1, which is based on [8]. Bed agglomeration happens as the inorganic alkali ash components interact with the bed material to form a sticky layer on the surface of the bed materials. As the ash particles and the bed material continue to collide, the ash coating grows thicker. Eventually, the bed particles grow towards larger agglomerates that will interfere with the fluidization process [4].

The main problem with ash melting and agglomeration in fluidized beds is the issue of de-fluidization. The agglomerated ash-particles (Fig. 2) differ considerably from the bed particles in shapes, sizes and densities, and are therefore difficult to fluidize adequately. At the time of de-fluidization, a sudden decrease in the pressure drop over the bed is observed as the sticky and cohesive agglomerated ash particles form small volumes in the bed. These volumes are not fully fluidized, leading to improper circulation of the biomass and thereby non-uniform temperature distribution and decreased heat transfer in the bed. Inside the de-fluidized volumes, the temperatures will be increased, which in turn increases the stickiness of the particle surfaces resulting in enhanced agglomeration [7].

The poor mixing and the decreased heat transfer that occur due to bed agglomeration change the bubble behavior in the bed. While normal fluidization conditions give well-distributed bubble frequency through all sections along the bed, the fluidization in the agglomerated bed is characterized by instabilities with frequent bubbling and channeling of fluid. Eventually, the bed takes a sluggish appearance. The unwanted collapse of the fluidized bed is rarely recognized until sudden de-fluidization occurs, and might lead to shutdown of the whole installation [4]. Figure 3 illustrates the bubble behavior in a normal fluidized bed compared to the bubble behavior in an agglomerated fluidized bed.

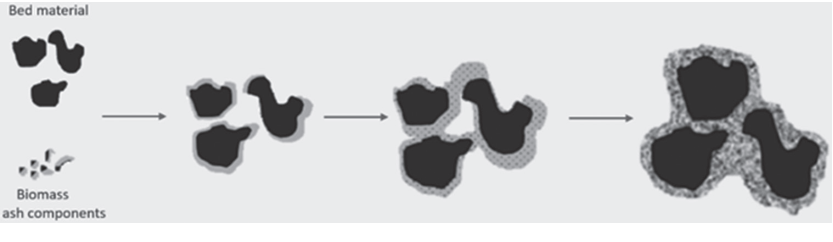

Figure 1: Formation of agglomerates.

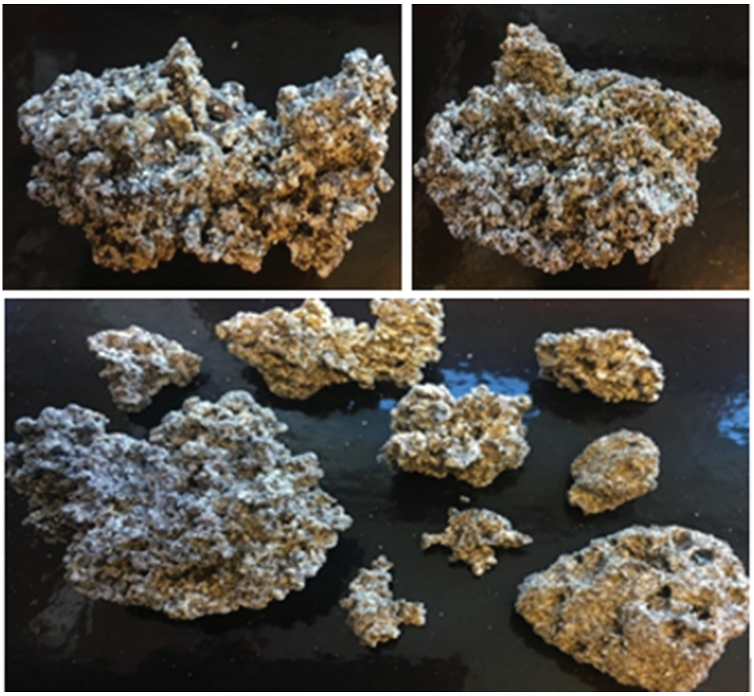

Figure 2: Agglomeration of silica sand particles.

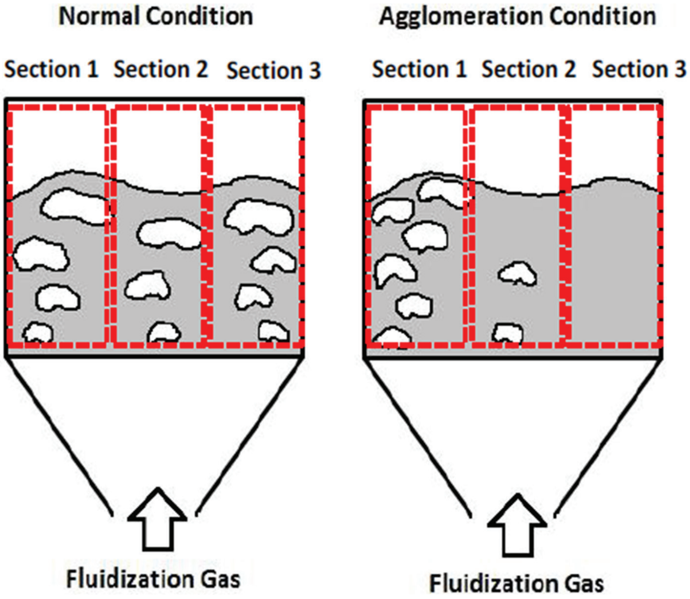
Normal Condition
Agglomeration Condition
Section 1
Section 2
Section 3
Section 1
Section 2
Section 3
Fluidization Gas
Fluidization Gas

Figure 3: Bubble frequency in a fluidized bed [9].

3 MODEL DEVELOPMENT

3.1 Model description

The CPFD software package Barracuda VR 17.1.0 was used to simulate the flow characteristics in an agglomerated bubbling fluidized bed. Barracuda VR uses the Multiphase Particle In-Cell (MP-PIC) approach that is based on the Eulerian–Lagrangian approach, where the transport equations are solved for the continuous fluid phase and each of the discrete particles are tracked through the calculated fluid field. The fluid–particle interaction is considered as source terms in the transfer of mass, momentum and energy between the two systems. CPFD simulations are hybrid numerical methods where the Eulerian approach is used for solving the fluid phase, and the Lagrangian computational particle approaches for the modeling of the particle phase [10]. Chladek *et al.* [11] and Jayarathna *et al.* [12] describe the transport equations in detail.

The Barracuda software package includes several drag models. In order to find the most suitable model for the simulations of flow characteristics in an agglomerated fluidized bed gasifier, different drag models were tested. The best fit between the numerical model (simulation) and the experimental results was achieved with the Wen–Yu drag model. Wen–Yu drag model is based on a variety of experiments performed by Richardson and Zaki [13]. The correlation developed from the experimental data achieved by Richardson and Zaki [13] is valid when the internal forces are negligible, meaning that the viscous drag forces dominate the flow behaviour.

In general, the drag force caused by the fluid on the particles is calculated from:

$$F_p = m_p \cdot D \cdot \left(u_f - u_p\right) \tag{1}$$

where m_p is the particle mass, D the drag function, u_f the superficial velocity of the fluid and u_p the superficial velocity of the particles. The Wen–Yu drag function is dependent on the fluid and the particle properties and is expressed by the drag coefficient (C_d):

$$D = \frac{3}{8} \cdot C_d \cdot \frac{\rho_f \cdot \left(u_f - u_p\right)}{\rho_p \cdot r_p} \tag{2}$$

where ρ_f and ρ_p is the density of the fluid and the particle, respectively, and r_p the particle radius. C_d is a function of Reynolds number *(Re)* and the fluid volume fraction *(θ_f)*, and is determined according to a set of conditions shown in eqn (3).

$$C_d = \begin{cases} \frac{24}{Re} \cdot \theta_f^{n_0}\ 0.5 < Re \\ . \\ \frac{24}{Re} \cdot \theta_f^{n_0} \cdot \left(c_0 + c_1 \cdot Re^{n_1}\right) 0.5 \le Re \le 1000 \ . \\ . \\ c_2 \cdot \theta_f^{n_0}\ Re > 1000 \end{cases} \tag{3}$$

Reynolds number is determined by

$$Re = \frac{2 \cdot \rho_f \cdot r_p \cdot \left(u_f - u_p\right)}{\mu_f} \tag{4}$$

where μ_f is the viscosity of the fluid. More detailed information of the Wen–Yu drag model are presented by Wen and Yu [14].

3.2 Computational setup

The cold flow model of the fluidized bed used in the experimental study is shown in Fig. 4.

A three-dimensional Cartesian coordinate system was used to describe the cylindrical column with a height of 140 cm and a diameter of 8.4 cm. In the present study, the static bed height was 21 cm. The computational grid is shown in Fig. 5. The mesh size was 0.01 m x 0.01 m x 0.01 m and the number of control volumes was 13,284. Isothermal temperature at 300 K was used, and the fluidizing gas was air at atmospheric pressure that was flowing through the gas distributor from the bottom of the column. The total pressure was monitored at positions 3.5 cm (P1) and 13.5 cm (P2) above the distributor. The simulation was run for 50 s with a time step of 0.001 s. The simulation parameters are summarized in Table 1. The Wen–Yu drag model was selected, and the coefficient values c_0, c_1, c_2, n_0 and n_1 were equal to 1.0, 0.15, 0.44, –2.65 and 0.687, respectively.

Quartz sand with a Solid density of 2,650 kg/m^3 was used as bed material. The particle size of the sand ranged from 150 μm to 340 μm with a mean diameter of 175 μm. The particle size distribution was determined by sieving analysis. The maximum close pack volume fraction was set to 0.54, which was calculated based on the ratio of the bulk density and the particle density. The maximum momentum from the redirection of particles collision was

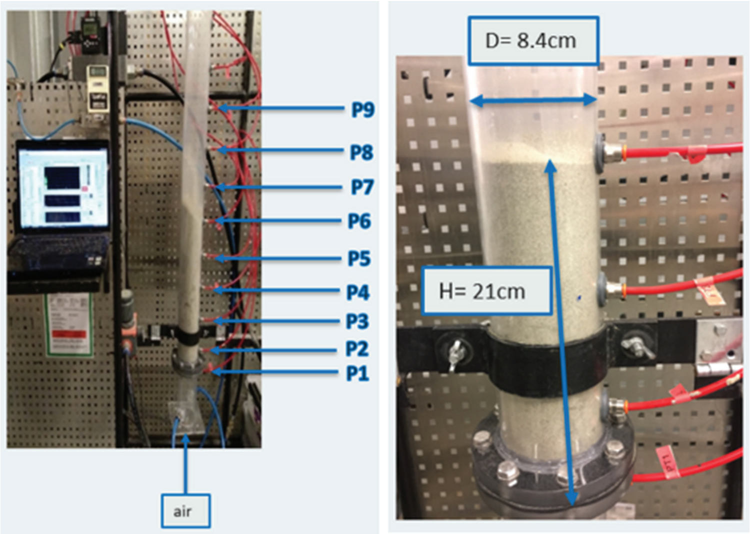

Figure 4: Cold flow model of bubbling fluidized bed.

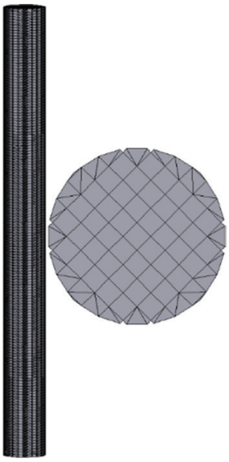

Figure 5: Computational grid.

Table 1: Simulation parameters.

Parameter	**Value**
Number of grid cells	13,284
Static bed height	21 cm
Fluidizing agent	Air
Type of flow	Isothermal @ 300 k
Superficial gas velocity	0.02: 0.005: 0.15 m/s
Simulation time for each flowrate	50 s
Drag model	Wen–Yu
Drag coefficients (c_0, c_1, c_2, n_0, n_1)	Default values

assumed to be 40%, the normal-to-wall and tangential-to-wall momentum retention were 0.3 and 0.99, respectively. The particle properties are listed in Table 2.

The flow behavior in an agglomerated fluidized bed was studied by comparing three different CPFD simulations, where agglomerates were present in the bed. The different cases were defined with 5%, 10% and 15% of agglomerates. In order to simulate agglomerates, a coarser

Table 2: Particle properties.

	Property			
Particle	**Mean diameter (µm)**	**Density (kg/m^3)**	**Sphericity**	**Close pack volume fraction**
Bed material	175	2,650	0.86	0.54
Agglomerates	N/A	1,506	0.6	N/A

grid was used and the number of grid cells was reduced from 13,284 to 5,782. The size of the agglomerates was limited by the chosen grid, which allowed a maximum particle size of 1.0 cm. The agglomerates ranged from 0.5 cm to 1.0 cm in diameter, with density equal to 1,506 kg/m^3. The density of the agglomerates was determined based on mass and volume [7].

4 RESULTS AND DISCUSSION

The Wen–Yu drag model was used in the CPFD simulations. The model was validated by customizing it to the previous performed experimental results for sand particles with a mean diameter of 175 μm [7]. The pressure drop in the bed was plotted as a function of the superficial air velocity. As the superficial velocity is steadily increased, the bed expands slightly. The drag caused by the fluid on the particles increases and at some point, the particles begin to move. At a certain velocity, the particles will be suspended by the upward-flowing fluid [15]. This state is referred to as the minimum fluidization and the corresponding superficial velocity is the minimum fluidization velocity (u_{mf}). Figure 6 compares the simulation with the experimental result. The simulated minimum fluidization velocity was 0.039 m/s, which is slightly higher than the experimental value of 0.035 m/s.

The deviation between the simulation and the experiment can be related to how the characteristics of the particles influence on the fluidization processes, and how the numerical model accounts for the particle size distribution. Barracuda uses the MP-PIC-based Euler–Lagrangian approach, which means that instead of tracking each individual particle in the bed separately, particles with the same properties are grouped into parcels. Each parcel is represented by one computational particle, in which the equation for motion is solved as the discrete particle moves through the flow field [16]. Another explanation for the deviation might be erroneous assumptions for the drag model coefficients, c_0, c_1, n_0 and n_1. The value of c_2 will not influence on the results as it only has significance when $Re > 1{,}000$. Which is not the case for the present work. In order to find the model that shows the best agreement with the experimental results, several simulations with different values for the coefficients were performed. Finally, the default values provided in Barracuda were chosen for all the coefficients. In Fig. 6, it is seen that the simulation has a significant peak in the pressure drop at the onset of fluidization. However, the pressure drop decreases quickly after fluidization and stabilizes at approximately the same value as in the experiment, corresponding to the weight of the particles [11].

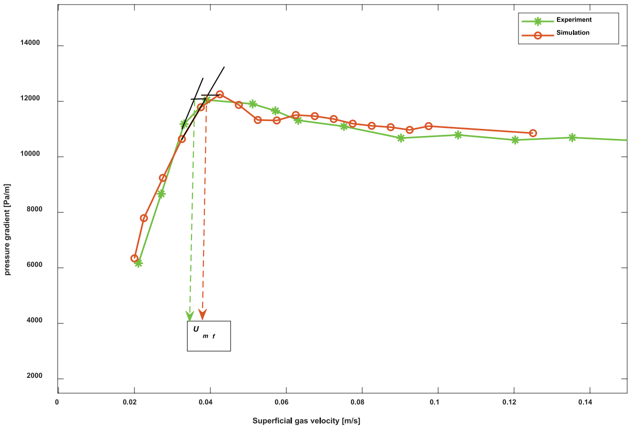

Figure 6: Pressure drop as a function of increasing superficial air velocity.

The result shows that the validated CPFD model describes the fluidization of the sand particles with good agreement, and the model was used to simulate the fluidization conditions in an agglomerated fluidized bed. Figure 7 shows how bed agglomeration changes the fluidization characteristics of the bed. Smooth fluidization is a result of hydrodynamic, gravitational and inter-particle forces. When agglomerates are present in the bed, the inter-particle forces take control over the bed behavior, and the agglomerates will interfere with the fluidization process. As the sticky particles grow into larger entities, the particles lose their original weight and are no longer able to be fluidized by the initial gas velocity. Under fluidized conditions, the pressure drop through the bed is equal to the total hydrostatic pressure of the bed, but due to channeling and agglomerated zones, agglomerated fluidized beds are characterized by lower pressure drop than normal fluidized beds.

The decreased pressure drop in the agglomerated fluidized beds indicates that the beds are not completely fluidized, as the bubbles collapse at the bottom of the bed instead of passing through the entire bed. Figure 8 illustrates the distribution of the particle species in the agglomerated fluidized bed, initially (Fig. 8a) and after fluidization (Fig. 8b). Blue color indicates bed

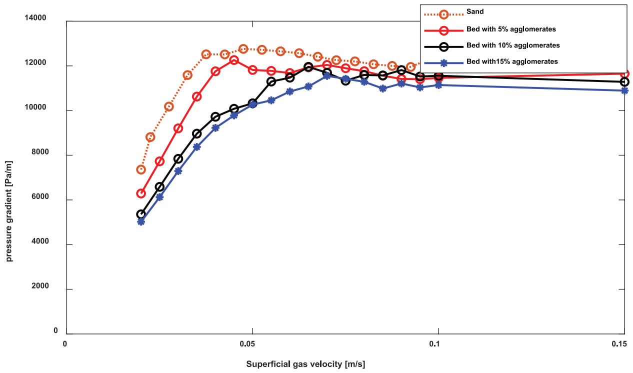

Figure 7: Simulation of fluidization in normal and agglomerated fluidized bed.

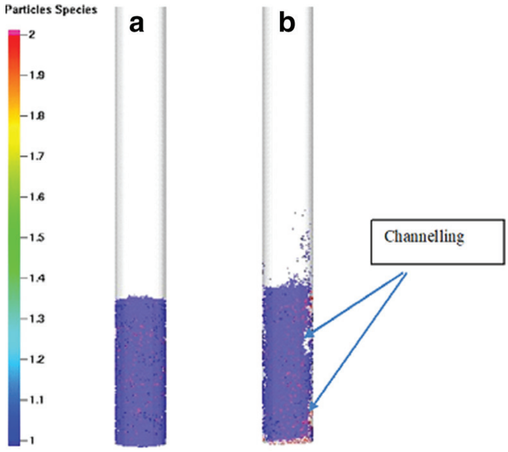

Figure 8: (a) Initial particle species and (b) particle species after fluidization.

particles, while red color indicates agglomerates. The bed material are in motion at the top of the bed, while the agglomerates remain at the bottom and one side of the column resulting in the gas flowing in channels. In biomass gasification, agglomeration causes improper circulation of the biomass and non-uniform temperature distribution in the bed. The non-uniform temperature distribution forms zones with de-fluidized volumes and increased temperatures. Higher temperatures increase the stickiness of the particle surfaces and might result in enhanced formation of agglomerates. Eventually, the bed takes a sluggish appearance.

5 CONCLUSION

The objective of this study was to develop a CPFD model for simulation of the flow behavior in an agglomerated fluidized bed gasifier. The simulations were performed using the commercial CPFD software package Barracuda VR.

The agglomerates consist of a large amount of primary particles clustered together. They have irregular shapes, sizes and structures, and are therefore difficult to fluidize and handle adequately.

The simulations show that bed agglomeration influences the fluidization characteristics of a bubbling fluidized bed. The pressure drop decreases and the minimum fluidization velocity increases when agglomerates are present in the bed. Moreover, the formation of agglomerates cause large instabilities with uneven distribution of bubbles and channeling that lead to loss of fluidization. When channeling occurs in the bed, there is less contact between gas and particles and the heat and mass transfer operation is weakened. Consequently, de-fluidized zones occur, which in turn can lead to unscheduled shutdowns of the whole installation.

ACKNOWLEDGEMENTS

This study is funded by The Research Council of Norway, Program for Energy Research (ENERGIX), Project 280892 FLASH – Predicting the FLow behavior of ASH mixtures for production of transport biofuels in the circular economy.

REFERENCES

[1] Sansaniwal, S.K., Rosen, M.A. & Tyagi, S.K., Global challenges in the sustainable development of biomass gasification: an overview. *Renewable and Sustainable Energy Reviews*, **80**, pp. 23–43, 2017. https://doi.org/10.1016/j.rser.2017.05.215

[2] World Bioenergy Association, *WBA Global Bioenergy Statistics*, 2017.

[3] Basu, P., *Biomass Gasificaion, Prolysis and Torrefaction*, 2nd edn., Academic Press Inc.: UK, 2013.

[4] Bartles, M., Lin, W., Nijenhuis, J., Kapteijn, F. & Ommen, R., Agglomeration in fluidized beds at high tempearures: Mechanisms, detection and prevention. *Progress in Energy and Combustion Science*, **34(5)**, pp. 633–666, 2008. https://doi.org/10.1016/j.pecs.2008.04.002

[5] Wang, L., Weller, C.L., Jones, D.D. & Hanna, M.A., Contemporary issues in thermal gasification of biomass and its application to electricity and fuel production. *Biomass and Bioenergy*, **32(7)**, pp. 573–581, 2008. https://doi.org/10.1016/j.biombioe.2007.12.007

[6] Khadilkar, A.B., Rozelle, P.L. & Pisupati, S.V., Investigation of fluidized bed agglomerate growth process using simulations and SEM-EDX characterization of laboratory-generated agglomerates. *Chemical Engineering Science*, **184**, pp. 172–185, 2018. https://doi.org/10.1016/j.ces.2018.03.035

[7] Furuvik, N.C.I.S., Jaiswal, R. & Moldestad, B.M.E., Flow behaviour in an agglomerated fluidized bed gasifier. *International Journal of Energy and Environment*, **10(2)**, pp. 55–64, 2019.

[8] Moradian, F.A., *Behaviour in Fluidized-Bed Combustion and Gasification of Biomass and Waste Fuels*, Thesis for the Degree of Doctor of Philosophy, University of Borås, Sweden, 2016.

[9] Montes, A., *Factors Affecting Bed Agglomeration in Bubbling Fluidized Bed Biomass Boilers*, Electronic Thesis and Dissertation Repository, September 2014.

[10] Thapa, R.K. & Halvorsen, B.M., Stepwise analysis of reactions and reacting flow in a dual fluidized bed gasification reactor. *WIT Transactions on Engineering Sciences*, **82**, pp. 37–48, 2014.

[11] Chladek, J., Jayarathna, C.K., Moldestad, B.M.E. & Tokheim, L.A., Fluidized bed classification of particles of different size and density. *Chemical Engineering Science*, **177**, pp. 155–162, 2018. https://doi.org/10.1016/j.ces.2017.11.042

[12] Jayarathna, C.K., Moldestad, B.E. & Tokheim, L.A., Validation of results from Barracuda® CFD modelling to predict minimum fluidization velocity and pressure drop of Geldart A particles. *Proceedings of the 58th SIMS Conference*, 2017.

[13] Richardson, J.F. & Zaki, W.N., Sedimentation and fluidisation: Part I. *Chemical Engineering Research and Design*, **75**, pp. S82–S100, 1997. https://doi.org/10.1016/s0263-8762(97)80006-8

[14] Wen, C. & Yu, Y., Mechanics of fluidization. *Chemical Engineering Progress Symposium Series*, **62**, pp. 100–111, 1966.

[15] Kunii, D. & Levespiel O., *Fludization Engineering*, 2nd edn., Butterworth-Heinemann: USA, 1994.

[16] Crowe, C.T., Schwarzkopf, J.D., Sommerfield, M. & Tsuji, Y., *Multiphase Flows with Droplets and Particles*, 2nd edn., Taylor & Francis Group: USA, 2012.

Paper 3

Study of agglomeration in fluidized bed gasification of biomass using CPFD simulations

This paper was presented in the 60th International Conference of Scandinavian Simulation Society, SIMS 2019 was held in Västerås, Sweden on August 2019.

The paper is published in Linköping Conference proceedings, Volume 170 (2019), page 176-181. DOI: 10.3384/ecp20170176.

Study of agglomeration in fluidized bed gasification of biomass using CPFD simulations

Nora C I S Furuvik Rajan Jaiswal Rajan K Thapa Britt M E Moldestad

Department of Process, Energy and Environmental Technology, University of South-Eastern Norway, Norway,
{nora.c.i.furuvik rajan.k.thapa, britt.moldestad}@usn.no
Rajanjaiswal357@outlook.com

Abstract

Fluidized beds have been widely applied for the gasification of biomass. However, at high temperatures ash melting and subsequently bed agglomeration may occur. When biomass is used for thermal conversion processes, inorganic alkali components present in the biomass fuels can be responsible for major problems. Understanding the ash melting and agglomeration in various gasification temperatures is crucial to optimize the design and operation conditions of a fluidized bed gasifier. This study focuses on the ash melting and the agglomeration process in a bubbling fluidized bed biomass gasification reactor. Using standard techniques, ash-melting analyses were performed to determine the initial agglomeration temperature in laboratory prepared ash samples from woodchips from Austria. Computational Particle Fluid Dynamic (CPFD) simulations were carried out using the commercial CPFD software package Barracuda Virtual Reactor (VR). The results show that the fluid dynamics gives important indications of unwanted agglomeration processes in a biomass gasification in a bubbling fluidized bed.

Keywords: bubbling fluidized bed, biomass gasification, agglomeration, CPFD simulations

1 Introduction

Climate changes are perhaps the biggest and most challenging environmental problems the world faces today. Greenhouse gas emissions from burning of fossil fuels for heat and power generation are major contributors to the earth's global warming. Over the last decades, it has been a growing attention to the use of renewable energy as an effective tool to fight the climate changes. On global basis, renewable energy were estimated to account for 14.1% of the total 573 EJ of primary energy supply in 2014, of which the largest energy contributor was biomass (10.3%) (World Bioenergy Association, 2017).

Fluidized bed gasification (FBG) is an important route for conversion of biomass into useful gaseous products, including syngas that can be further utilized into biofuels. Fluidized bed gasifiers offer distinct advantages over other conversion technologies, especially regarding to their uniform temperatures and excellent heat transfers. (Basu, 2013) However, because of the special ash-forming constituents of biomass fuels, biomass ash has shown to be particularly problematic in high temperature FBG processes (Wang et al., 2008). Generally, these problems are associated with the ash melting and following agglomeration of bed material (Van der Drift, 1999). Bed agglomeration is a result of interaction between the bed material and molten biomass ash with high content of alkali metals. When biomass is used for thermal conversion, alkali species from the fuel can react readily with silica (Si) from the bed material. As a consequence, the particles become coated with an adhesive layer that glue the particles together forming larger agglomerates. (Bartles et al., 2008) Bed agglomeration leads to poor fluidization conditions, and in the most severe cases it causes de-fluidization and subsequently total shutdown of the gasification process. Fundamental understanding of the ash behavior in thermal conversion of biomass, is necessary to improve the operational conditions in FBG (Khadilkar, 2018).

The objective of this work is to (a) study the melting behavior of woody biomass ash in correlation to standard ash melting tests (b) use a previous validated CPFD model to simulate agglomeration in a bubbling fluidized bed gasifier.

The ash-melting analyses are performed using a Leco Ash Fusion Determinator (AF700). In this test, the temperature at which the ash starts to melt is determined, giving a good indication of the temperature at which agglomerates can be formed. Laboratory prepared ash from woodchips from Austria are used for the ash melting analyses. The CPFD model is developed to get a better understanding of the problem with agglomeration phenomenon in a bubbling fluidized bed biomass gasification reactor. The connection between the ash melting behavior, operating temperatures and bed agglomeration in a FBG is investigated. The simulations are carried out using the commercial CPFD software package Barracuda VR.

DOI: 10.3384/ecp20170176

2 Theory

2.1 Bed agglomeration

In the literature, there is good agreement that alkali metals are the main components causing problems with bed agglomeration in FBG of biomass. (Bartles et al., 2008) The agglomeration process happens in two ways, either as melt-induced agglomeration or as coating-induced agglomeration. The melt-induced mechanism is direct adhesion of the bed particles because of alkali compounds from the molten ash acting as a glue that forms hard bridges between the particles. The coating-induced mechanism happens due to chemical reactions, between the bed material and the molten ash components, causing formation of a sticky uniform coating layer on the surface of the bed particles. (Visser et al., 2008) Bed agglomeration is in most cases a result of the inorganic alkali ash components combining with Si, either from the bed material or from the ash itself, to form low-melting silicates (eutectics) that coat the bed particles. These eutectics are characterized by a lower melting point than the individual components. If the alkali concentrations are too high, the coating melts and adheres the particles together. As a consequence of repeated collisions between these sticky ash-coated particles, the particles eventually grow towards larger agglomerates. (Badhoilya, 2018) The phenomenon is shown in Figure 1, an illustration based on (Moradian).

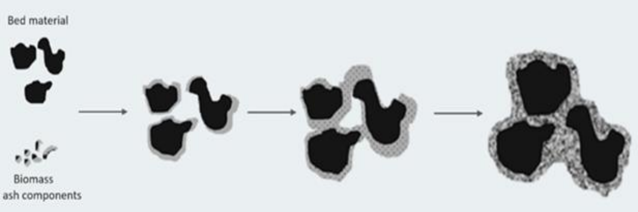

Figure 1. Agglomeration process.

Ash melting and following bed agglomeration is a key concern in fluidized bed biomass gasification reactors. The problems are mainly coupled to the high temperature chemistry of ash, i.e. its melting at different gasification temperatures. Proper fluidization of the particles needs to be maintained in order to stabilize the operational conditions of the fluidized bed (Badholiya 2018). As the agglomerated particles are of greatly irregular shape, size and structure, they will interfere with the fluid dynamics in the bed. In Figure 2 agglomerates from bubbling fluidized bed gasification of biomass is pictured.

In FBG the particle movement is one of the most important factors due to the corresponding transfer of energy. Under normal conditions, this energy transfer is so effective that the temperature difference across the cross section of the bed is kept approximately equal to zero. When agglomerates are present in the bed, the bed mixing becomes more ineffective due to obstructed particle movement. If this agglomeration process comes out of control, it can lead to severe agglomerate formation and subsequently shutdown of the gasification process. (Bartles et al., 2008, Badhoilya 2018) The obstruction in the particle movement can result in local temperature deviations that in turn creates de-fluidized volumes in the bed. De-fluidization is described as a total collapse of the fluidized bed leading to rapidly decreasing pressure drop and substantial temperature changes. (Van der Drift, 1999)

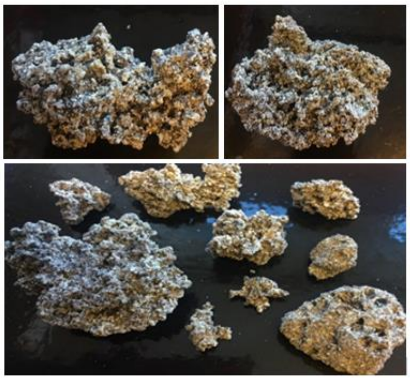

Figure 2. Agglomerates from silica sand particles.

2.2 Ash melting

Biomass is greatly varying in its physical properties and chemical composition, and the ash melting behavior is greatly affected by the ash composition. The biomass ash composition is in turn essential when it comes to the efficiency of a FBG process. (Badholiya, 2016) Biomass fuels with high ash content and low ash melting temperatures have limited possibilities for successful applications due to problems with ash melting, and agglomeration that occur under certain conditions. (Dragutinovic 2017) In general, woody biomass has very low ash content, typically below 1 %, of which approximately 40 % calcium (Ca), 15 % potassium (K) and 20 % Si. (Vassilev et al., 2017)

Previous studies have indicated that the bed agglomeration process is heavily dependent on the chemical characteristics and melting behaviors of the coating on the surface of the bed particles (Vassilev et al., 2017). Typically, elements such as Ca and magnesium (Mg) increase the ash melting temperature, while Si, K and sodium (Na) decreases the ash melting temperature. The combination of high Si and high alkali content is especially problematic for fluidized bed biomass gasification because of the formation of silicates with low melting temperature. (BISYPLAN, 2012)

Apart from the chemical reactions that happens when ash melts and interacts with the fluid dynamics in the bed, the operating temperature is the most important factor determining the time-scale of the agglomeration process in fluidized beds. (Van der Drift, 1999) Good knowledge about the ash melting temperatures is therefore of great relevance to avoid operational problems during biomass gasification in fluidized beds. In general terms, ash is used to describe the inorganic matter in fuels. In biomass fuels, the content of the critical inorganic alkali metals tends to vary within the same type of biomass, as well as between the different biomass species. (Badholiya, 2016) This makes it difficult to determine the ash melting behavior on the basis of the melting temperature of the individual components. Another challenge when it comes to determination of the melting behavior for biomass ash, is that it under certain conditions can react to form eutectics with lower melting point than the individual components. (Dragutinovic, 2017) Performing ash melting analyses can be a useful way to estimate the tendency of bed agglomeration. The method for analyzing the ash melting behavior involves heating the ash in a controlled manner and then determining the temperatures at which the ash begins to deform, soften and completely fuse. This method gives a realistic prediction of the initial agglomeration temperature, i.e. the temperature where the first molten phases that are able to glue particles together are visible. (BISYPLAN, 2012)

3 Material and methods

3.1 Ash melting analysis

The biomass fuel was ashed at 600°C using a muffle furnace, and the ash was subsequently analyzed using a Leco Ash Fusion Determinator (AF700). To prepare the biomass ash sample for ash-melting analysis, the ash was milled and wetted with a few drops of Dextrin solution (Part no: 502-010) before it was pressed into a cylindrical test piece (Figure 3) with specified dimensions. The test piece was mounted on a ceramic tray and placed in the high-temperature furnace.

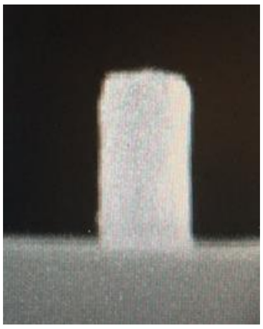

Figure 3. Cylindrical test piece ready for ash melting analysis.

For the ash-melting analyses, the Approved Standard Test Method (ASTM) D1857 was used. This test involves heating of the ash samples at a defined heating rate in reducing conditions. Table 1 shows the ASTM method specifications.

Table 1. Ash melting analyses specifications.

Step	*1*	*2*	*Unit*
Start temperature	400	700	°C
End temperature	700	1500	°C
Ramp rate	20	10	°C /min
Ramp time	00:15	01:20	H:min
Hold time	00:00	00:00	H:min
Total time	00:15	01:20	H:min

Four characteristic temperatures were determined for the ash sample: (ST) Shrinking starting Temperature, (DT) Deformation Temperature, (HT) Hemispherical temperature and (FT) Flow Temperature. Each of these temperatures correspond to a specific shape of the cylindrical ash test piece, and are described in Table 2 (BISYPLAN, 2012).

Table 2. Characteristic temperatures in ash melting analyses.

Characteristic temperature	*Description*
ST	First sign of shrinking of the cylinder
DT	First sign of rounding due to melting of the corners of the cylinder
HT	The cylindrical test piece forms a hemisphere
FT	The cylindrical test piece has effectively melted and the ash are spread out over the supporting tile in a layer

3.2 CPFD model description

The CPFD software package Barracuda VR 17.1.0 was used to simulate the agglomeration process in a biomass bubbling FBG. Barracuda VR uses the Multiphase Particle-in-Cell (MP-PIC) based Eulerian-Lagrangian approach, where the transport equations are solved for the continuous fluid phase and each of the discrete particles are tracked through the calculated fluid field. The fluid-particle interaction is considered as source terms in the transfer of mass, momentum and energy between the two systems. CPFD simulations are hybrid numerical methods, where the Eulerian approach is used for solving the fluid phase and the Lagrangian computational particle approach is used for solving the particle phase (Thapa and Halvorsen, 2013). Chladek et al. (2018) and Jayarathna et al. (2017) have described the transport equations in detail.

The Barracuda software package includes several drag models. For the present simulations, the Wen-Yu drag model was used. The CPFD model are previously developed and validated against experiments performed in a lab-scale cold flow model by Furuvik et al (2018). The model was scaled up to a full-scale bubbling FBG reactor using Glicksman's scaling rules that are based on a set of dimensionless parameters. The scaling rules are explained in detail by Thapa et al (2013).

A three-dimensional Cartesian coordinate system was used to describe the cylindrical column with height of 250 cm and 42 cm in diameter. In the present study, the static bed height was 105 cm. The mesh size was 0.0466 m x 0.0466 m x 0.0466 m and the number of control volumes was 4 536. The simulations were carried out at three different temperature conditions: (I) 850 ^{o}C, (II) 900 ^{o}C and (III) 1000 ^{o}C, and for each temperature, two different agglomeration processes were simulated. The fluidizing gas was air at atmospheric pressure. Pressure transducers are placed with an interval of 10 cm along the height of the bed, and the first monitor point is 10 cm above the distributor. The simulations were run for 50 seconds with a time step of 0.001 s. The simulation conditions are summarized in Table 3.

Table 3. CPFD simulation conditions.

Operating parameter	*Value*
Number of grid cells	4 536
Static bed height	105 cm
Fluidizing agent	Air
Type of flow	Isothermal@ (I) 850^{o}C (II) 900^{o}C (III) 1000^{o}C
Superficial air velocity	0.02; 0.005; 0.15 m/s
Simulation time for each flowrate	50 s
Drag model	Wen-Yu

Quarts sand with a solid density of 2 650 kg/m^3 was used as bed material. The particle size of the sand were 300 µm. The agglomerates ranged from 1.0 cm to 4.0 cm in diameter, with a particle density of 1 506 kg/m^3. (Furuvik et al., 2018). The maximum close pack volume fraction was set to 0.54. The maximum momentum from the redirection of particles collision was assumed to be 40 %, the normal-to-wall and tangential-to-wall momentum retention were 0.3 and 0.99 respectively. The particle properties are listed in Table 4.

Table 4. Particle properties.

Property	*Bed material*	*Agglomerates*
Diameter	300 µm	1.0 - 4.0 cm
Density	2650	1506
Sphericity	0.86	0.6
Close pack volume fraction	0.54	N/A

For the present simulations, it was assumed that the agglomeration process started at the DT measured by the ash melting analyses, and that the size and amount of agglomerates accumulate once the process has been initiated. In total, six different simulation cases were performed. Specific details on the agglomeration processes in the different simulation cases are presented in Table 5.

Table 5. CPFC simulation specification

	850^{o}C	*900^{o}C*	*1000^{o}C*
Amount of agglomerates	0 15%	20% 20%	20% 30%
Size of agglomerates	- 1-2 cm	2-3 cm 3-4 cm	3-4 cm 3-4 cm

4 Results and discussion

4.1 Ash melting analysis

Woodchips from Austria were used for the laboratory prepared ash samples. The ash-processing temperature was 600^{o}C. In Figure 4, the form of the cylindrical test piece is pictured for each of the defined characteristic temperatures.

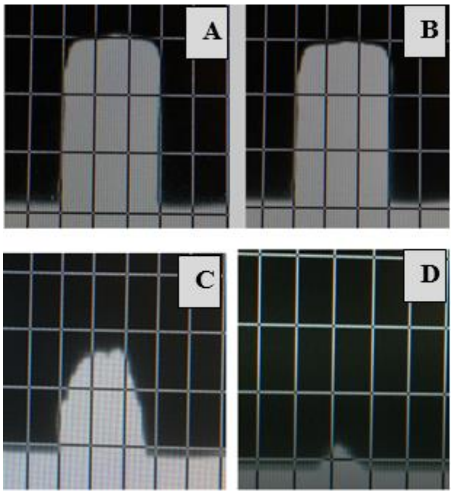

Figure 4. Results from ash melting analyses showing the test piece at (A) ST, (B) DT, (C) HT and (D) FT.

In order to obtain reasonable results, three separate measurements were carried out. The four characteristic temperatures were determined for all the three measurements. The results from the ash melting analyses are listed in Table 6.

Table 6. Results from ash melting analyses.

	ST	*DT*	*HT*	*FT*
1	861^{o}C	870^{o}C	1466^{o}C	1492^{o}C
2	867^{o}C	874^{o}C	1472^{o}C	1492^{o}C
3	859^{o}C	865^{o}C	1463^{o}C	1490^{o}C

For all the three measurements, the ash started to show sign of shrinking around 860^{o}C and deformation and rounding were observed at approximately 870^{o}C, these are the temperatures that correspond to ST and DT respectively. For biomass fuels, the DT is considered as a valid indication for the tendency of the ash to cause problems during thermal conversion processes. (BISYPLAN, 2012) In the present study, the received data for the DT are further related to the initial agglomeration temperatures.

4.2 CPFD simulations

The CPFD simulations were carried out at three different temperatures, and with varying combination of size and amount of agglomerates in the bed. The chosen simulation temperatures were based on the measured DT from the ash melting analyses, assuming the initial ash-melting temperature will start the agglomeration process. It was also assumed that the process continues once it has been initiated. The CPFD simulation results are presented as plots of the pressure drop in the bed as a function of the superficial air velocity.

Figure 5 represents the results of the simulations at 850^{o}C. The red line represents fluidization of the bed material, and is used as a reference bed. The purple line represents 15 % agglomeration in the bed. From the figure it is seen that there is a clear correlation between the fluid dynamics and the bed agglomeration processes. The difference between the pressures drops in the two cases increases with increasing superficial velocity until the bed is fluidized, at about 0.06 m/s. The pressure drop at minimum fluidization is approximately 14 000 Pa/m in the reference bed, while it is decreased to approximately 12 000 Pa/m in the agglomerated bed.

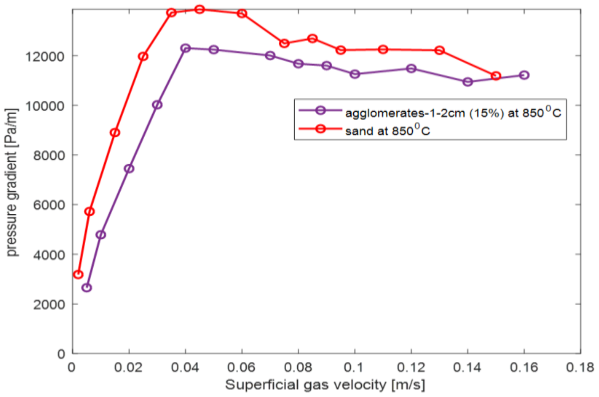

Figure 5. CPFD simulations at 850^{o}C, (I) silica sand, no agglomeration (II) agglomerate size 1-2 cm and 15% agglomeration.

Figure 6 shows the results from the two simulation cases at 900^{o}C. In both of the cases 20 % agglomerates are present in the bed. The blue line represents the case with agglomerates of 2-3 cm, while the black line represents agglomerates of 3-4 cm. The deviation between the two curves indicates that the fluidization is greatly affected by the size of the agglomerates. When the maximum size of the agglomerates is increased from 3 cm to 4 cm, the minimum fluidization velocity is increased from about 0.05 m/s to 0.08 m/s. The minimum fluidization velocity is a key parameter in fluidized beds, and works as a rough indication of the quality of the fluidization. Minimum fluidization is the point at which the bed conditions are at the boundary between fixed and fluidized, and the corresponding superficial velocity is referred to as the minimum fluidization velocity. The superficial velocity should therefore always be kept well above the theoretical minimum fluidization velocity to prevent de-fluidization of the bed

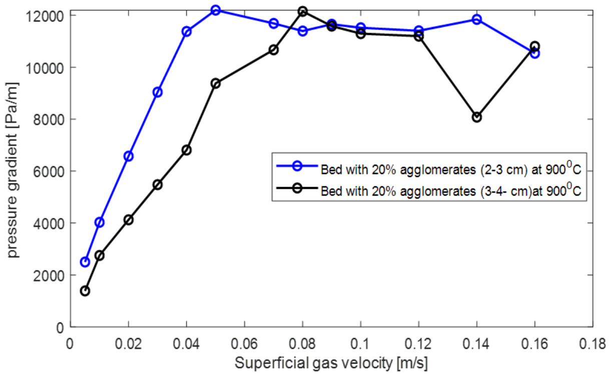

Figure 6. CPFD simulations at 900^{o}C, (I) agglomerate size 2-3 cm and 20% agglomeration (II) agglomerate size 3-4 cm and 20% agglomeration.

Figure 7 shows the results from the simulations at 1000^{o}C. The size of the agglomerates is 3-4 cm in both the simulation cases. The green line represents the case with 20 % agglomeration and the yellow line is simulation with 30 % agglomeration. The simulation results displayed in Figure 5 indicates that agglomeration causes decreased pressure drop in the fluidized bed. From Figure 7, it is seen that as the agglomerates grow larger it results in heavy instabilities in the bed. The pressure drop across the bed start to fluctuate as soon as the bed achieves fluidized state. The fluctuation in the pressure drops becomes worse as the amount of agglomerates increases. This improper bed control indicates de-fluidization. Apparently around 20% agglomeration seems to be enough to initiate de-fluidization of the bed.

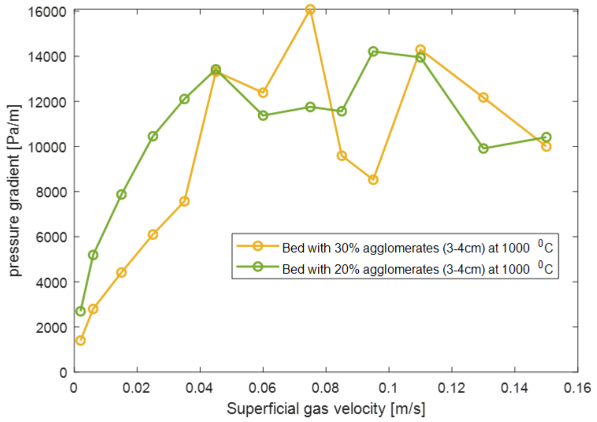

Figure 7. CPFD simulations at 1000^{o}C, (I) agglomerate size 3-4 cm and 20% agglomeration (II) agglomerate size 3-4 cm and 30% agglomeration.

DOI: 10.3384/ecp20170176

5 Conclusion

The objective of this work was to use a previous developed and validated CPFD model to study the ash melting and agglomeration in biomass gasification in a bubbling fluidized bed. The study included ash melting analyses, and CPFD simulations using the commercial software Barracuda VR. Ash related problems are the main obstacle in fluidized bed gasification of biomass, and are generally associated with high content of alkali components in the fuels. These elements might form low-melting temperature compounds that will coat the surface of the bed particles. If the coating have high enough fraction of molten ash, it will cause bed agglomeration.

The measurement of ash melting temperatures provides a direct correlation between laboratory data and the temperature at which the ash might have the tendency to melt. The simulations shows that the agglomeration process will affect the fluid dynamics in a bubbling fluidized bed gasifier. Bed agglomeration is often seen as a consequence of improper bed control. The more and larger agglomerates, the more severe are the problems. The point where agglomeration starts to cause problems is characterized by a sudden drop or instability in pressure. The simulations shows that around 20% agglomerates seems to be enough to initiate de-fluidization of the fluidized bed.

Acknowledgements

This study is funded by The Research Council of Norway, Program for Energy Research (ENERGIX), Project 280892 FLASH – Predicting of FLow behavior of ASH mixtures for production of transport biofuels in the circular economy.

References

A.B. Khadilkar, P.L. Rozelle, and S.V. Pisupati. Investigation of fluidized bed agglomerate growth process using simulations and SEM-EDX characterization of laboratory-generated agglomerates. *Chemical Engineering Science,* 184: 172-185, 2018.

A. van der Drift. Conversion of Biomass, prediction and solution methods for ash agglomeration and related problems. Final Report, ECN-C-99.090, 1999.

BISYPLAN. Web-based handbook, 2012. Available from: *http://bisyplan.bioenarea.eu/ash_appendix.html*. 02.06.2019.

C.K. Jayarathna, B.M.E. Moldestad, and L.A. Tokheim. Validation of results from Barracuda® CFD modelling to predict minimum fluidization velocity and pressure drop of Geldart A particles. *Proceedings for the 58th SIMS conference,* 2017.

J. Chladek, C.K. Jayarathna, B.M.E. Moldestad, and L.A. Tokheim. Fluidized bed classification of particles of different sixe and density. *Chemical Engineering Science,* 177: 155–162, 2018.

L. Wang, C.L. Weller, D.D., and M.A. Hanna. Contemporary issues in thermal gasification of biomass and its application to electricity and fuel production. *Biomass and Bioenergy*, 32: 573-581, 2008.

M. Bartles, W. Lin, J. Nijenhuis, F. Kapteijn and R. Ommen. Agglomeration in fluidized beds at high temperatures: Mechanisms, detection and prevention. *Progress in Energy and Combustion Science,* 34: 633-666, 2008.

N. Dragutinovic, B. Nakomcic-Smaragdakis, and Z. Cepic. Comparison of ash melting behavior of crop residues and woody biofuels with recommended measures. *The 8th PSU-UNS International Conference on Engineering and Technology* (ICET-2017), Novi Saf, Serbia, June 8-10, 2017.

N.C.I.S. Furuvik, R. Jaiswal, and B.M.E. Moldestad. Flow behavior in an agglomerated fluidized bed gasifier. *International Journal for Energy and Environment,* 10(2): 55-64, 2019.

N.C.I.S. Furuvik, R. Jaiswal, R.K. Thapa, and B.M.E. Moldestad. CPFD model for prediction of flow behavior in an agglomerated fluidized bed gasifier. *International Journal for Energy Production and Management*, 4(2):105-114, 2019.

P. Basu. Biomass Gasificaion, Prolysis and Torrefaction, Second Edition. *Academic Press Inc.*, UK, 2013.

R.K. Thapa and B.M. Halvorsen. Study of Flow Behavior in Bubbling Fluidized Bed Biomass Gasification Reactor using CFD simulation. T*he 14th International Conference on Fluidizatio*n *- From Fundamentals to Products,* Eds, ECI Symposium Series, 2013.

R.K. Thapa, C. Pfeifer, and B.M. Halvorsen. Scaling of biomass gasification reactor using CFD simulations. In *International conference on Polygeneration strategies (IPCS),* Vienna, Austria, June 3-5, 2013.

S.K. Badholiya and A. Kothari. A review on ash agglomeration phenomenon in fluidized bed combustion boiler. *International Journal of Scientific Research Engineering & Technology* (IJSRET), 5(11): 533-541, 2016

S.K Badholiya, S.K. Pradhan and A. Kothari. Investigations on ash agglomeration in CFBC boiler using computational fluid dynamics. *International Journal of Mechanical Engineering and Technology* (IJMET), 9(7): 1464-1476, 2018.

S.V. Vassilev, C.G. Vassilev, Y. Song, W. Li and J. Feng. Ash contents and ash-forming elements of biomass and their significance for solid biofuel combustion. *Fuel*, 208: 377-409, 2017.

S. Visser, S. van Lith and J. Kiel J. Biomass Ash – Bed Material Interactions Leading to Agglomeration in FBC. *Journal of Energy Resources Technology,* 2008.

World Bioenergy Association. WBA Global Bioenergy Statistics, 2017.

Paper 4

Computational Modelling of Fluidized Bed behaviour with agglomerates

This paper was presented in the 61st International Conference of Scandinavian Simulation Society, SIMS 2020 was organized as a virtual conference on September 2020.

The paper is published in Linköping Conference proceedings, Issue 176 (2020), page 421-427. DOI: 10.3384/ecp20176421.

Computational modeling of fluidized bed behavior with agglomerates

Krister Jakobsen Rajan Jaiswal Nora C. I. S. Furuvik Britt M. E. Moldestad

Department of Process, Energy and Environmental Technology, University of South-Eastern Norway, Norway
Krister.Jako@gmail.com {Rajan.Jaiswal, Nora.C.I.Furuvik, Britt.Moldestad}@usn.no

Abstract

Fluidized bed reactors can be used for biomass gasification. The product from biomass gasification is syngas, which can be used for production of bio oil. The main challenge when using fluidized bed for gasification is ash melting and agglomeration of the bed material. Agglomeration of the bed material influences on the flow behavior in the fluidized bed reactor and thus affects the gasification efficiency. A Computational Particle Fluid Dynamic (CPFD) model is developed to predict the flow behavior in a fluidized bed gasifier. The CPFD model was validated against experimental data from a cold fluidized bed. The model was then tested against the results from a biomass gasifier, and a few modifications were needed. Glickman's scaling parameters were used to scale up from a lab-scale to a full-scale gasifier. Simulations using the modified model were performed to study the flow behavior in a full-scale gasifier with agglomerates. It was found that the CPFD model is capable of predicting the effect of agglomerates on flow behavior in a fluidized bed gasifier.

Keywords: biomass, gasification, ash, agglomeration, CPFD, Barracuda

1 Introduction

Biomass is considered a renewable energy source, and it is crucial to make the biomass conversion processes more energy effective. Biomass is converted via gasification into a syngas consisting of mainly CO and H_2. Different technologies are used for gasification of biomass, and one of the most promising technologies is fluidized bed reactor. Fluidized bed reactors are used to ensure proper mixing of biomass and fluidizing gas, and thus increase the heat and mass transfer. Fluidized bed reactors are also very flexible when it comes to the type and quality of the biomass feed. The challenges when using fluidized bed gasifiers are ash melting and agglomeration of the bed material. Agglomeration may disrupt the flow behavior in the fluidized bed and thus affect the overall efficiency of the gasifier (Basu, 2013).

2 Ash melting and agglomerates

Ash melting is a big challenge in operation of biomass fluidized bed gasifiers. The amount of ash from biomass varies a lot depending on the type of biomass used. The typical content of ash in wood chips, straw and solid municipal waste is about 1 wt%, 8 wt% and 50 wt% respectively. However, even a small amount of ash can harm the gasification process, and it is therefore important to study how ash melting and agglomeration affect the flow behavior in a fluidized bed. Biomass such as grasses, demolition wood, and straw have a high potential to create agglomeration, fouling, and corrosion in a gasifier. (Basu, 2013)

The operating temperature for biomass fluidized bed gasifiers is usually kept in the range of 700-900°C to avoid ash melting. Ideally, the temperature should be increased to obtain a higher quality of the syngas and to avoid problems with tar. The ash melting temperature varies depending on the composition of the biomass. The melting temperature for spruce wood is 1170°C, whereas the melting point for wheat straw is 915°C (Basu, 2013).

The most significant ash-forming elements in biomass are silica (Si), potassium (K), calcium (Ca), magnesium (Mg), aluminum (Al), phosphor (P), chlorine (Cl), sodium (Na) and sulphur (S). (Balland et al., 2017; Furuvik et al., 2020). The ash-forming elements are released from the biomass during the heating process. When the ash melts, the inorganic elements from the melted ash can create a sticky component, which functions as a glue between the ash and the sand particles, and agglomerates are formed. Figure 1 shows agglomerates which are created by melted biomass ash and sand particles. (Furuvik et al., 2019a; Furuvik et al., 2019b). The agglomerates are of various sizes and shapes, and may change the fluidization properties in a biomass gasifier significantly. An agglomerated bed creates instability in the bubble frequency and can cause fluid channeling. Agglomeration can also result in defluidized zones in the gasifier. In the most severe cases, particle agglomeration may lead to unscheduled shutdowns of the whole installation. (Öhman et al., 2000)

DOI: 10.3384/ecp20176421

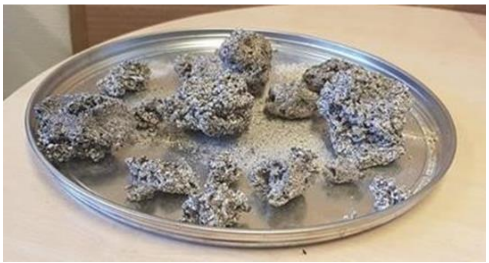

Figure 1. Agglomerates formed during gasification of biomass.

3 Material and methods

3.1 Experimental set-up

Two different experimental set-ups have been used in this study. One is a cold fluidized bed, where the fluid dynamic properties and flow behavior are studied. The other one is a biomass gasification reactor used to study the gasification yield at different operation conditions.

3.1.1 Cold fluidized bed set-up

The cold fluidized bed consists of a transparent cylindrical tube open to the atmosphere, and with a gas distributor plate at the bottom. The height and diameter of the cylinder are 140 cm and 8.4 cm, respectively. Pressure transducers are installed along the height of the bubbling fluidized bed, and the distance between the transducers is 10 cm. The model is shown in Figure 2. Experiments were performed with sand particles with density 2650 kg/m^3 as the bed material. A sieving analysis of the sand particles was performed and it was found that the particles had a size range of 300-700 µm. The weighted mean particle diameter was calculated to 535 µm. An aspect ratio (bed height/bed diameter) of 2.5 was used in the experiments. Pressure drop in the bed was monitored and plotted versus the superficial air velocity.

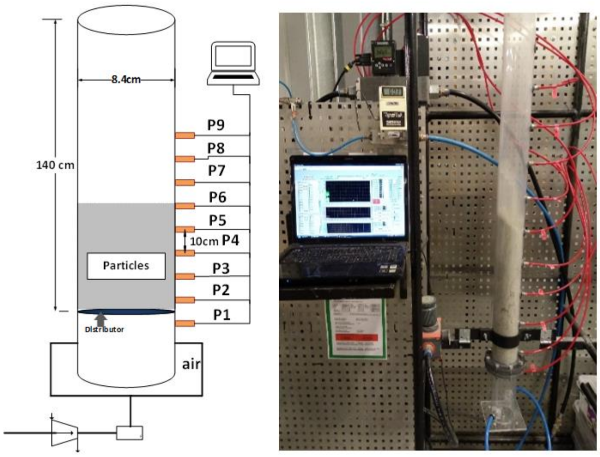

Figure 2. Experimental set-up; cold fluidized bed (Jaiswal *et al*, 2018).

3.1.2 Biomass gasifier set-up.

A lab-scale bubbling fluidized bed reactor with a feed capacity of 3–5 kg/h was used for the experimental biomass gasification tests. A drawing of the reactor is presented in Figure 3. The experimental rig is composed of a feeding system, a fluidized-bed reactor, a pre-heating system for the fluidizing gas stream, a sampling line and an exhaust line. The biomass gasification rig is made of stainless steel. It has three electrical heating elements, which are installed externally. The gasifier is insulated with refractory material on the inside, and a 200 mm thick fiberglass layer on the outside to minimize the heat losses.

The feeding system consists of a silo followed by a cold and a hot screw feeder. The cold screw feeder conveys the feed from the silo to the hot screw feeder. The hot screw feeder transports the feed into the reactor. The reactor is a cylindrical vessel with an inner diameter of 0.1 m and a height of 1.0 m. Air is used as the fluidizing agent, and flows through a pre-heater with a capacity of 18 kW. The exhaust line goes from the top of the reactor and transports the product gases into a flare. At the top of the reactor, there is also a sampling line, where samples of the syngas are taken at regular intervals and analyzed in a gas chromatograph (GC SRI 8610C). Two experiments were performed at temperature 735°C using gas flow rates of 1.5 and 2 kg/h. The bed material was sand with a mean particle diameter of 367 µm and density 2650 kg/m^3. The pressure drop over the particle bed was monitored.

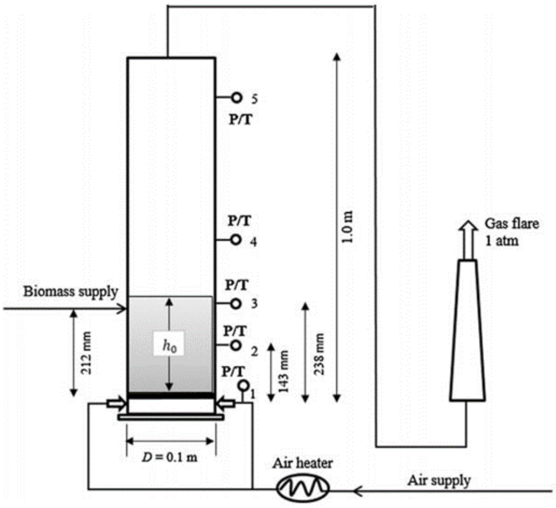

Figure 3. Experimental set-up; biomass gasifier.

3.2 CPFD modelling

Computational Particle Fluid Dynamics (CPFD) simulations are used to predict the minimum fluidization velocity and the flow behaviour in a cold fluidized bed and in a gasification reactor. The bed dimensions and the fluid and particle properties were the same as in the experimental tests. The CPFD model is developed using Barracuda VR. The CPFD numerical methodology incorporates the multi-phase-particle-in-cell (MP-PIC) method, where particles with the same properties are grouped into parcels and each parcel is represented by one computational particle (Snider, 2001; Amarasinghe, 2017). The gas phase and the particle phase are modelled using the Eulerian and the Lagrangian approaches respectively. Chladek et al. (2018) and Jayarathna et al. (2017) have described the transport equations in detail. Several drag models are available in Barracuda, and five of them were tested in this study. The five drag models are Ergun, Wen-Yu, Wen-Yu&Ergun, Turton-Levenspiel and Nonspherical Haider-Levenspiel. The Ergun drag model is derived based on dense bed systems, and is only valid for gas volume fractions lower than 0.8. The Wen–Yu drag model (Wen and Yu, 1966) is developed based on a series of experiments performed by Richardson and Zaki in 1954. The experimental data are available in (Richardson and Zaki, 1997). The Wen-Yu correlation is valid when the internal forces between particles are negligible, meaning that the viscous drag forces dominate the flow behavior. The Wen-Yu drag coefficient is a function of the Reynolds number and the void fraction. Researchers have reported good agreement between experiments and simulations using the Wen-Yu drag model (Furuvik et al., 2019). The Wen-Yu & Ergun drag model, is a combination of the two drag models. Wen-Yu's drag model is for dilute systems, and the Ergun drag model is for dense systems. This blend of drag models is controlled by the conditions set by the particle volume fraction and close pack volume fraction. Bandara et al. obtained good results when using the Wen-Yu & Ergun drag model in simulation of a circulating fluidized bed system (Bandara et al., 2019). The Turton-Levenspiel model (Turton and Levenspiel, 1986) and the non-spherical Haider-Levenspiel model (Haider and Levenspiel, 1989; Chhabra et al., 1999) utilize a single particle drag function dependent on the fluid volume fraction.

3.3 Scaling

Fluidized bed reactors are operating under relatively high temperatures, and it is difficult to observe the flow behavior during operation. Therefore, cold fluidized beds are often used for these types of studies. A CFD or CPFD model can be developed and validated against experimental data from cold bed tests. The model can further be used for a biomass gasifier operating at high temperatures. The cold bed has to be scaled based on scaling rules to get the correct dimensions for the particles and reactor, and to fit with the flow behavior observed in the cold fluidized bed. Scaling rules are used to scale from cold to hot, and also for up-scaling from lab scale to pilot or industrial sized reactors. To obtain the fluid dynamic similarities between two reactors, properly developed scaling rules must be used.

The most commonly used scaling rules for fluidized bed reactors are the rules proposed by Glicksman (Glicksman, 1984; Glicksman
study, a simplified set of Glicks
parameters is used. This simplified set is known as Glicksman's viscous limit set of dimensionless parameters, and can be used when Reynolds number is less than 4. The dimensionless numbers are: $\frac{}{U_0^2}, \frac{L}{d_p}, \frac{L_1}{L_2}, \frac{U_0}{U_{mf}}, \varphi$

$g\cdot L$

where U_0 is the operating gas velocity,
minimum fluidization velocity,
diameter, L is a reactor dimension (eg. diameter, height, bed height) and φ is the sphericity.

4 Results and discussion

4.1 Validation of CPFD model

A CPFD model of the cold fluidized bed was developed and validated against experimental data.
was to find the drag model that gave the best fit
experimental data. The grid resolution was set to
cells, which resulted in a uniformly distributed grid of 9536 cells. Figure 4 shows the simulated pressure drop versus the superficial velocity for the different drag models.

The Turton-Levenspiel model fits well with the experimental results in the fixed bed area (velocities lower than 0.17 m/s), whereas the Wen
a good agreement with the experimental data in the fluidized regime (velocity between 0.16 and 0.20 m/s). A fluidized bed reactor will operate in the fluidized regime, and therefore it was decided to use the Wen
drag function for the further validation of the CPFD model.

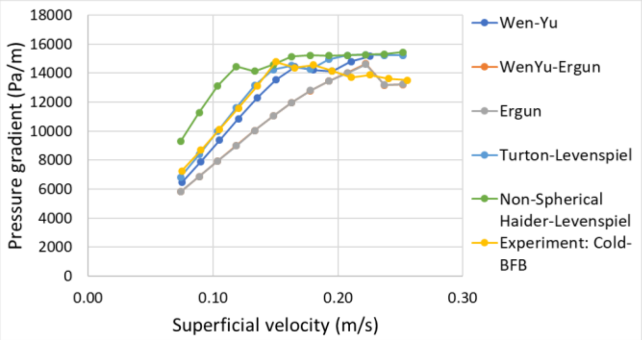

Figure 4. Comparison of different drag models against experimental data.

The next was to perform a grid resolution test. The number of cells was reduced from 12000 to 4000, and it was clear that using 4000 cells gave a significant deviation from the experimental results.
was also run with 20000 cells, but this did not give any significant difference compared to using 12000 cells. Since simulation with 20000 cells are more time

consuming, the further simulations were run with 12000 cells. A time step dependency test was carried out, The time steps were changed from 0.001 s to 0.0001 s. The results are presented in Figure 5. The plot shows that the CPFD model using Wen-Yu drag model, 12000 cells and time step 0.0001 s gives a good agreement with the experimental data. This model is further used to simulate agglomerates in an up-scaled fluidized bed reactor.

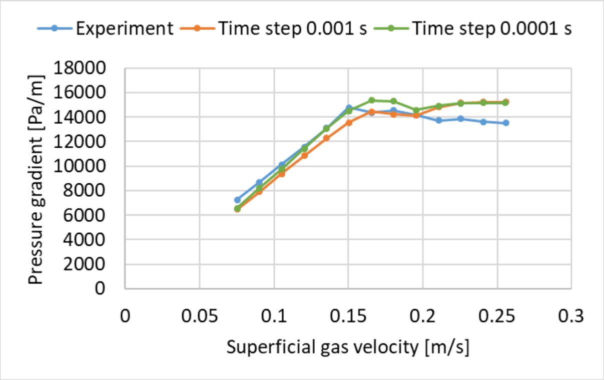

Figure 5. Comparison of simulations with different time step.

Figure 6 shows a comparison of the minimum fluidization velocity from the experiments and the simulation using the final model. The simulated minimum fluidization velocity is about 10% higher than the experimental. The deviation may be due to small differences in particle size distribution and the closed packed volume fractions. The drag model could have been tuned to fit the experimental data better. However, the model is capable of predicting the flow behavior in a fluidized bed with acceptable accuracy.

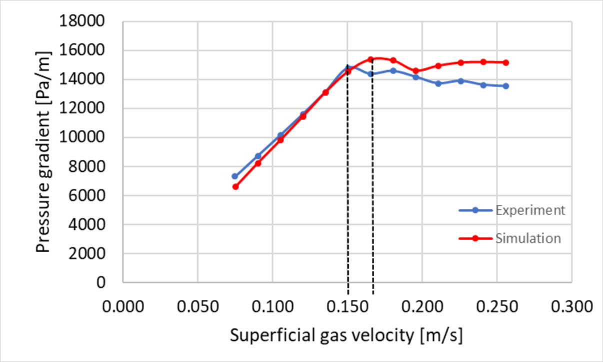

Figure 6. Comparison of minimum fluidization velocity. Dotted lines mark the minimum fluidization velocities.

The CPFD model was further tested against the results from the biomass gasifier, and it gave a good fit regarding the pressure drop over the bed at gas velocity 0.20 m/s.

4.2 Scaled model

The lab scale fluidized bed gasifier was up-scaled using Glicksman's viscous limit set of dimensionless parameters. Before doing the scaling, the diameter ratio of the two beds was set to 1:5, which means that the up-scaled gasifier has a diameter of 0.5 m. The reason why the geometry ratio was fixed, was to be able to simulate large agglomerates by using the same number of cells as in the simulation of the lab scale gasifier. In CPFD simulations of gas particle systems, the particle sizes cannot exceed the size of the computational cells. The scaling parameter L/d_p had to be neglected to avoid unreasonably large sand particles to be used in the up-scaled bed. The scaling parameters $\frac{U_0^2}{g \cdot L}, \frac{L_1}{L_2}, \frac{U_0}{U_{mf}}, \varphi$, were used for the up-scaling. The calculated parameters for the scaled and the lab scale gasifier are presented in Table 1. The highlighted values in the table are calculated based on the scaling rules.

Table 1: Parameters for the lab-scale and the up-scaled gasifier.

Parameters	Lab-scale	Up-scaled
D	0.1 m	0.5 m
H_{bed}	0.21 m	**1.05 m**
T	735°C	735°C
ρ_p	2650 kg/m^3	2650 kg/m^3
ρ_g	0.35 kg/m^3	0.35 kg/m^3
μ_g	0.000042Pa·s	0.000042Pa·s
d_p	367 µm	**549 µm**
U_0	0.153 m/s	**0.342 m/s**
U_{mf}	0.051 m/s	**0.114 m/s**
d_{aggl}	-	3-4 cm
ρ_{aggl}	1506 kg/m^3	1506 kg/m^3

Simulation with pure sand particles and with sand particles together with agglomerates were performed. The operating air velocity was set constant to 0.15 m/s in both simulations. In the simulation with agglomerates, agglomerates were fed continuously to the gasifier at a mass flow rate of 1.0 kg/s. The simulations were run for 90 s, and the pressure drop over the bed versus superficial gas velocity was monitored. The aim of these simulations was to find the amount of agglomerates required to influence on the flow behavior in the bed. Figure 7 shows the comparison of the simulations with and without agglomerates. As can be seen from the figure, there is a drop in the pressure for the agglomerated bed already after 20 s (20 kg of agglomerates fed to the reactor). The reason can be that the average density of the bed decreases due to the presence of agglomerates having a lower density than the sand. The lower pressure drop can also be due to air channeling caused by the large agglomerates. Between 45 and 70 s the pressure drop over the agglomerated bed decreases gradually from 13500 Pa/m to 12300 Pa/m. During this time interval, the mass of agglomerates in the bed has increased from 45 kg to 70 kg, and it seems that the agglomerates have started to affect the flow behavior significantly. A higher concentration of agglomerates may lead to higher degree of channeling of the air, which again gives a lower pressure drop over the bed. The problem is that a large part of the air leaves the bed through channels, and that the remaining air is not sufficient to fluidize the bed. This can result in defluidized zones in the bed, low mass and heat transfer and uneven temperature in the bed. Zones with very high temperature can occur, which promotes ash melting and formation of more and bigger agglomerates. In the end, the bed will collapse, and the gasification process has to be shut down. Ash melting and agglomeration of bed material can also plug the reactor totally, and thereby lead to a dangerous situation. It is therefore crucial to ensure that the gasifier is always running in the fluidized regime.

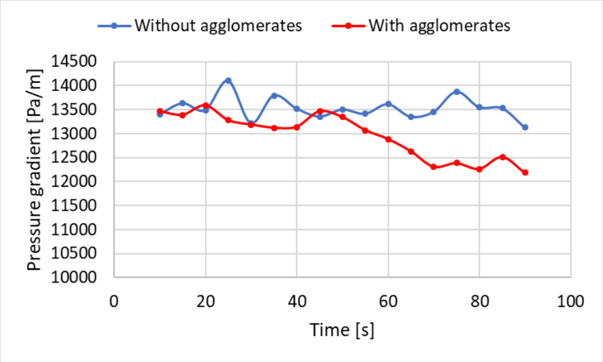

Figure 7. Simulation of gasifier with and without agglomerates. Gas velocity 0.15 m/s. Agglomerate feeding 1 kg/s.

Figure 8 shows the distribution of agglomerates (red) in the gasifier at time 0 s (no agglomerates), 60 s (60 kg of agglomerates and 90 s (90 kg of agglomerates). The agglomerates seems to segregate towards the bottom of the bed as the fraction of agglomerates increases. Figure 9 shows the flow behavior in the bed with 14 kg, 60 kg and 90 kg of agglomerates. The shape and frequency of the bubbles (areas with low particle fractions) change as the fraction of agglomerates increases. Also, the bubbles are getting more diffuse, meaning that the fraction of particles in the bubbles is increasing. This indicates that most of the air is leaving the bed in channels or through the emulsion.

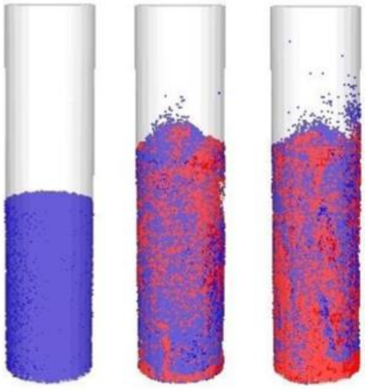

Figure 8. Distribution of agglomerates in the bed at time 0 s, 60 s and 90 s. Sand is blue, agglomerates are red.

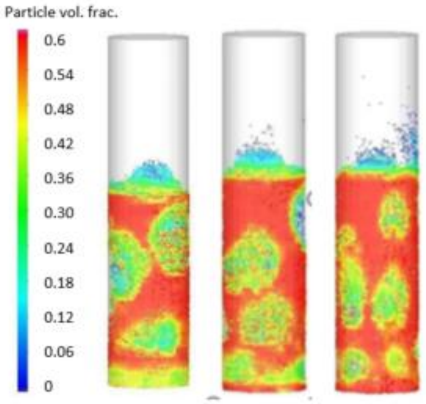

Figure 9. Flow behavior in agglomerated fluidized bed. Gas velocity 0.15 m/s, agglomerates 14, 60 and 90 kg.

The next simulations were run to predict the minimum fluidization velocity for pure sand and for sand with 60 kg (26% by volume) of agglomerates. The results are presented in Figure 10.

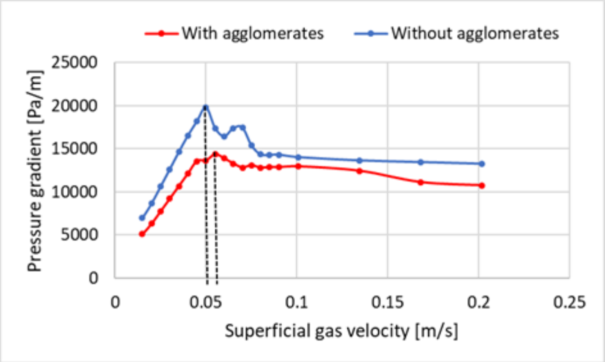

Figure 10. Minimum fluidization velocities (marked with dotted lines) for sand bed and agglomerated bed.

The pressure drop over the bed is significantly lower for the agglomerated bed than for the sand bed both in the fixed bed regime and in the fluidized regime. The minimum fluidization velocities are 0.05 m/s for the sand bed and 0.055 m/s for the agglomerated bed, which is significantly lower than the operating velocity of 0.15 m/s in the previous simulations. It is also observed that the minimum fluidization velocity for the sand bed (0.05 m/s) is less than half of the scaled minimum fluidization velocity (0.114 m/s). The reason is that the scaled minimum fluidization velocity is calculated from the Ergun's equation using the mean particle diameter. The minimum fluidization velocity very much depends on the particle size and the particle size distribution, and the smallest particles in a mixture influence significantly on the minimum fluidization velocity (Jayarathne and Halvorsen, 2009). In the simulations with Barracuda, the particle size distribution is included, and the simulations are therefore giving a more realistic value for the minimum fluidization velocity.

Figure 11 shows the distribution of the agglomerates (red) in the bed at minimum fluidization velocity (0.055 m/s) and at velocity 0.085 m/s. The volume fraction of agglomerates is 26%. At minimum fluidization velocity, the agglomerates are uniformly distributed in the gasifier. However, when the gas velocity is increased to 0.085 m/s, the agglomerates segregates towards the bottom of the bed. Segregation of agglomerates can have unfortunate consequences for the gasification process, as it can lead to defluidized zones with high temperature at the bottom of the bed. This can trigger the formation of more and also larger agglomerates.

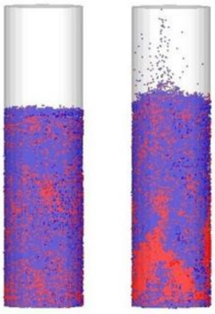

Figure 11. Distribution of agglomerates in the bed at gas velocity 0.055 m/s and 0.085 m/s.

Figure 12 shows the comparison of the flow behavior in the bed without agglomerates (left) and with 26% agglomerates (right) at gas velocity 0.101 m/s. In the sand bed, the bubbles seem to be well distributed in the bed, whereas in the agglomerated bed it seems like the gas (bubbles) is channeling through the bed in the center. The channeling of the air will cause bad mixing and limited mass and heat transfer. It is crucial to run the gasifier at temperatures well below the ash melting temperature to avoid agglomeration of the bed material. It is also important to operate the gasifier well above the minimum fluidization velocity to avoid defluidization and segregation of the larger particles if agglomeration occurs. Reduction in pressure drop over the bed indicates that formation of agglomerates has occurred.

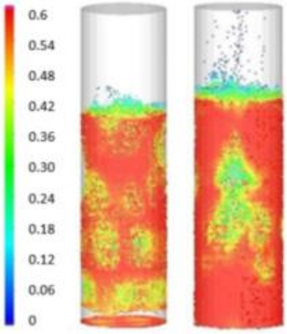

Figure 12. Distribution of particles in bed without agglomerates (left) and with agglomerates (right). Gas velocity 0.101 m/s.

5 Conclusion

The objective of this study was to develop a model to predict the flow behavior in a fluidized bed gasifier. A CPFD model is developed using the commercial software Barracuda VR. Experiments were performed using a cold model of a fluidized bed reactor to study the flow behavior and determine the minimum fluidization velocity. Additional experiments were performed in a lab-scale biomass gasifier 735℃ to determine the pressure drop over the bed.

The CPFD model was first validated against experimental data from the cold fluidized bed. Grid resolution tests, tests with different time steps, and tests with different drag models were performed, and the final model gave good agreement with the experimental results. The average deviation between the experimental results and the simulations regarding pressure drop and minimum fluidization velocity was 6% and 10% respectively. The model was further tested against the results from the biomass gasifier, and it gave a good fit for the pressure drop over the bed at gas velocity 0.20 m/s. A few modifications were needed to be able to simulate an agglomerated fluidized bed gasifier. Glicksman's scaling rules were used to scale up the lab-scale gasifier to a full-scale gasifier. Simulations using the modified model were performed to study the flow behavior in a full-scale gasifier with agglomerates. The pressure drop over the bed decreased with increasing mass of agglomerates. The minimum fluidization velocity for the bed with 26 vol % agglomerates was about 10% higher than for the sand bed. The bubble shape and bubble frequency changed with the fraction of agglomerates in the bed. This may be due to gas channeling and segregation of agglomerates. The developed CPFD model is capable of predicting the effect of agglomerates in a fluidized bed gasifier.

Acknowledgements

This work is funded by the Research Council of Norway, Program for Energy Research (ENERGIX). Project 280892 FLASH - Prediction of FLow behavior of ASH mixtures for transport biofuels in the circular economy.

References

C. E. Agu, C. Pfeifer, M. S. Eikeland, L. A. Tokheim, and B. M.E. Moldestad. Measurement and characterization of biomass mean residence time in an air-blown bubbling fluidized bed gasification reactor, *Fuel*, 253: 1414-1423, 2019.

W. S. Amarasinghe, C. K. Jayarathna, B. S. Ahangama, B.E.M. Moldestad, and L. A. Tokheim. Experimental study and CFD modelling of fluidization velocity for Geldart A, B and D particles. *International Journal of Modelling and Optimization*, 7(3): 152-156, 2017

M. Balland, K. Froment, G. Ratel, S. Valin, J. Roussely, R. Michel, J. Poirier, Y. Kara, and A. Galnares. Biomass ash Fluidized-Bed Agglomeration: Hydrodynamic Investigations. *Waste Biomass*, 8: 2823-2841, 2017.

J. Bandara, B. M. E. Moldestad, and M. S. Eikeland. Analyzing the Effects of Geometrical and Particle Size Uncertainty in Circulating Fluidized Beds using CPFD

Simulation, *Linköping Electronic Conference Proceedings*, 170: 182-189, 2019.

P. Basu. Biomass gasification, pyrolysis and torrefaction, 2nd ed. Elsevier Inc, 2013.

R Chhabra, L. Agarwal, and N. Sinha. Drag on non-spherical particles: an evaluation of available methods, *Powder Technology*, 101(3): 288-295, 1999.

J. Chladek, C. K. Jayarathna, and B. M. E. Moldestad. L. A. Tokheim, Fluidized bed classification of particles of different sixe and density, *Chemical Engineering Science*, 177: 155–162, 2018.

N. C. I. S Furuvik, R. Jaiswal, and B. M. E. Moldestad. Flow behavior in an agglomerated fluidized bed gasifier, *International Journal of Energy and Environment*, 10(2): 55-64, 2019a.

N. C. I. S Furuvik, R. Jaiswal, R. K. Thapa, and B. M. E. Moldestad. CPFD model for prediction of flow behavior in an agglomerated fluidized bed gasifier", *International Journal of Energy Production and Management*, 4(2): 105-114, 2019b.

N. C. I. S Furuvik, R. Jaiswal, and B. M. E. Moldestad. Experimental study of agglomeration of grass-pellets in fluidized bed gasification, *WIT Transactions on Ecology and Environment*, 246: 9-17, 2020.

L. Glicksman. Scaling relationships for fluidized beds, *Chemical Engineering Science*, 39(9): 1373-1379, 1984.

L. Glicksman, M. Hyre, and P. Farrell. Dynamic similarity in fluidization, *International Journal of Multiphase Flow*, 20: 331-386, 1994.

A. Haider and O. Levenspiel. Drag coefficient and terminal velocityof sperical and nonspherical particles, *Powder Technology*, 58(1): 63-70, 1989.

R. Jaiswal, C. E. Agu, R. K. Thapa, and B. M. E. Moldestad. Study of fluidized bed regimes using Computational Particle Fluid Dynamics. *Linköping Electronic Conference Proceedings*, 153: 271-276, 2018

C. K. Jayarathna and B. M. Halvorsen. Experimental and computational study of particle minimum fluidization velocity and bed expansion in a bubbling fluidized bed. SIMS 50 Conference, Fredericia, Denmark: Technical University of Denmark (ISBN 978-87-89502-88-5)-285290, 2009.

C. K. Jayarathna, B. M. E.Moldestad, and L. A. Tokheim. Validation of results from Barracuda® CFD modelling to predict minimum fluidization velocity and pressure drop of Geldart A particles, *Linköping Electronic Conference Proceedings*, 138: 76-82, 2017.

J. F. Richardson and W.N. Zaki, Sedimentation and fluidization: Part I. *Chemical Engineering Research and Design*, 75: 82–100, 1997.

D. M. Snider. An incompressible three-dimensional multiphase particle-in-cell model for dense particle flows. *Journal of Computational Physics*, 170(2): 523-549, 2001.

R. Turton and O. Levenspiel. A short note on the drag correlation for spheres, *Powder Technology*, 47(1): 83-86, 1986.

C. Wen and Y. Yu. Mechanics of fluidization, *Chemical Engineering Progress Symposium Series*, 62: 100–111, 1966.

M. Öhman and A. Nordin. The Role of Kaolin in Prevention of Bed Agglomeration during Fluidized Bed Combustion of Biomass Fuels. *Energy & Fuels* 14(3): 618-624, 2000.

Paper 5

Comparison of Experimental and Computational study of Fluid Dynamics in Fluidized Beds with agglomerates

This paper was presented in the 61st International Conference of Scandinavian Simulation Society, SIMS 2020 was organized as a virtual conference on September 2020.
The paper is published in Linköping Conference proceedings (2020), Issue 176, page 414-420. DOI: 10.3384/ecp20176414

Comparison of experimental and computational study of the fluid dynamics in fluidized beds with agglomerates

Nora C I S Furuvik Rajan Jaiswal Britt M E Moldestad

Department of Process, Energy and Environmental Technology, University of South-Eastern Norway, Norway,
{nora.c.i.furuvik, rajan.jaiswal, britt.moldestad}@usn.no

Abstract

Particle agglomeration is one of the obstacles for successful application and commercial breakthrough of fluidized bed biomass gasification. The problem is generally associated with molten ash components that interact with the bed particles, forming agglomerates that interfere with the flow behavior.

In this work experimental and computational study are combined in order to gain more insight into the fluid dynamics in a bubbling fluidized bed gasifier. The goal is to develop a Computational Particle Fluid Dynamic (CPFD) model that can be used in further investigations of the correlation between flow behavior and bed agglomeration during biomass gasification in fluidized beds. The experimental part was performed in a 20 kW laboratory scale bubbling fluidized bed system. The commercial CPFD software Barracuda Virtual Reactor (VR) version 17.4.1 was used for the computational study. Simulation results were compared to the experimental data in order to validate the CPFD model. Pressure drops predicted by the simulations were in good agreement with the experimental measurements, which indicate that the model is well capable of studying the fluid dynamics in a fluidized bed system.

Keywords: biomass gasification, fluidized bed, agglomeration, CPFD simulations

1 Introduction

Fluidized bed reactors have a broad use in various industrialized applications and are common in both petroleum and petrochemical processes, as well as heat and power production. A typical fluidized bed system consists of a cylindrical column packed with a suitable bed material, which is kept in a fluidized state by passing a fluid through at a velocity that is sufficiently high to “loosen” the bed particles. The fluidized bed design allows for good mixing in all directions within the reactor, resulting in enhanced fuel/fluid contact and thereby increased heat and mass transfer (Sansaniwal, 2017). As a result of the combination of intense solid mixing and bed materials with large thermal capacity, the fluidized beds can be operated under nearly isothermal conditions. Additionally, they have the benefit of continuous and controlled operations (Basu, 2013). Due to their homogenous operation conditions, the fluidized bed reactors are capable of handling a wide range of fuels, and compared to other conversion technologies they are considered well suited for processing highly reactive fuels such as biomass (Basu, 2013; Capareda, 2014).

Despite the many advantages with the fluidized beds, some difficulties are reported related to the gasification process of biomass-derived fuels. Generally, these problems are associated with ash-melting and following agglomeration of bed material. Biomass fuels refer to a broad variety of feedstock, and are characterized as heterogeneous with widely varying chemical and physical properties (Capareda, 2014). Due to the differences in chemical and physical properties, the biomass fuel characteristics are associated with diversity in composition of ash forming elements, which may represent significant barriers for successful fluidized bed gasification processes (Tiffault *et al*, 2018).

Understanding the fluid dynamics in the fluidized bed is essential for maintaining ideal operational conditions for an appropriate fluidized regime. This work is divided into one experimental part and one simulation part. The experimental setup is a 20 kW laboratory scale bubbling fluidized bed gasifier. The laboratory scale model is used to study the fluidized conditions at different gasification temperatures. Additional experiments with a mix of bed material and agglomerates are performed to investigate the dependence of fluidization on particle shape, size and density. For the simulation part, the commercial CPFD software Barracuda VR version 17.4.1 is used for simulations of the flow behavior in a bubbling fluidized bed gasifier. The data and measurements achieved from the fluidization experiments are used to develop and validate a CPFD-model that can be used for further investigations.

2 Particle agglomeration in fluidized beds

Ash related problems are a key concern in gasification of biomass in fluidized beds. The problems are generally related to alkali ash components that interact with the bed particles, forming agglomerates that cause fluid dynamic disturbances in the bed. The agglomerates interfere with the flow behavior, change the fluidized conditions and make further fluidization impossible. During bed agglomeration processes, the solid mixing becomes ineffective because the agglomerates tend to

DOI: 10.3384/ecp20176414

obstruct the particles movement, resulting in decreased heat transfer and local temperature deviations that in turn create de-fluidized volumes in the bed (Bartles *et al*, 2008). De-fluidization is described as a total collapse of the fluidized bed, and is recognized by a rapidly decreasing bed pressure drop and/or a substantial change in the bed temperature. In the most severe cases, particle agglomeration results in unscheduled shutdowns of the whole installation (Öhman and Nordin, 2000).

Particle agglomeration in fluidized bed biomass gasification is highly coupled to the high temperature chemistry of the biomass ash, i.e. its melting and the consequently appearance of an alkali liquid phase that glue the ash to the surface of the bed particles (Öhman et al., 2000). The mechanisms are dominated by a combination of ash particles attaching the surface of the bed material and chemical reactions that occur between the ash-coated bed particles and the condensed gaseous alkali components (Figure 1).

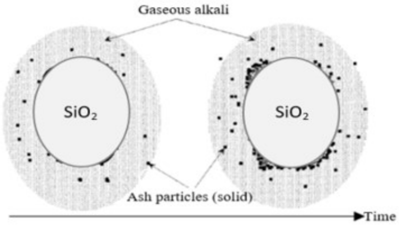

Figure 1. Ash deposition onto the surface of silica sand bed material (Öhman et al., 2000).

As a consequence of repeated collisions between the ash-coated particles in the bed, the particles stick together and eventually they grow towards larger agglomerates. Figure 2 shows a photo of agglomerate formed during gasification experiments with grass pellets in a bubbling fluidized bed gasifier (Furuvik *et al*, 2020).

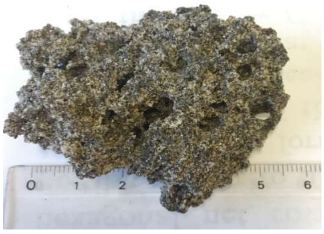

Figure 2. Agglomerate of biomass ash and silica sand particles, formed in a bubbling fluidized bed gasifier.

3 Experimental setup

The fluidization experiments were performed in a 20 kW laboratory scale bubbling fluidized bed reactor with a height of 100 cm and an inner diameter of 10 cm. A schematic of the experimental setup is shown in Figure 3. The fluidizing agent was air introduced into the bed through two pipes from the bottom of the column. The air mass flow rate was controlled with a Brook air flowmeter, with an operating range between 0.5 kg/h – 4.7 kg/h. Five pressure transducers placed along the height of the reactor were constantly monitoring the operating conditions in the bed. Each pressure transducer measures the gauge pressure in the given position, i.e. the fluid pressure above the atmospheric pressure. The temperature and pressure sensors are connected to the LabVIEW software for data acquisition. The locations of the pressure and temperature sensors (P1/T1, P2/T2, P3/T3, P4/T4 and P5/T5) are seen in Table 1.

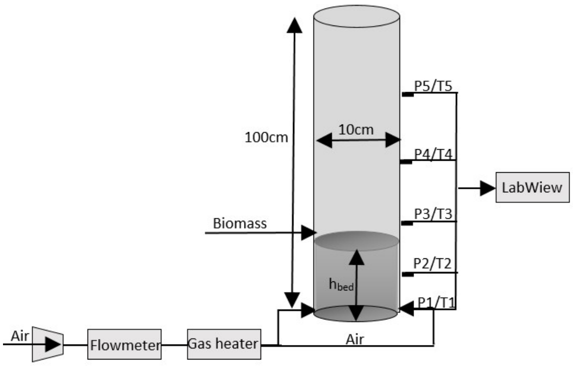

Figure 3. Schematic of the laboratory scaled bubbling fluidized bed used in fluidization experiments.

Silica sand particles with a mean diameter of 305 µm and particle density 2600 kg/m^3 were used as bed material. The sand particles were preheated to the operating temperature by letting the air pass through a preheated chamber before entering the reactor. The experiments were run without feeding biomass to the reactor. The externally heated reactor was operated at temperatures that were kept constant throughout each test run. Five thermocouples were used to determine the temperature profile in the bed and to control the temperatures at experimental conditions of 300^{o}C, 600^{o}C, 700^{o}C and 800^{o}C. For each temperature, a fluidization experiment of the bed particles were performed. The pressure drop in the bed were recorded at different superficial air velocities ranging from 0.029 to 0.330 m/s. The superficial air velocities (u_f) were calculated from the mass flow rate $(\dot{m})$, the area of the reactor (A) and the air density at the specific temperatures (ρ_f):

$$u_f = \frac{\dot{m}}{A \cdot \rho_f} \tag{1}$$

Table 1 lists the operating parameters for the bubbling fluidized bed reactor. The minimum fluidization velocity for each experimental condition was calculated using the equation for minimum fluidization derived from Ergun's equation (Kuuni and Levenspiel, 1991).

Table 1. Operating parameters for fluidization experiments.

Description	*Value*
Operating temperatures	300, 600, 700 and 800°C
Air flow rate	0.5 – 3.0 kg/h
Superficial air velocity range	0.029 - 0.172 m/s @ 300°C 0.044 - 0.262 m/s @ 600°C 0.049 - 0.292 m/s @ 700°C 0.054 - 0.330 m/s @ 800°C
Calculated minimum fluidization velocity	0.050 m/s @ 300°C 0.038 m/s @ 600°C 0.036 m/s @ 700°C 0.034 m/s @ 800°C
Pressure and temperature measurement locations	P1/T1: 0.023 m P2/T2: 0.143 m P3/T3: 0.238 m P4/T4: 0.538 m P5/T5: 0.838 m

The mass of the bed particles was 2.355 kg, corresponding to a static bed height of 20 cm. For the temperatures of 700°C and 800°C additional test runs were carried out, for these runs a mix of agglomerates of different sizes was introduced to the bed together with the bed materials. The mass of agglomerates was 116 g corresponding to a bed agglomeration of 5% by weight. The agglomerates were produced from previous performed gasification experiments (Furuvik *et al*, 2020). Detailed specification of the properties of the bed material and the agglomerates are shown in Table 2.

Table 2. Specification of particle properties.

Particle properties	*Value*
Mass of bed material	2.355 kg
Bed material particle size range	180 – 710 μm
Particle density of bed material	2600 kg/m^3
Mass of agglomerates	116 g
Size of agglomerates	1.0 – 3.0 cm
Agglomerate density	1510 kg/m^3

4 Simulation model

4.1 CPFD model description

CPFD simulations are useful tools in modelling of fluid-particle interaction in fluidized bed reactors. In this study, the commercial software package Barracuda VR was used to simulate the fluid dynamics in a 20 kW laboratory scale bubbling fluidized bed system. Barracuda VR uses the three-dimensional Multiphase Particle-in-Cell (3D-MP-PIC) method for calculating the fluid-particle flow. The method is based on the Eulerian-Lagrangian approach, wherein the Eulerian approach is used for solving the continuum phase and the Lagrangian approach is used for solving the particle phase. In the MP-PIC method, the solid particles are modeled as computational particles with a proper size and density distribution (Jayarathna *et al*, 2017; Thapa and Halvorsen, 2014). The governing equations include the conservation of mass, momentum and energy in the system. The interphase momentum transfer is an important term when modelling fluidized bed systems, and is described in details by Chladek *et al.* (Chladek *et al*, 2018) and Jayarathna et al. (Jayarathna *et al*, 2017).

The particle fluidization results from the drag forces exerted by the fluid on the particles. The drag forces are the main cause of transfer of mass, momentum and energy between the different phases in the fluidized bed system (Marchelli *et al*, 2020). In Barracuda VR the drag forces (F) have their general form:

$$F = m_p D(u_f - u_p) \qquad (2)$$

Where m_p is the mass of the particles, u_f is the fluid velocity, u_p is the particle velocity and D is the drag function (CPFD Software, 2020). The dimensionless drag function is the fluid-particle interphase exchange coefficient and differs for the different drag models. Common for all systems are that D always has a complex dependency on the bed porosity and the particle Reynolds number (Re) (Marchelli *et al*, 2020). The Re is defined as:

$$Re = \frac{2r_p \rho_f (u_f - u_p)}{\mu_f} \qquad (3)$$

Where r_p is the particle radius, ρ_f is the fluid density and μ_f is the fluid viscosity. The drag models determine the drag forces acting on the particles, and several drag models are available in Barracuda. In order to study the behavior of different drag models for the chosen system, the Wen-Yu drag model (CPFD Software, 2020; Wen and Yu, 1966), the Ergun drag model (CPFD Software, 2020; Ergun, 1952) and the Wen-Yu/Ergun drag model (CPFD Software, 2020) were tested.

The Wen-Yu model is considered most valid for dilute systems. The drag function for the Wen-Yu model (D_{WY}) is dependent on the fluid conditions and the particle properties, and is related to the drag coefficient (C_d) (CPFD Software, 2020; Wen and Yu, 1966):

$$D_{WY} = \frac{3}{8} C_d \frac{\rho_f (u_f - u_p)}{\rho_p r_p} \qquad (4)$$

Where ρ_p is the particle density.

The drag coefficient (C_d) is defined as a function of Re and is calculated by the following set of equations (CPFD Software, 2020; Wen and Yu, 1966):

$$C_d = \begin{cases} \dfrac{24}{Re}\theta_f^{n_0} & Re < 0.5 \\ \dfrac{24}{Re}\theta_f^{n_0}\left(c_0 + c_1 Re^{n_1}\right) & Re \le 0.5 \le 10000 \\ c_2\theta_f^{n_0} & Re > 10000 \end{cases} \qquad (5)$$

Where θ_f is the fluid volume fraction, c_0, c_1, c_2, n_0 and n_1 are model constants with default values 1.0, 0.15, 0.44, -2.65 and 0.687 respectively.

The Ergun drag model is developed from dense bed data and is primarily most suitable for picturing flow through static packed beds. The drag function (D_E) is given by (CPFD Software, 2020; Ergun, 1952):

$$D_E = 0.5\left(\frac{k_1\theta_p}{\theta_f Re} + k_0\right)\frac{\rho_f(u_f - u_p)}{\rho_p r_p} \qquad (6)$$

Where θ_p is the particle volume fraction, k_0 and k_1 are constants with default values 2 and 180 respectively.

Wen-Yu/Ergun drag model is a combination of the Wen-Yu and the Ergun models. This allows it to be able to work well in both dense and dilute systems. The drag function (D_{WYE}) is controlled by the close pack volume fraction (θ_{cp}) with a switch from Ergun to Wen-Yu at defined values. Wen-Yu/Ergun uses the Ergun function for $\theta_p > 0.85\cdot\theta_{cp}$ and the Wen-Yu function at higher voidage (CPFD Software, 2020).

$$D_{WYE} = \begin{cases} D_{WY} & \theta_p < 0.75\theta_{cp} \\ D_{E\_WY} & 0.75\theta_{cp} \ge \theta_p \ge 0.85\theta_{cp} \\ D_E & \theta_p > 0.85\theta_{cp} \end{cases} \qquad (7)$$

Where D_{E_WY} is defined as:

$$D_{E\_WY} = (D_E - D_{WY})\left(\frac{\theta_p - 0.75\theta_{cp}}{0.85\theta_{cp} - 0.75\theta_{cp}}\right) + D_{WY} \qquad (8)$$

4.2 CPFD simulations

CPFD simulations of a 20 kW laboratory scale fluidized bed were performed. The 3D computational grid was created using 10000 control volumes. The reactor was initially loaded with silica sand particles with mean particle diameter of 305 μm and a particle density of 2600 kg/m^3. The particle size distribution is determined based on the discrete mass frequency distribution (Crowe *et al*, 2012), the result is shown in Figure 4.

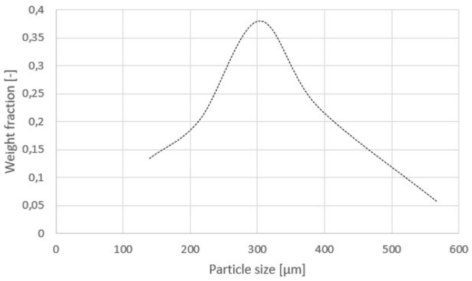

Figure 4. Particle size distribution of bed material.

Fluidizing agent was air at atmospheric pressure. Flow boundary conditions were applied at the bottom of the reactor. The pressure in the bed was measured at positions P1= 0.023 m, P2 = 0.103 m and P3 = 0.183 m above the bottom of the column. The simulations were run for 70 s with a time step of 0.0001 s. Table 3 shows the values of the model parameters used in the simulations. In order to add agglomerates to the fluidized bed a coarser grid was required, and the number of grid cells was therefore reduced from 10000 to 5120. The size of the agglomerates was limited by the chosen grid, which allowed a maximum particle size of 1.0 cm. In the present simulations, the size of the agglomerates ranged from 0.5 cm to 1.0 cm with a particle density approximately equal to 1510 kg/m^3 (Furuvik *et al*, 2019).

Table 3. Model parameters used in the CPFD simulations.

Description	*Value*
Particle density	2600 kg/m^3
Fluidizing agent	Air
Type of flow	Isothermal@ 300, 600, 700 and 800°C
Particle size	Range: 180 - 710 μm Mean diameter: 305 μm
Close-pack volume fraction	0.6
Particle sphericity	0.86
Static bed height	0.20 m
Superficial gas velocity	0.005 – 0.200 m/s
Agglomerate particle size	1.0 cm
Agglomerate density	1510 kg/m^3

5 Results and discussion

The bed pressure drop was measured experimentally at different superficial gas velocities. The operating temperatures were 300°C, 600°C, 700°C and 800°C. Figure 5 shows that the pressure drops decrease with increasing bed temperatures. The drag equations explain how the bed operating temperature alters the fluidized conditions in the bed. All drag functions indicate that the drag forces are strongly dependent on both the bed porosity and the Re. Moreover, increased bed temperature results in increased fluid viscosity (μ_f) and decreased fluid density (ρ_f), and hence lower Re. From the Wen-Yu drag functions, equation (3) and (4), it is obvious that changing the Re will cause a change in the magnitude of drag forces exerted on the bed particles. Stronger drag forces acting on the bed material give lower pressure drop in the fluidized bed.

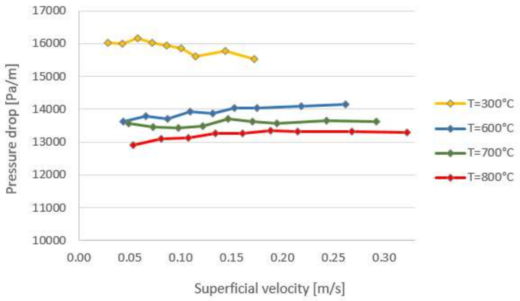

Figure 5. Comparison of experimental bed pressure drops with different operating temperatures.

Additional two fluidization experiments were carried out, where 5 wt% of agglomerates were mixed together with the bed particles. The experimental temperature conditions were 700°C and 800°C. Figure 6 shows that adding agglomerates to the process alters the character of the fluidized conditions. This can also be seen in drag force calculations using the drag functions described in equation (3), (5) and (7). The drag functions describe how the relation between the superficial velocity and the particle shape, size and density determine the bed conditions during fluidization.

The agglomerates are relatively big, but porous, which give them low particle density (ρ_p). A change in the ρ_p alters the gravitational forces acting on the particles. Looking at the drag equations, lower ρ_p gives increased drag function that further results in stronger drag forces and decreased pressure drop.

The agglomerates are more angular compared to the sand particles. Lower sphericity alters the packing properties of the bed and leads to change in the associated void spaces. Larger voids in the bed result in higher fluid volume fraction, which based on the Wen-Yu drag coefficient give increased drag forces and thereby lower bed pressure drop.

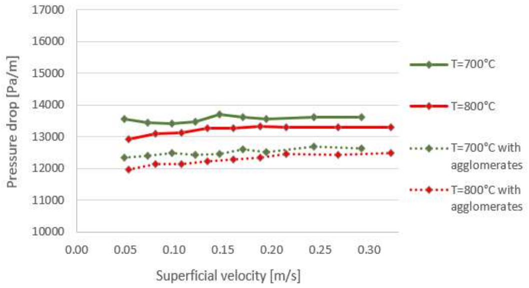

Figure 6. Comparison of experimental bed pressure drops with and without agglomerates.

To predict the fluidized conditions in the bubbling fluidized bed, the experimental setup was modeled using CPFD calculations. The simulation model was validated by comparing the measured pressure drop from experiments with results from the CPFD simulations. Wen-Yu, Ergun and the combined Wen-Yu/Ergun drag models were tested in order to study the behavior of the different drag models for the present system. Figure 7 compares the experimental results and the results from the simulations of the three different CPFD models at bed temperature of 300°C. The results show that the Wen-Yu drag function gives better prediction compared to the other drag models.

The advantage of Wen-Yu is that the drag force only depends on the fluid volume fraction and the Re, which make it very suitable for predicting the fluid dynamics in stabilized systems with isothermal bed conditions. The Wen-Yu drag function is based on a dependence on the Re, with a switch between different functions for Re<0.5 and Re>1000. Re increases as the superficial fluid velocity increases. However, Re will never exceed 1000 nor fall below 0.5 in the selected superficial velocity range. For this system, Wen-Yu therefore uses the same equation to calculate the bed conditions for all measuring points during the simulations. As the bed temperature is kept constant during the whole simulation time, it can be assumed that both the fluid conditions and the particle properties are unchanged. Fluid volume fraction will admittedly fluctuate slightly as a result of where and how bubbles are formed in the bed. These fluctuations are relatively small, hence they will not give large disturbances in the fluidized conditions.

Ergun drag model is based on data from fixed bed experiments and is therefore expected to be more appropriate at higher packing fractions. The superficial fluid velocity has large contribution to Ergun equation. For low velocities, the bed conditions are mainly controlled by the particle packing. As the superficial velocity increases, the velocity takes more control over the bed conditions. At higher velocities, Ergun gives large fluctuations in the pressure drop. As seen in Figure 7, the drag model fails in the fluidized regime.

Wen-Yu/Ergun drag model is a combination of the Wen-Yu model and the Ergun model, whereas the close-pack volume fraction (θ_{cp}) determines which drag function that are used. For this system with $\theta_{cp} = 0.6$, the Ergun equation is applied when the particle volume fraction (θ_p) > 0.51, and Wen-Yu is applied when $\theta_p < 0.45$. The results indicate that the only drag function used for the present CPFD calculations is Ergun, which explains why the simulated pressure drop for Ergun and Wen-Yu/Ergun drag models are about the same.

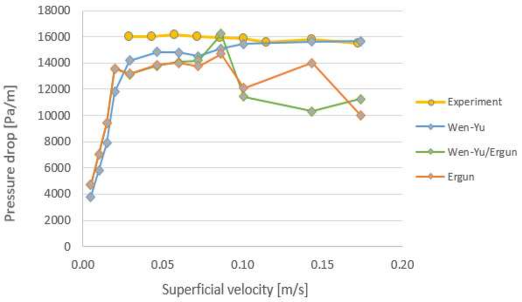

Figure 7. Comparison of experimental result and simulations using different drag models.

Figure 8 shows the experimental and the simulated pressure drops in the fluidized bed for temperature conditions of 300°C. The theoretical minimum fluidization velocity (u_{mf}) for the particles was previously calculated to $u_{mf,theoretical} = 0.05$ m/s. From the CPDF simulations, the minimum fluidization velocity is found at approximately the same value, $u_{mf,simulated} = 0.05$ m/s. Comparison of the experimental pressure drop and the simulations using the Wen-Yu drag model shows that the CPFD model can predict fluid dynamic behavior of fluidized bed reasonably well.

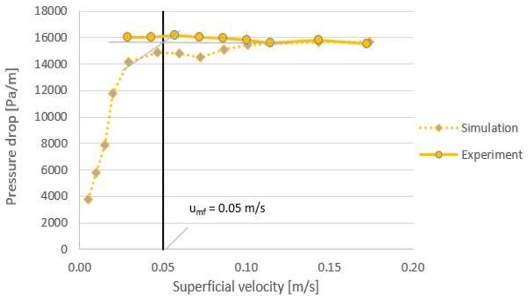

Figure 8. Comparison of experimental and simulated bed pressure drops for 300°C.

Figure 9 shows the experimental and the simulated pressure drops in the fluidized bed for temperature conditions of 800°C. As seen in the figure, the minimum fluidization velocities have decreased with the increased temperature. u_{mf} is indicated by black vertical lines in the figure, which read off $u_{mf,theoretical} = 0.034$ m/s and $u_{mf,simulated} = 0.046$ m/s. The large deviation between $u_{mf,theoretical}$ and $u_{mf,simulated}$ can be explained by the theoretical calculation using the mean particle diameter of 305 µm, while the CPFD calculation use the particle size distribution (Figure 4) where the particle diameter ranges from 180-710 um. However, the CPFD simulation correctly predicts the fluidized regime and pressure drops in the fluidized bed system.

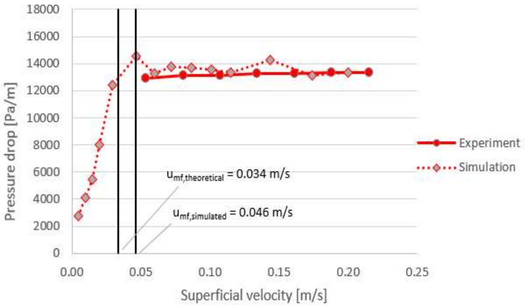

Figure 9. Comparison of experimental and simulated bed pressure drop at 800^{o}C.

Figure 10 and 11 compare the experimental and the simulated pressure drops for fluidization of sand and sand mixed with agglomerates for the temperature conditions of 700°C and 800°C respectively. One problem in the application of CPFD modelling of the agglomerated fluidized bed systems is that the agglomerates exist in all types of size, shapes and structures, which makes it difficult to define the agglomerated particles properties correctly. Although the simulations show instabilities in the fluidized regimes, the CPFD model maintains good agreement for the fluidized operation conditions in the fluidized regime.

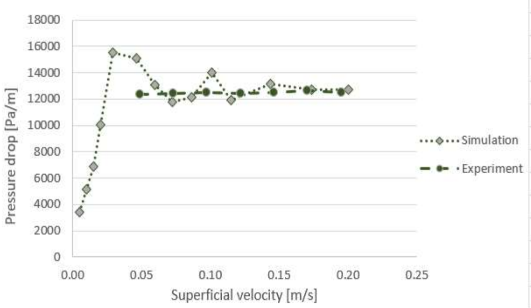

Figure 10. Comparison of experimental and simulated pressure drop for agglomerated bed at 700°C.

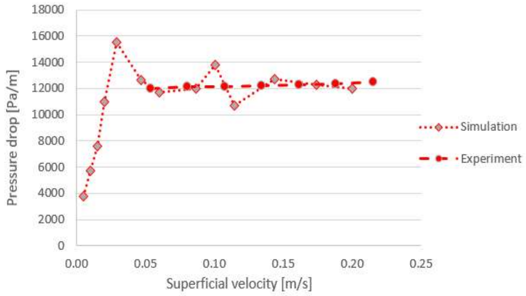

Figure 11. Comparison of experimental and simulated pressure drop for agglomerated bed at 800°C.

6 Conclusion

In this study, the fluid dynamics of a bubbling fluidized bed gasification system were investigated computationally and experimentally. The study included CPFD simulations of fluidization of silica sand particles and agglomerates using the commercial simulation software Barracuda VR version 17.4.1. Comparison of experimental and simulated pressure drops over the bed showed that the model can predict fluid dynamic behavior of fluidized bed reasonably well. Furthermore, the comparison showed that the Wen-Yu drag model gave better prediction of the fluidized conditions in the bed compared to the Ergun and the Wen-Yu/Ergun drag models.

The agglomerates are large sized and porous, which give them low density. The fluid dynamics in the bed depend upon the particle shape, size, density and diameter. Thus, the agglomeration process disturbs the fluidized conditions in the bed. The CPFD model is well capable of predicting the effect of agglomerates on flow behavior in a fluidized bed gasifier, and can be used for further studies including ash from different types of biomass.

Acknowledgements

This work is funded by the Research Council of Norway, Program for Energy Research (ENERGIX). Project 280892 FLASH - Prediction of FLow behavior of ASH mixtures for transport biofuels in the circular economy.

References

M. Bartles, W. Lin, J. Nijenhuis, F. Kapteijn and R. Ommen. *Agglomeration in fluidized beds at high temperaures: Mechanisms, detection and prevention*. Progress in Energy and Combustion Science 34:633-666, 2008.

P. Basu. *Biomass Gasification, Pyrolysis and Torrefaction*, Second Edition. Academic Pess, UK, 2013.

S. C. Capareda. *Introduction to Biomass Energy Conversions.* CRC Press, Boca Raton, US, 2014. ISBN: 978-1-4665-1334-1 (eBook-PDF).

J. Chladek, C. K. Jayarathna, B. M. E. Moldestad and L- A. Tokheim. *Fluidized bed classification of particles of different size and density.* Chemical Engineering Science 177: 155-162, 2018.

CPFD Software, LLC. *Barracuda VR Solutions,* (2020). Available from: https://cpfd-software.com/barracuda-vr-solutions/barracuda-vr (Accessed July, 2020)

C. T. Crowe, J. D. Schwarzkopf, M. Sommerfield and Y. Tsuji. *Multiphase Flows with Droplets and Particles*, Second Edition. CRC-Press, USA, 2012.

S. Ergun. *Fluid flow through packed columns*. Chemical Engineering Progress, 48: 89, 1952.

N. C. I. S. Furuvik, R. Jaiswal and B.M.E. Moldestad. *Experimental study of agglomeration of grass pellets in fluidized bed gasification.* WIT Transactions on Ecology and the Environment, 246, 2020.

N. C. I. S. Furuvik, R. Jaiswal and B. M. E. Moldestad. *Flow behavior in an agglomerated fluidized bed gasifier.* International journal of Energy and Environment 10(2):55-64, 2019.

C. K. Jayarathna, B. M. E. Moldestad and L. A. Tokheim. *Validation of results from Barracuda® CFD modelling to predict minimum fluidization velocity and pressure drop of Geldart A particles*. Proceedings of the 58th SIMS conference, 2017.

D. Kunii and O. Levenspiel. *Fluidization Engineering*, Second Edition. Butterworth-Heinemann, USA, 1994

F. Marchelli, Q. Hou, B. Bosio, E. Arato and A. Yu. *Comparison of different drag models in CFD-DEM simulations of spouted beds.* Powder Technology 360:1253-1270, 2020.

S. K. Sansaniwal, K. Pal, M. A. Rosen and S. K. Tyagi. *Global challenges in the sustainable development of biomass gasification: An overview*. Renewable and Sustainable Energy Reviews 80: 23-43, 2017.

R. K. Thapa and B. M. Halvorsen. *Study of Flow Behavior in Bubbling Fluidized Bed Biomass Gasification Reactor using CFD simulation.* The 14th International Conference on Fluidization - From Fundamentals to Products, Eds, ECI Symposium Series, 2013.

E. Tiffault, S. Sokhansanj, M. Ebadian, H. Rezaei, E. O. B. Ghiasi, F. Yazdanpanah, A. Asikainen and J. Routa. *Biomass pre-treatment for bioenergy. Case study 2: Moisture, physical property, ash and density management as pre-treatment practices in Canadian forest biomass supply chains.* IEA Bioenergy, 2018.

C. Wen and Y. Yu. *Mechanics of fluidization*. Chemical Engineering Progress Symposium Series, 62: 100-111, 1966.

L. C. Williams, T. L. Westover, R. M. Emerson, J. S. Tumuluru and C. Li. *Sources of Biomass Feedstock Variability and the Potential Impact on Biofuels Production.* Bioenergy Resource 9: 1-14, 2016.

M. Öhman, A. Nordin, B.J Skrifvars, R. Backman and M. Hupa. *Bed Agglomeration Characteristics during Fluidized Bed Combustion of Biomass Fuels.* Energy & Fuels 14(1): 169-178, 2000. DOI: 10.1021/ef990107b

M. Öhman and A. Nordin. *The Role of Kaolin in Prevention of Bed Agglomeration during Fluidized Bed Combustion of Biomass Fuels.* Energy & Fuels 14(3): 618-624, 2000. DOI: 10.1021/ef990198c

Paper 6

Experimental study of agglomeration in Fluidized Bed Gasification of Grass pellets.

This paper was presented in the 4th International Conference on Energy Production and Management. The conference was organized as a virtual conference on June 2020.
The paper is published in WIT Transactions on Ecology and the Environment, Volume 246 (2020) page 9-17. DOI: 10.2495/EPM200021

EXPERIMENTAL STUDY OF AGGLOMERATION OF GRASS PELLETS IN FLUIDIZED BED GASIFICATION

NORA C. I. S. FURUVIK, RAJAN JAISWAL & BRITT M. E. MOLDESTAD
Department of Process, Energy and Environmental Technology, Faculty of Technology,
Natural Science and Maritime Science, University of South-Eastern Norway, Norway

ABSTRACT

The agglomeration tendency during gasification of grass pellets in a bubbling fluidized bed reactor was studied. Particle agglomeration occurs as a consequence of interactions between the bed particles and the biomass ash during the thermal conversion of biomass in fluidized beds. The continuous operation and high efficiency of the fluidized beds are in these cases limited by partial or complete de-fluidization. In order to study the agglomeration tendency of grass pellets at defined operating conditions, controlled agglomerations tests are performed in a laboratory scaled 20 kW bubbling fluidized bed reactor. The effect of the ratio between the superficial fluidization velocity (u_0) and the minimum fluidization velocity (u_{mf}) on the agglomeration tendency for grass pellets is reported. The results show that agglomeration in the bed can be recognized by fluid dynamic disturbances in the bed, and if not counteracted, de-fluidization will occur. The ratio u_0/u_{mf} influences the agglomeration tendency and the de-fluidization of bed. As the ratio u_0/u_{mf} increases, the agglomeration tendency and the de-fluidization time decreases. The de-fluidization temperature was not influenced by the changes in the superficial velocity ratio.

Keywords: biomass fluidized bed gasification, particle agglomeration, de-fluidization.

1 INTRODUCTION

The massive expansion in the use of fossil fuels and the world-rising fear over the effects of climate changes, have brought to light the search for a renewable and climate-friendly alternative to fossil fuels [1]. Among the different sustainable energy conversion technologies, fluidized bed biomass gasification is considered a promising contribution to the shift towards renewable energy production. Fluidized beds offer homogenous operation conditions and excellent fuel/gas contact, and are therefore ideally suited for converting biomass into an energy-rich synthetic gas. The produced gas has several applications, and can be used either directly for production of heat and power or it can be further processed into biofuels and other conventional chemicals [2].

Despite the many advantages with fluidized bed biomass gasification, the process introduces ash-related challenges that are the main drawback for the commercial breakthrough [3]. These problems are generally associated with molten biomass ash that interacts with the bed materials, forming agglomerates that create fluid dynamic disturbances in the bed. Particle agglomeration is a key concern in fluidized bed biomass gasification. The presence of agglomerates results in instabilities with bubbling and channeling in the bed, which changes the fluidization character of the particles and makes further fluidization impossible [4]. The phenomenon may further cause decreased heat transfer and local temperature deviations followed by de-fluidized volumes in the bed [4]. De-fluidization is described as a total collapse of the fluidized bed, and can be recognized as rapidly decreasing pressure and substantial temperature changes during the gasification process. In the most severe cases, particle agglomeration transforms the fluidized bed into fixed bed conditions and may lead to unscheduled shutdowns of the whole installation [1]. Fig. 1 pictures a photo of biomass ash particles melted together with bed material that are grown to a larger agglomerate in a bubbling fluidized bed reactor.

WIT Transactions on Ecology and the Environment, Vol 246, © 2020 WIT Press
www.witpress.com, ISSN 1743-3541 (on-line)
doi:10.2495/EPM200021

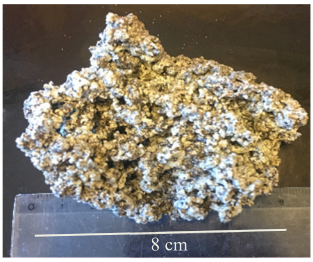

Figure 1: Agglomerates from biomass ash and silica sand particles.

Particle agglomeration during gasification of biomass in fluidized beds typically originates from certain ash-forming elements, which are released from the biomass during the heating process. The most significant ash-forming elements in biomass are silica (Si), potassium (K), calcium (Ca), magnesium (Mg), aluminium (Al), phosphor (P), chlorine (Cl), sodium (Na) and sulphur (S) [2]. The tendency of particles to agglomerate is highly coupled to the physical characteristics and the high temperature chemistry of the biomass ash. Melting processes and chemical reactions produce an alkali liquid phase that can form a bridge between the ash and bed particles [5]. With increased bed temperatures, the viscosity of the liquid phase will decrease and cause larger adhesive forces that glue the particles together. The agglomeration process is initiated by ash deposition and formation of a coating layer on the surface of the bed particles, and is dominated by a combination of the three mechanisms illustrated in Fig. 2 [5]. First, the transfer of solid ash particles onto the surface of the bed material (here: Silica sand, SiO_2) through van der Waals forces. The second mechanism is the condensation of volatilized ash on the bed particles, while the third mechanism is the attachment of molten or partially molten ash to the surface of the bed particles due to chemical reactions between the gaseous alkali components and the particles (solid ash + bed material) [5].

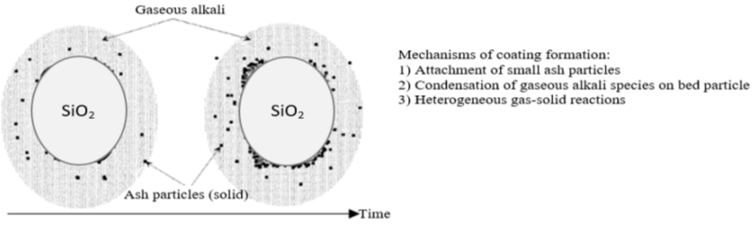
Gaseous alkali
SiO₂
SiO₂
Ash particles (solid)
Time
Mechanisms of coating formation:
1) Attachment of small ash particles
2) Condensation of gaseous alkali species on bed particle
3) Heterogeneous gas-solid reactions

Figure 2: Deposition of biomass ash on the bed particles.

The ash melting and following agglomeration process depends on the ash characteristics, and can also be influenced by the bed operation conditions or the nature of the bed material [2]. In most ash-layer coatings, Si is the dominating element [5]. The agglomeration process happens as Si combines with other alkali ash components to form low-melting silicates (eutectics), which are characterized by lower melting points that the individual components [6]. The attachment of ash on the bed particles surface, and the subsequently growth of agglomerates can follow two main routes: Melting-induced or coating-induced agglomeration. Most dominant among the mechanisms is the coating-induced agglomeration, where the biomass ash attaches to the surface of the bed particles resulting in formation of an ash-layer enriched in alkali metals. This coating tends to soften and will become sticky at high temperatures, and thereby cause particles to agglomerate due to repeated collisions between the sticky ash-coated particles. In some cases, especially with fuels that are rich in Si and K, melting-induced agglomeration can occur. The melting-induced agglomeration is a result of direct adhesion of the bed particles due to alkali ash compounds that melt and form a liquid phase at conventional gasification temperatures. The molten ash acts as a glue, which forms liquid bridges between the particles and causes agglomeration. In Fig. 3, the two agglomeration mechanisms between bed material particles (SiO_2) and the biomass ash are illustrated [5], [7].

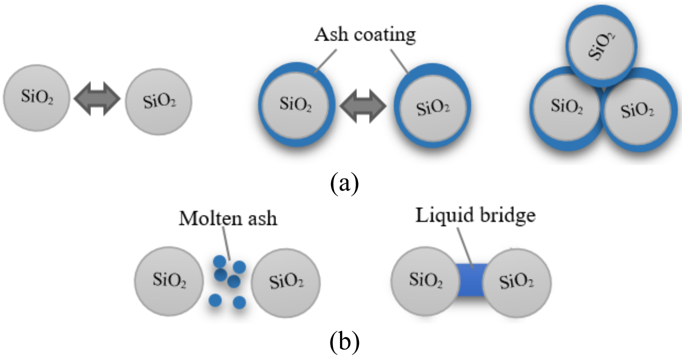

(a)

(b)

Figure 3: Coating-induced (a); and melting-induced (b) agglomeration.

This study focuses on agglomeration during gasification of grass pellets in a bubbling fluidized bed reactor. The fuel characteristics indicate that the major ash-forming elements in the investigated grass pellets are K, Si and Ca. In addition, the grass pellets are enriched with less amounts of P, Na, Mg and Al. The ash obtained from the grass pellets are composed of various inorganic elements, which are present as oxides dominated by SiO_2 and K_2O.

The main objective of this work is to study the agglomeration tendency of grass pellets during a gasification process. The experiments are carried out in a 20 kW laboratory scale bubbling fluidized bed gasifier under normal bed fluidization conditions. The effect of the ratio of the superficial air velocity over the minimum fluidization velocity (u_0/u_{mf}) in relation to the agglomeration tendency of grass pellets is examined. The operating parameters, i.e. the bed temperature (T_{bed}) and bed pressure drop (ΔP_{bed}) are continuously monitored throughout the experiments in order to develop data to determine the de-fluidization time (t_{def}) on the onset of de-fluidization.

2 EXPERIMENTAL SETUP

The experimental set-up consists of a 20 kW laboratory scaled bubbling fluidized bed gasifier; the system is divided into seven blocks as illustrated schematically in Fig. 4. The reactor is a stainless steel cylindrical column with inner diameter of 10 cm and a height of 130 cm. Three electrical heating elements are coiled around the wall of the reactor and are used for external heating of the gasification process. Five thermocouples and five pressure transducers are placed along the height of the column, and are constantly monitoring the operating conditions in the bed. The gasification agent is preheated air, which flows into the reactor through two 10 mm steel pipes that are placed 27.5 mm from the bottom of the column. The mass flow rate of air is controlled with a BROOK air flowmeter operating in the range of 0.48–4.7 kg/h. The distance between the pressure and temperature sensors are 10 cm, whereas the first sensor is at the same level as the air supply. Each pressure transducer measures the gauge pressure, i.e. the fluid pressure in excess of the atmospheric pressure, in the given position. The biomass fuel is supplied through a screw conveyor and enters the reactor 21.2 cm above the air inlet. The product gas leaves the reactor from the top and flows through a pipe into the chimney where it is burned directly. Gas samples for use in analytical setup are collected from a gas sampling point installed in the outlet pipe of the reactor.

The temperature and pressure sensors are connected to the LabView software for data acquisition, and the bed conditions are continuously observed from the temperature and pressure measurements. Fig. 5 pictures a screenshot of the control panel.

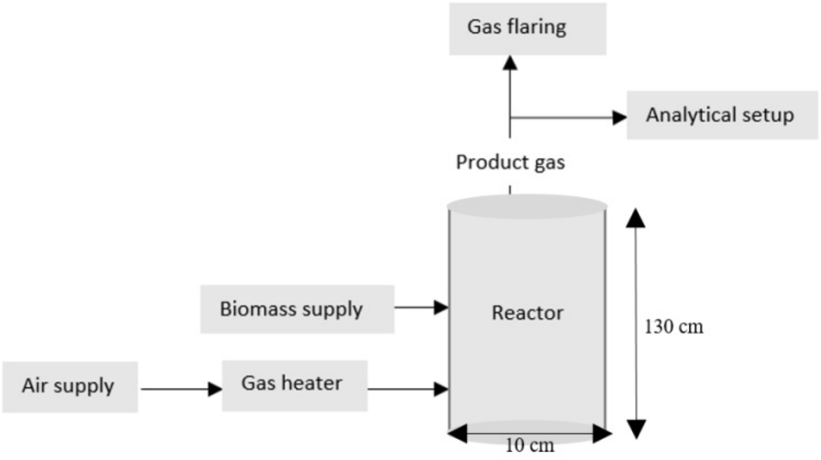
Gas flaring
Analytical setup
Product gas
Reactor
130 cm
Biomass supply
Air supply
Gas heater
10 cm

Figure 4: Block diagram of the bubbling fluidized bed gasifier.

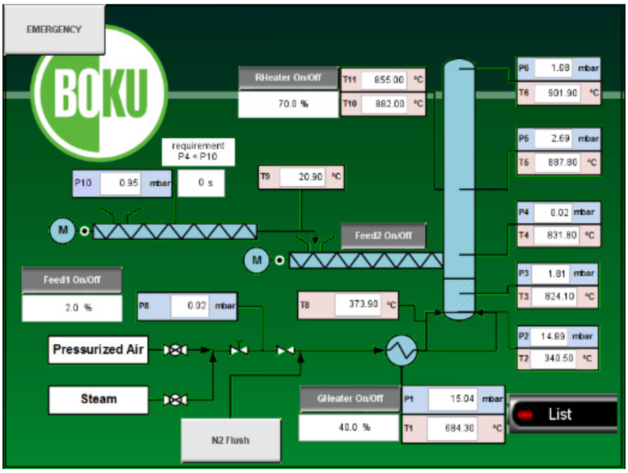
EMERGENCY
BOKU
RHeater On/Off
Feed2 On/Off
Feed1 On/Off
Pressurized Air
Steam
N2 Flush
GHeater On/Off
M
M
List

RHeater On/Off 70.0 %
T11 855.00 °C
T10 882.00 °C
requirement P4 < P10
P10 0.95 mbar
0 s
T9 20.90 °C
Feed1 On/Off 2.0 %
P8 0.02 mbar
T8 373.90 °C
GHeater On/Off 40.0 %
P1 15.04 mbar
T1 684.30 °C
P6 1.08 mbar
T6 901.90 °C
P5 2.69 mbar
T5 887.80 °C
P4 0.02 mbar
T4 831.80 °C
P3 1.81 mbar
T3 824.10 °C
P2 14.89 mbar
T2 340.50 °C

Figure 5: LabView control panel.

3 FUEL AND BED MATERIAL CHARACTERISTICS

Grass pellets sized in the range from 0.5 cm to 2.0 cm are used for the agglomeration tests. Prior to the experiments, chemical analyses of the pellets and the ash were carried out by Eurofins Environment Testing Norway AS. The analyses were performed in accordance with the requirements of European Standards SS-EN 14961, SS-EN 15359 and EN 13656. The fuel characterization is presented in Table 1, and the chemical properties of the grass pellets and the ash are listed in Tables 2 and 3, respectively.

Table 1: Ultimate and proximate analyses of grass pellets, dry basis (wt %).

	Ash content	Volatiles	Moisture	Fixed C	C	O	H	N	S
Fuel	9.5	75.9	8.4	6.2	46.9	33.7	5.7	3.2	0.3

Table 2: Major ash-forming elements of grass pellets, dry basis (mg/kg).

	K	Si	Ca	P	Na	Mg	Al
Fuel	20,000	16,000	6,500	3,400	2,100	2,000	340

Table 3: Ash composition of grass pellets, dry basis (mg/kg).

	SiO_2	K_2O	CaO	P_2O_5	MgO	Na_2O	Al_2O_3	Other
Ash	34,000	25,000	9,300	7,600	3,400	3,100	1,300	850

Quartz sand with particle size ranging from 200 μm to 425 μm was used as bed material. The mean diameter of the particles is 355 μm, and the particle density is 2,650 kg/m^3. The sand particles are classified as round to angular. Table 4 lists the chemical composition of the bed material.

Table 4: Chemical composition of bed material (wt %).

	SiO_2	Al_2O_3	K_2O	Na_2O	Fe_2O_3	CaO	MgO	TiO_2	LOI*
Bed material	83.6	7.83	2.49	2.31	1.5	1.49	0.45	0.22	0.4

*LOI = Loss of Ignition.

4 EXPERIMENTAL PROCEDURE

The bed materials were filled into the bubbling fluidized bed reactor from the top, the mass of the bed particles was 2.0 liters corresponding to a bed height of 20 cm. The agglomeration tests were initiated by loading the grass pellets to the bed with a fuel feed ratio of 2.46 kg/h. The air mass flow was controlled in the range between 2.0–3.0 kg/h. The reactor was operated in a controlled gasification range, with bed temperature maintained between 800–900°C throughout all experiments. The temperature sensor T3 was used as reference for the bed temperature. Three agglomeration tests were carried out, where the ratio of the superficial air velocity (u_0) over the minimum fluidization velocity (u_{mf}) varied. Prior to the experiments, the minimum fluidization velocity for the bed particles was calculated to 0.0446 m/s from Erguns equation [8]. The bubbling fluidized bed gasifier was operated according to the parameters in Table 5. All three experiments were carried out continuously and separately for approximately 30 minutes, or until the fluidized bed collapsed as a consequence of particle agglomeration. The onset of bed agglomeration was determined by observing fluctuations in bed temperature (T_{bed}) and bed pressure drop (ΔP_{bed}). Agglomerates and the bed material and ash were removed from the gasifier after each test.

Table 5: Operating parameters for the agglomeration tests of grass pellets.

Air flow rate (kg/h)	Fuel feed rate (kg/h)	T_{bed} (°C)	u_0 (m/s)	u_{mf} (m/s)	u_0/u_{mf} (-)
2.0	2.46	800–900	0.225	0.0446	5.0
2.5	2.46	800–900	0.281	0.0446	6.3
3.0	2.46	800–900	0.338	0.0446	7.6

Ash melting behavior from laboratory prepared ash from the grass pellets was determined according to the CEN/TS 15730-1:2006. Generally, the ash melting takes place over a melting range where the solid phase coexists with its liquid phase [2]. The ash melting behavior is useful to make a qualitative statement about the agglomeration tendency of the fuel at given temperatures. The evaluation is done automatically by monitoring a shadow profile of the sample where the changes of the geometry are documented, and the information given from the images defines four characteristic temperatures that are explained in Table 6.

Table 6: Characteristic ash melting temperatures, based on [9].

Characteristic temperature	Shrinking temperature (ST)	Deformation temperature (DT)	Hemispherical temperature (HT)	Flow temperature (FT)
Shadow profile	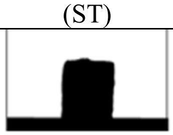	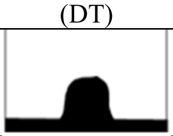	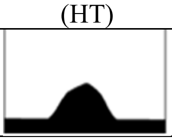	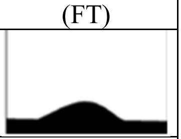
Description	Initial deformation. First sign of shrinking.	Spherical appearance. First sign of rounding.	Hemispherical form. Half the original height.	The cylindrical test piece has effectively melted.

5 RESULTS

The influence of the ratio u_0/u_{mf} on the de-fluidization time is examined by changing the air flow rate for three controlled bed agglomeration tests. The experimental results are shown in Fig. 6, where the bed temperature (T_{bed}) and bed pressure drop (ΔP_{bed}) are plotted as a function of time for each of the test runs. De-fluidization can be clearly seen as an unusual decrease in ΔP_{bed} or/and an increase in T_{bed}. For the test run where $u_0/u_{mf} = 5.0$, the gasification process reaches instabilities in the bed parameters after 14 minutes; the drastic fluctuations in ΔP_{bed} and T_{bed} suggest the presence of agglomerations in the bed. If not counteracted, the modifications in particle size result in segregation of the bed where the agglomerated particles accumulate and either settle at the bottom or stick to the walls of the reactor. Segregation is indicated by a slow decline in ΔP_{bed} due to formation and build-up of channels in the bed. Channeling creates de-fluidized volumes that act as “hot-spots”, which are the cause of a heterogenous temperature profile. Complete de-fluidization finally occurs at 24 minutes and is detected by a sudden decrease in the ΔP_{bed}. For the test run where $u_0/u_{mf} = 6.3$, the bed parameters are stable with no fluctuations in ΔP_{bed} and homogenous T_{bed} during the first 18 minutes of the run. At this time, the temperature profile makes a sudden change and shows a significant increase in the temperature gradient, suggesting onset of particle agglomeration in the bed. However, the lack of variation in ΔP_{bed} indicates that only small fractions of the bed particles have been agglomerated. After 30 minutes, no de-fluidization is observed. When $u_0/u_{mf} = 7.6$, the bed conditions are recognized by higher ΔP_{bed} and higher T_{bed} at the start-up of experiment. ΔP_{bed} shows no fluctuations while T_{bed} shows a decreasing temperature profile during the first 8 minutes of the run. At this time, a sharp reduction in ΔP_{bed} occurs at the same time as the bed reaches homogenous T_{bed}, indicating that agglomerates are refluidized as the ΔP_{bed} drops to a stable value. No disturbances or de-fluidization were observed during the next 25 minutes of the test run. During normal gasification conditions, ΔP_{bed} is stabilized in the range between 10–15 mbar for all experiments. When de-fluidization occurs, the differential pressure drops drastically with over 10 mbar to below 3 mbar. From the observed bed conditions, it is found that u_0/u_{mf} does not influence the de-fluidization temperature (T_{def}). For grass pellets, de-fluidization of the bed was observed when the temperature reached 860°C, $T_{def} = 860°C$.

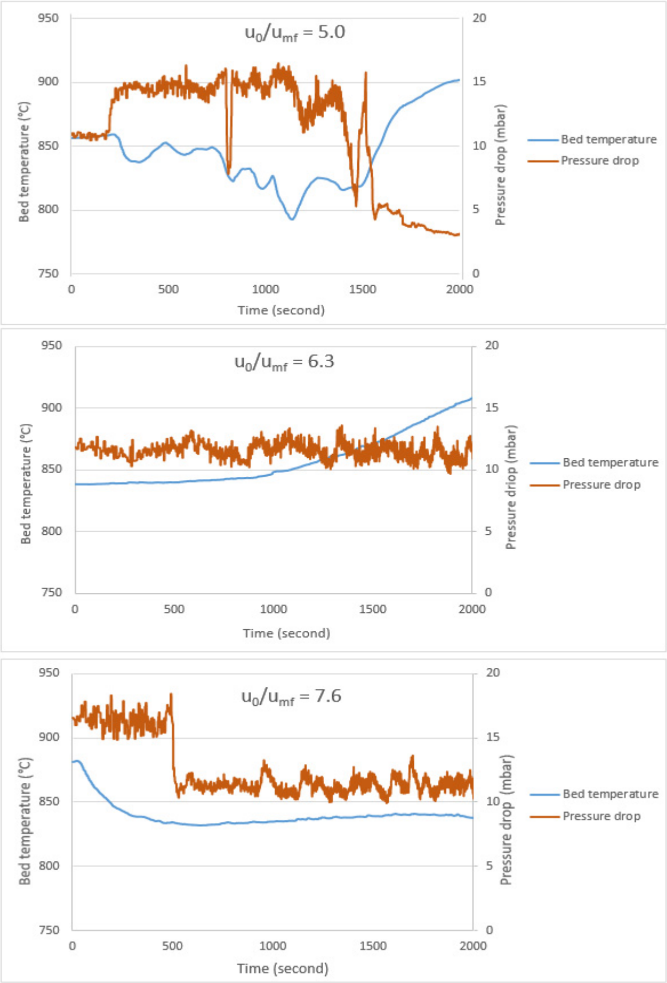

Figure 6: Bed temperatures and pressure versus time for agglomeration tests.

The results from the agglomeration tests indicate that higher ratio of u_0/u_{mf} will decrease the onset of agglomeration and increase the de-fluidization time. Increasing the air superficial velocity gives better mixing of the particles, and may result in breaking of formed agglomerates due to increased forces acting on the particles. Additionally, high fluidization velocity reduces the amount of ash in the bed as some of the ash particles may flow out of the reactor together with the producer gas. Increasing the ratio of u_0/u_{mf} can slow the particle agglomeration and prevent de-fluidization. However, upper limits for air mass flow exist during the gasification process; if the amount of air exceeds the stoichiometric amount, the process will go from gasification to combustion.

The observation of the bed material at the end of the agglomeration tests shows presence of agglomerates of various sizes after each of the three experiment. The agglomerates are of distinct types, as pictured in Fig. 7. For the test with the lowest u_0/u_{mf} ratio, the agglomerates are formed as result of melting-induced mechanism. These agglomerates clearly show that the bed particles are melted together by hard bridges, resulting in faster agglomeration due to increased adhesive forces between the particles. If the adhesive forces are equal or exceed the drag forces, de-fluidization appears [10]. Once formed, this type of agglomerates tend to stick to the walls of the reactor, or process equipment, causing increased de-fluidized volumes with temperatures around the agglomerates. For the tests with higher u_0/u_{mf} ratio, the agglomerates are closely connected to the coating-induced agglomeration mechanism. The agglomerates show that bed materials coated with ash have clustered together. These agglomerates interfere with the flow behaviour in the bed. However, as long as the bed maintains homogenous T_{bed} and the fluidization velocity remains high enough to fluidize the particles, these agglomerates will easily break into smaller particles. If not controlled, the agglomerated particles might grow into larger agglomerates that cause de-fluidization.

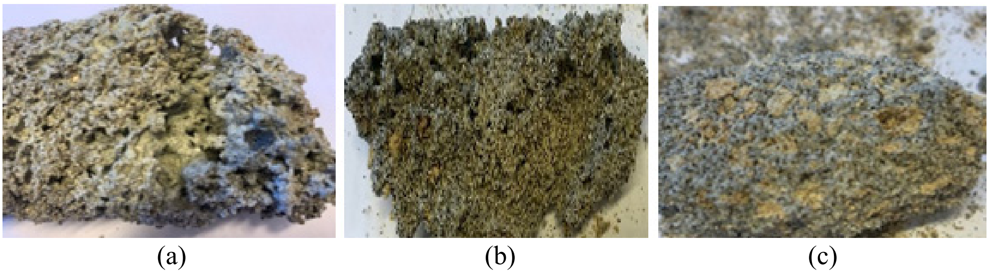
(a) (b) (c)

Figure 7: Agglomerates from grass pellets. (a) $u_0/u_{mf} = 5.0$; (b) $u_0/u_{mf} = 6.3$; and (c) $u_0/u_{mf} = 7.6$.

The particle agglomeration tendency is represented by T_{def}. The agglomeration tests indicate that $T_{def} = 860°C$ for grass pellets, which are far below the characteristic temperatures given by the ash melting analyses shown in Table 7. High Si and high K characterize the content of ash-forming elements in grass pellets, and the low T_{def} occurs most probably because sticky K-silicates are formed during the thermochemical process.

Table 7: Ash melting behaviour of grass pellets.

ST (°C)	DT (°C)	HT (°C)	FT (°C)	T_{def} (°C)
1090	1150	1180	1190	860

6 CONCLUSION

The objective of this work was to study the agglomeration tendency and the related de-fluidization time in gasification of grass pellets in a bubbling fluidized bed gasifier. The chemical analyses of the grass pellets show that the fuel is rich in K and Si, and has relatively low content of Ca, P and other ash-forming elements. The ash content of the examined grass pellets is 9.5 wt %. In order to develop data to determine the agglomeration tendency of the grass pellets, agglomeration tests were carried out in a laboratory scaled bubbling fluidized bed gasifier. Three different experiments were carried out, at different air mass flow. De-fluidized condition in the bed was detected by observation of a sudden decrease in the differential pressure in the bed, or by significant changes in the temperature profile in bed. The de-fluidization temperature for grass pellets was determined to $T_{def} = 860°C$. As the ratio of the superficial air velocity over the minimum fluidization velocity (u_0/u_{mf}) increases, the agglomeration tendency decreases and the de-fluidization time increases. The results indicate T_{def} is not affected by the u_0/u_{mf} ratio.

ACKNOWLEDGEMENT

This work is funded by the Research Council of Norway, Program for Energy Research (ENERGIX). Project 280892 FLASH – Prediction of FLow behavior of ASH mixtures for transport biofuels in the circular economy.

REFERENCES

[1] Öhman, M. & Nordin, A., The role of kaolin in prevention of bed agglomeration during fluidized bed combustion of biomass fuels. *Energy and Fuels*, **14**(3), pp. 618–624, 2000.

[2] Balland, M. et al., Biomass ash fluidized-bed agglomeration: Hydrodynamic investigations. *Waste Biomass Valor*, **8**, pp. 2823–2841, 2017.

[3] Wang, L., Weller, C.L., Jones, D.D. & Hanna, M.A., Contemporary issues in thermal gasification of biomass and its application to electricity and fuel production. *Biomass and Bioenergy*, **32**, pp. 573–581, 2008.

[4] Bartles, M., Lin, W., Nijenhuis, J., Kapteijn, F. & Ommen, R., Agglomeration in fluidized beds at high temperatures: Mechanisms, detection and prevention. *Progress in Energy and Combustion Science*, **34**, pp. 633–666, 2008.

[5] Öhman, M. & Nordin, A., Bed agglomeration characteristics during fluidized bed combustion of biomass fuels. *Energy and Fuels*, **14**(1), pp. 169–178, 2000.

[6] Visser, S., van Lindt, S. & Kiel, J., Biomass ash-bed material interactions leading to agglomeration in FBC. *Journal of Energy Resource Technology*, 2008.

[7] Gatternig, B., Predicting agglomeration in biomass fired fluidized beds. PhD thesis, Der Technichsen Fakultät der Friedrich-Alexander-Universität Erlangen-Nürnberg, 2015.

[8] Kunii, D. & Levenspiel, O., *Fluidization Engineering*, Butterworth-Heinemann: Berlin, p. 69, 1994.

[9] Hesse Instruments, The Heating Microscope and EMII Software, 2016. www.hesse-instruments.de/fileadmin/downloads/Prospekt/BRO_EM301_EN_160608.pdf. Accessed on: 7 Feb. 2020.

[10] Zhong, Y., Gao, J., Guo, Z. & Wang, Z., Mechanism and prevention of agglomeration/defluidization during fluidized-bed reduction of iron ore. Volodymyr Shatokha, IntechOpen, 2017. DOI: 10:5772/intechopen.68488.

Paper 7

Experimental study and SEM-EDS analyses of agglomerates from gasification of biomass in fluidized beds

This paper is submitted to the journal, Energy. Status: Under review.

Not available online

Paper 8

Modelling of ash melts in fluidized bed gasification of biomass

This paper is submitted to the journal, Chemical Engineering Science X.

Status: Under review.

Not available online

Doctoral dissertation no. 120
2022

—

Modelling of ash melts in gasification of biomass

Dissertation for the degree of Ph.D

—

Nora Cecilie Ivarsdatter Skau Furuvik

—

ISBN: 978-82-7206-649-8 (print)
ISBN: 978-82-7206-650-4 (online)

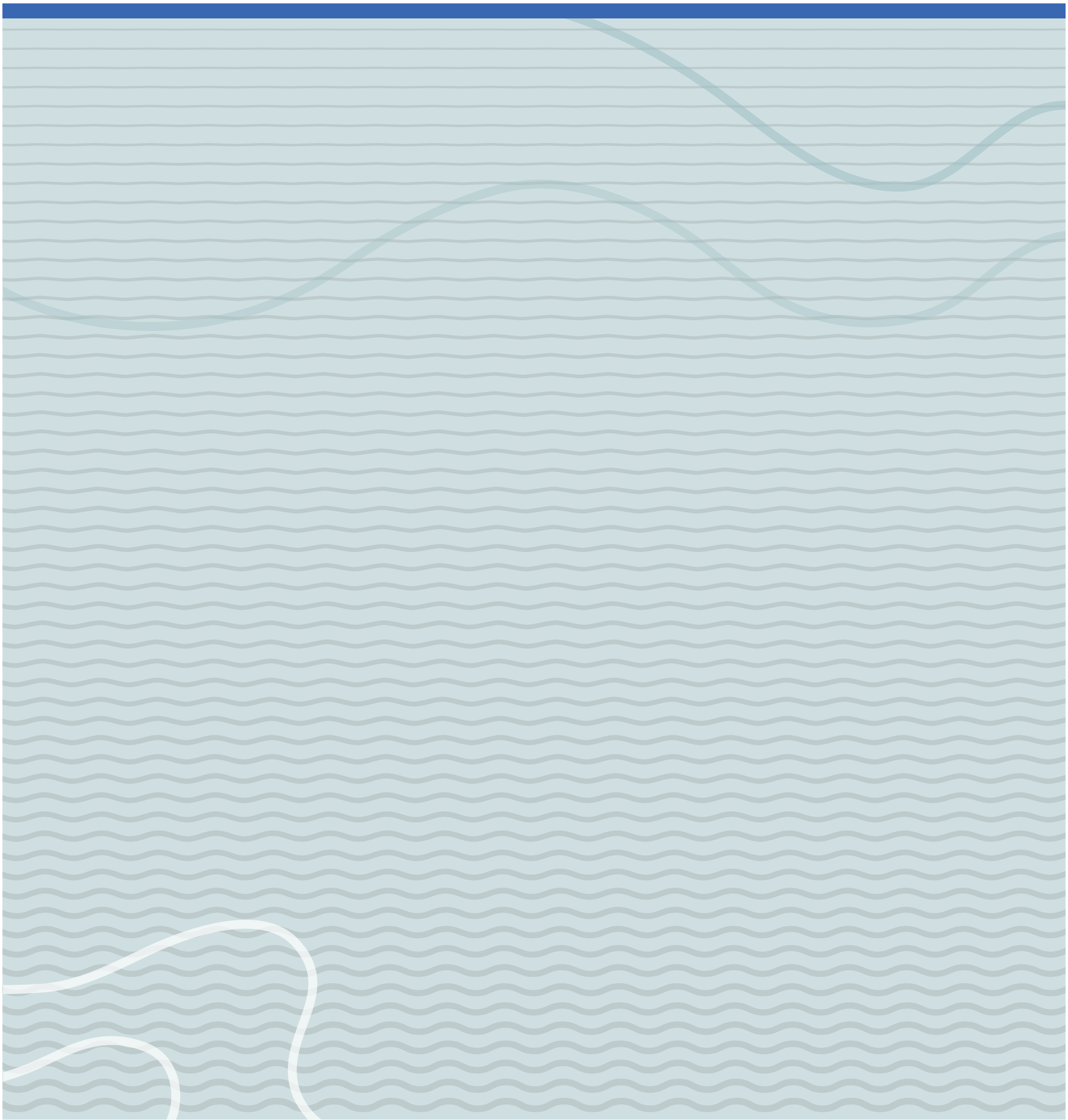usn.no